UNIVERSITÀ DEGLI STUDI DI UDINE

CORSO DI DOTTORATO DI RICERCA IN
SCIENZE BIOMEDICHE E BIOTECNOLOGICHE

CICLO XXVI

Tesi di Dottorato di Ricerca

Role of LIMP-2 in the trafficking of Acid β-Glucosidase

RELATORE
Prof. Claudio Brancolini

DOTTORANDA
Dott.ssa Erika Malini

CORRELATORI
Dott.ssa Andrea Elena Dardis
Dott. Bruno Bembi

ANNO ACCADEMICO 2013/2014

Table of contents

Abstract

Acid β-glucosidase (GCase) is a lysosomal enzyme defective in most cases of Gaucher disease (GD). GCase, encoded by the *GBA* gene, is targeted to the lysosomes through its interaction with the lysosomal integral membrane protein type 2 (LIMP-2). To date, more than 300 mutations of the *GBA* gene have been reported, most of them lead to the synthesis of misfolded proteins that are retained in the endoplasmic reticulum (ER) and rapidly degradated by endoplasmic reticulum associated degradation (ERAD). It has been proposed that mutations in the *SCARB2* gene, encoding LIMP-2, may modify the phenotypic expression of GD. However, the nature of the GCase-LIMP-2 interaction has not been characterized in detail and the impact of *GBA* mutations on this interaction has not been explored.

Recently, mutations in the human gene encoding LIMP-2 (*SCARB2*) were found to be responsible for action myoclonus-renal failure syndrome (AMRF), a disorder characterized by a mistargeting of GCase. The main feature of AMRF is the presence of progressive myoclonus epilepsy, a frequent sign found in patients affected by the chronic neurological form of GD. However, even if AMRF and GD affect the same metabolic pathway and share some neurological features, they present with different clinical and biochemical phenotypes, suggesting that an alternative lysosomal targeting pathway may be active in different tissues.

In this study we investigated the impact of *GBA* mutations on LIMP-2-GCase association and the role of LIMP-2 in the trafficking of GCase to the lysosomes in different human tissues.

First, we analyzed the impact of 9 novel *GBA* alleles, found in 8 GD Italian patients (P159S, N188I, E235K, P245T, W312S, S366R, W381C, [N188S;G265R], [E326K;D380N]) and two frequent *GBA* mutations (N370S and L444P) on GCase enzymatic activity and binding to LIMP-2. All mutants were inactive except for the P159S, which retained a 15% of wild type activity. The presence of N188I, [N188S;G265R] and W381C mutations significantly impaired the ability of GCase to associate with LIMP-2, suggesting that these residues may be important for LIMP-2-GCase interaction.

In addition, we performed an in vitro functional analysis of a *SCARB2* mutation (E471G) recently described to be associated with myoclonic epilepsy in a family affected by GD. The obtained results showed that the mutation do not affect the binding of LIMP-2 to GCase. However, in the presence of this mutation very low levels of LIMP-2 protein could be detected, suggesting that the mutation would severely impact LIMP-2 protein expression and/or protein degradation.

Then, we evaluated the role of LIMP-2 in the trafficking of GCase in different human tissues, by comparing the GCase enzymatic activity and intracellular localization in cells derived from a patient affected by AMRF, patients affected by GD and healthy controls.

The results strongly suggest that LIMP-2 is critical for the lysosomal targeting of GCase in human fibroblasts. In these cells LIMP-2 deficiency led to the retention of GCase in the ER and its degradation, which in turn, caused a severe impairment in GCase activity. A LIMP-2 dependent mechanism was also observed for the targeting of human recombinant GCase (hrGCase) to the lysosomes in human fibroblasts.

Instead, LIMP-2 deficient macrophages and lymphoblasts retained a quite high GCase residual activity and digestion with endo-H clearly showed that in these cells, a significant fraction of GCase is able to leave the ER and probably reaches the lysosomes. These data suggest the existence of a LIMP-2 independent mechanism for the lysosomal targeting of GCase in blood cells.

Finally, in a model of human LIMP-2 deficient neurons, obtained by neuronal differentiation of adult stem cells derived from human fibroblasts (hSKIN-MASC) of a patient affected by AMRF, GCase enzymatic activity was almost undetectable and GCase did not localize within the lysosomes. Furthermore, an accumulation of GM2 gangliosides was observed within lysosomes of these cells. These observations suggest that LIMP-2 is critical for the trafficking of GCase in neuronal cells and support the hypothesis that the neurological signs present in AMRF patients are caused by the lack of functional GCase in lysosomes with subsequent storage of glycosphingolipid material.

1. Introduction

1.1 The lysosomal system

Lysosomes are lytic organelles that contain numerous acid hydrolases for degradation and modification of substances, passing through the vacuolar membrane system. The material to be broken down may be intracellular or extracellular. Intracellular materials undergo autophagy, a process which degradates cellular components, including organelles, enclosing them in an autophagosome. Extracellular material enters the cell either by endocytosis or phagocytosis, depending on the nature of the molecule.

Endocytosis is a mechanism by which fluid and solutes are engulfed via clathrin-coated vescicles (receptor-mediated endocytosis), via clathrin-independent pathway or via caveolae. Instead, phagocytosis is a mechanism by which specialized cells engulf invading pathogens, apoptotic cells and other foreign particles (>250 nm in diameter) via large vesicles called phagosomes.

Lysosomes contain about 50-60 types of acid hydrolases, localized in the lysosomal lumen and able to degrade most macromolecules. Lysosomal enzymes include proteases, nucleases, glycosidases, lipases, phospholipases, phosphatases and sulphatases. To ensure optimal enzymatic activity, lysosomes maintain an internal acidic environment (pH 4.5-5.0) through the use of a hydrogen vacuolar ion pump ATPase (V-ATPase) located in the lysosomal membrane that drives ions from the cytoplasm into the lumenal space of the organelles (**Figure 1.1**).

Following the breakdown of macromolecules, the resultant amino acids, sugars, simple glycolipids, cholesterol, nucleotides etc are salvaged by transport through the lysosomal membrane for subsequent use in biosynthetic processes. Taken as a whole, the lysosomal system functions at the very hub of cellular metabolic homeostasis.

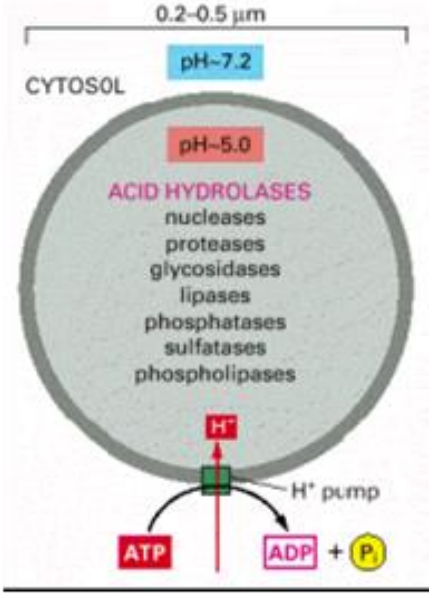

Figure 1.1 The Lysosome. The acid hydrolases are hydrolytic enzymes active under acidic conditions. The lumen is maintained at an acidic pH by an H+ ATPase located in the lysosomal membrane that acidifies the environment inside the lysosome. (From Alberts, 2002).

With the recent discovery of an overarching gene regulatory network referred to as CLEAR (Coordinated Lysosomal Expression and Regulation) and its master gene transcriprion factor EB (TFEB), it has been shown that many components of the lysosomal system are linked at the transcriptional level (Sardiello et al., 2009). These studies further establish the lysosomal system as a highly efficient and coordinated network.

As such, proper lysosomal function is essential, since failure of this system leads to catastrophic consequence for cells, organs and individuals.

1.2 Lysosomal storage diseases

Lysosomal storage diseases (LSD) encompass a wide spectrum of rare genetic disorders due to defects in proteins essential for normal function of the lysosomal system. Most LSD show widespread tissue and organ involvement, with brain, viscera, bone and connective tissues often being affected. Brain disease is particularly prevalent, being present in two-thirds of all lysosomal disorders.

To date, nearly 60 monogenic LSD have been described with a combined incidence of approximately of 1:500 to 1:7000 live births (Staretz-Chacham et al., 2009). They

are caused by deficiencies in lysosomal hydrolases, soluble non enzymatic proteins and membrane associated proteins critical for proper function of the lysosomal system. The deficient or missing activity of lysosomal proteins leads to the accumulation of macromolecules within the lysosome, such as sphingolipids, cholesterol, glycoproteins, mucopolysaccharides or glycogen.

LSD are inherited in an autosomal-recessive fashion, except for Fabry disease, Hunter disease (MPS II) and Danon disease that are all X-linked (Futerman and van Meer, 2004).

Certain disorders are more prevalent in certain geographic areas or among particular ethnic groups. For example Gaucher disease (Horowitz et al., 1998) and Tay-Sachs disease (Myerowitz et al., 1997) are almost 100 times more prevalent in Ashkenazi Jewish decent that in the general population.

Although most LSD affects children, the age at onset and the clinical course can vary significantly and the progressive course usually leads to premature death.

The genetic bases of most LSD are known. However, it is often difficult to correlate a genotype to a phenotype. In fact, the high phenotypic variability in patients affected by LSD suggests that the substrate accumulation leads to a cascade of secondary cellular events, which are responsible for the clinical manifestations. The nature of these secondary events is not fully understood.

1.3 Synthesis and transport of lysosomal proteins

Most soluble lysosomal enzymes are synthesized as *N*-glycosylated precursors in the endoplasmic reticulum (ER), and the initial steps of biosynthesis are shared with secretory proteins. However, the diversion of the lysosomal proteins from the secretory pathway is dependent on the acquisition of the mannose-6-phosphate (M6P) marker in the *cis*-Golgi that is recognized by transmembrane M6P receptor.

The generation of the M6P recognition marker depends on a reaction involving two different enzymes: UDP-N-acetylglucosamine 1-phosphotransferase and α-N-acetylglucosamine-1-phosphodiester α-N-acetylglucosaminidase.

The binding of ligands to the extracellular domain of the M6P receptor is pH dependent. In fact, this receptor binds lysosomal enzymes in the *trans*-Golgi network at pH 6.5 and releases the ligands in the acidic environment of the endosomal

compartment at pH < 6.0, from where they are delivered to lysosomes. The M6P receptors cycle back to the *trans*-Golgi network to mediate further transport.

Studies in fibroblast from patients affected by I-cell disease, caused by the deficiency of N-acetylglucosamine-1-phosphotransferase, have shown that the lack of M6P leads to a secretion of most lysosomal enzymes. However, not all lysosomal enzymes synthesized by these cells are secreted, suggesting the existence of a M6P-receptor-independent transport to the lysosomes (Ginsel and Fransen, 1991; Glickman and Kornfeld, 1993). In addition, mice lacking M6P receptors have provided further evidence for alternative M6P-receptor-independent trafficking of newly synthesized enzymes to lysosomes (Dittmer et al., 1999; Kasper et al., 1996; Ludwig et al., 1994).

In particular, the acid β-glucocosidase (GCase), the lysosomal enzyme responsible for the degradation of glucosylceramide in glucose and ceramide, is transported to the lysosomes in a M6P independent manner through its interaction with the lysosomal integral membrane protein 2 (LIMP-2) (Reczek et al., 2007).

1.4 GCase protein

Acid β-glucosidase (GCase) is synthesized on polyribosomes as a naked 55 kDa polypeptide of 497 amino acids. Like other lysosomal hydrolases, normal GCase is synthesized with a secretory signal sequence at the amino terminal of the nascent polypeptide. This sequence is proteolytically removed when the enzyme is translocated into the ER. There, GCase is modified by the addition of high mannose oligosaccharides chains on four of the five potential N-glycosilation sites (Asn 19, Asn 59, Asn 146 and Asn 270; Asn 462 residue is not occupied) (Berg-Fussman et al., 1993), generating a 63 kDa precursor which is then processed to an intermediate form of 66 kDa and then to a mature form of 59 kDa. It has been shown that glycosylation of Asn 19 is essential for the catalytic activity and the deglycosylated enzyme is more susceptible to proteolysis (Grace and Grabowski, 1990).

The oligosaccharide chains are remodelled as the protein is transported from *cis* and *trans* Golgi into lysosomes. However, unlike other soluble lysosomal hydrolases, the GCase becomes membrane associated and does not contain M6P for targeting to lysosomes.

The X-ray structure of GCase has been defined facilitating the structural analysis (Dvir et al., 2003). GCase comprises three non-contiguous domains. It has a characteristic $(\beta/\alpha)_8$ (TIM) barrel containing the catalytic residues, designated as domain III, and two closely associated β-sheets, resembling an immunoglobulin architecture, designed as domain II. In addition, it possesses an unusual structure containing one major β-stranded antiparallel β-sheet that is flanked by a perpendicular N-terminal β-strand and loop, designated as domain I. Domain I tightly interacts with domain III, while the other interactions do not seem to be significant in the crystal structure (**Figure 1.2**)

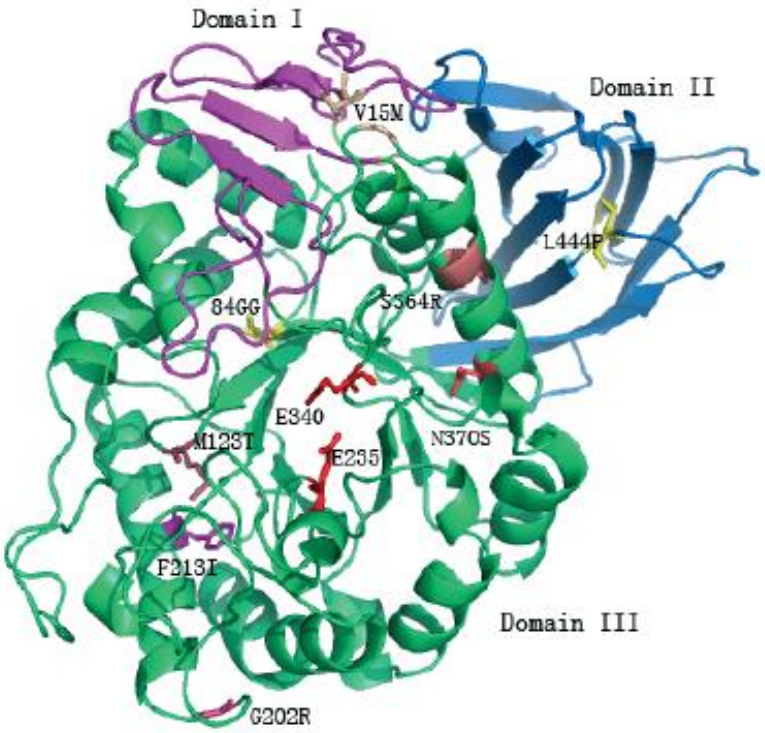

Figure 1.2 Ribbon diagram representation showing the location of some GD-associated point mutations (from Yu et. al., 2007).

The natural substrates of GCase are a mixture of N-acyl-sphingosyl-1-O-b-D-glucosides, glucosylceramides (GlcCer), members of a very heterogeneous group of lipids termed glycosphingolipids (GSL), characterized by a ceramide backbone linked to a single sugar head group, which in the case of GlcCer is glucose (**Fig. 1.3**). The ceramide component consists of a long-chain amino alcohol, sphingosine, in amide linkage to a fatty acid. Ceramide structures vary in length, hydroxylation, and

saturation of both the sphingosine and fatty acid moieties, resulting in lipid structural diversity. GCase is specific for D-glucose since L-glucosyl derivatives are not hydrolyzed by this enzyme (Sarmientos, et al., 1985).

Glucosylsphingosine (**Fig. 1.3**), the deacylated analog of glucosylceramide, is a minor substrate for the GCase.

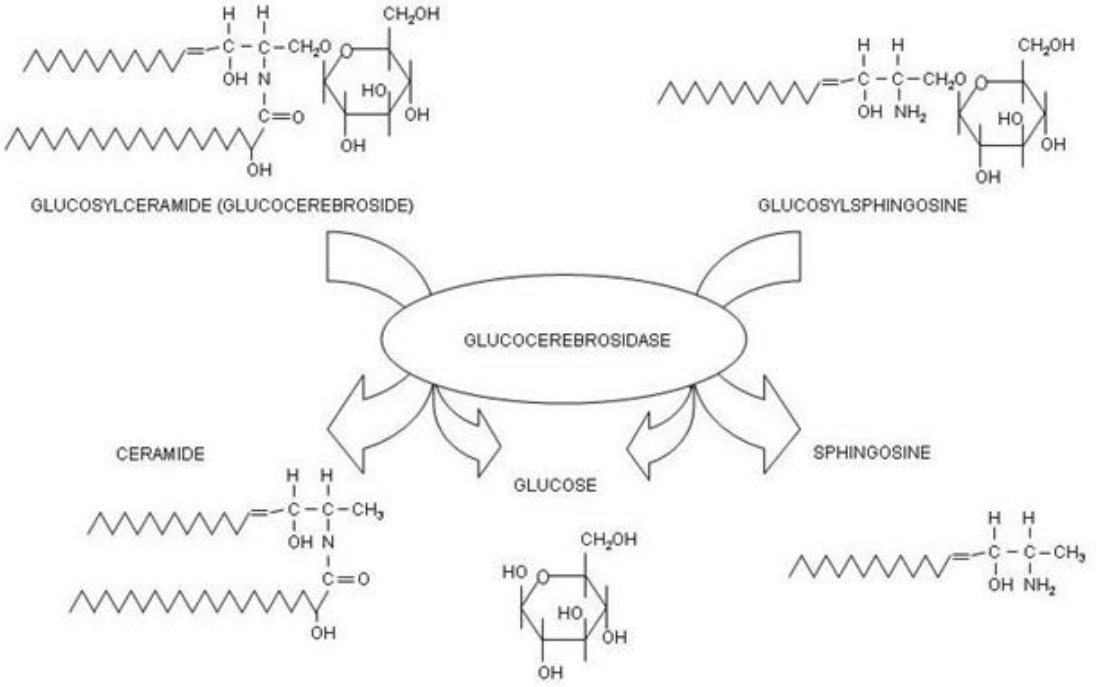

Figure 1.3 Glucocerebrosidase substrates.

1.5 β-glucosidase gene

The β-glucosidase gene, *GBA* (GenBank accession no. J03059.1), is located on chromosome 1q21 and contains 11 exons spread out in approximately 7.5 kb of genomic sequence. A highly homologous 5.7 kb pseudogene, *psGBA* (GenBank accession no. J03060.1) is located 16 kb downstream from the active gene (Horowitz et al., 1989).

The *psGBA* spans 5.7 kb with the same exon and intron number and the same structure as the functional gene, which is longer than the pseudogene because of several *Alu* insertions in intronic tracts. Despite of the length differences, *psGBA* has

maintained 96% sequence identity with the functional *GBA* gene. One important distinction between the two sequences is a 55-bp deletion in exon 9 of the pseudogene (Reiner, et al., 1988).

The 5' genomic region of *GBA* contains two TATA box and two CAAT-like box consensus sequences (Reiner and Horowitz, 1988). The expression of *GBA* is regulated by many transcription factors, such as OCT, AP-1 and CBP (Moran et al., 1997). When compared to the corresponding 5' sequence of *psGBA*, this region of the functional gene is 8- to 10-fold more potent in driving reporter gene expression (Reiner et al., 1988).

The *GBA* cDNA is approximately 2 kb in length. Northern blot analysis of the *GBA* mRNA in different cells showed the expression of several transcripts, which are generated from alternative splicing, alternative polyadenylation sites, or pseudogene transcription (Graves et al., 1988; Reiner et al., 1988). The GBA mRNA has two in-frame ATG translational start sites located in exons 1 and 2 (Sorge et al., 1985). Both start sites are efficiently used, producing two polypeptides with different sized signal peptides: the protein synthesized from the first ATG has a 39-residue leader, while the second ATG yields a 19-residue leader; both are processed to the same 497-residue mature enzyme (Pasmanik-Chor et al., 1996; Sorge et al., 1987). The levels of *GBA* mRNA are variable in different cell lines and the enzyme activity is not strictly related to transcription levels, suggesting that different post-transcriptional modifications are involved in the regulation of enzymatic activity.

1.6 Gaucher disease

Gaucher disease (GD) is the most frequent LSD, caused by the autosomal recessive deficiency of GCase due to *GBA* mutations. Since GCase hydrolyzes the β-glucosidic bond between glucose and ceramide of the glucosylceramide (GlcCer), the enzyme dysfunction leads to the accumulation of this glycolipid and other sphingolipids within the lysosomes.

The storage occurs predominantly in cells of the monocyte-macrophage lineage, but an increase in GlcCer concentration is detectable in most tissues (Beutler and Grabowski, 2001).

GD is a panethnic disorder but presents a higher prevalence among Ashkenazi Jews with a carrier frequency of 1:17 and expected birth frequency of 1:850. The estimated global frequency of Gaucher disease is 1:40,000 to 1:60,000 (Morris 2012).

To date, more than 300 mutation, including single base changes, insertions, partial and total deletions, splicing mutations and gene-pseudogene rearrangements, have been described in GD patients. (Hruska et al., 2008).

GCase operates in the presence of Saposin C (Sap C), which is required for the degradation of GlcCer in the lysosomal compartment (Ho et al., 1971). It is an essential activator of GCase and protects it from proteolitic degradation inside the cell (Sun et al., 2003).

A deficiency of Sap C is an extremely rare disease that causes a Gaucher-like disorder. However, unlike Gaucher patients, subjects affected by Sap C deficiency present normal GCase activity *in vitro*. Six patients with Sap C deficiency due to mutations in the PSAP gene have been reported in the literature to date, all of whom had symptoms resembling GD (Kuchar et al., 2009, Christomanou et al., 1986; Christomanou et al., 1989; Tylki-Szymanska et al., 2007; Tylki-Szymanska et al., 2011).

1.6.1 Clinical features

In all GD patients, the accumulation of GlcCer and other sphingolipids in the lysosomes, cause the enlargement of cells, in particular those of mononuclear phagocyte origin. Lysosomes within macrophages become engulfed of storage material giving rise to the so called “Gaucher cells” which, at light microscope, show the characteristic appearance of “wrinkled” cytoplasm with a displaced nucleus (**Figure 1.4**). The presence of “Gaucher cells” in bone marrow aspirates is a hallmark of GD and leads to a chronic dysfunction of blood cell production, causing fatigue, frequent hemorrhagic events and increase the risk of developing monoclonal gammopathies.

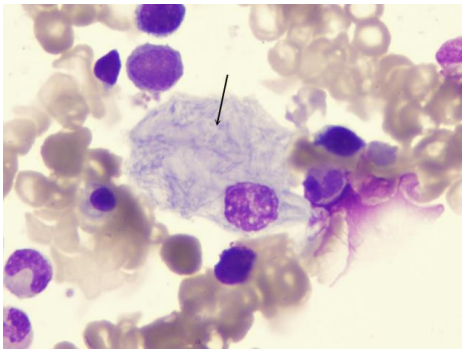

Figure 1.4 "Gaucher cell" from bone marrow aspirate of a patient with Gaucher Disease. It presents a typical wrinkled cytoplasm and an eccentrically located nucleus.

Splenomegaly and hepatomegaly are present in the majority of GD patients. Although GD presents as a continuum of disease states (**Figure 1.5**) ranging from milder forms, displaying only peripheral symptoms, to the most severe forms with early neurological onset, the disease has been classically classified in three major clinical variants based on the absence (type 1 non-neuronopathic GD) or presence of primary central nervous system involvement (type 2, acute neuronopathic and type 3, subacute neuronopathic GD) (Grabowski, 2008).

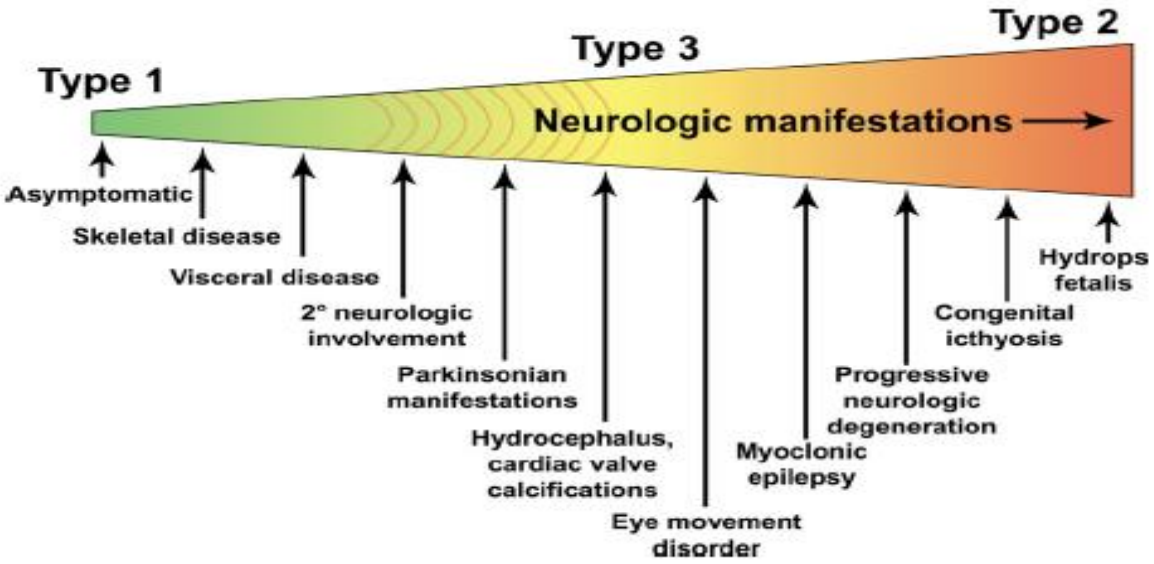

Fugure 1.5 Gaucher disease presents with a wide spectrum of phenotypes with the primary distinction being the presence or absence of neurologic manifestations. There is a ''grey zone,'' indicated by curved lines, where it is not clear if the neuropathology is the result of the enzyme deficiency or of a secondary cause (from Sidransky 2004).

Type 1 GD: the non neuronopathic form is the most prevalent (95% of cases). The age at onset and the phenotypic expression of the disease are extremely variable, generally the younger the age at presentation the more severe the clinical course. Type 1 GD is characterized by enlargement and dysfunction of liver and spleen and displacement of normal bone marrow by storage cells. Anemia and thrombocytopenia are common presenting findings. Type 1 GD, often develops a severe skeletal involvement, in that case, the infiltration of Gaucher cells causes the alteration of cortical region of bones causing osteoporosis and osteopenia with frequent spontaneous fractures (Zimran 2010). Although type 1 GD is considered a nonneuropathic form, there is increasing evidence that neurological involvement (i.e. Parkinson syndrome, seizures, oligophrenia, perceptive deafness) can also occur (Bembi et al., 2003).

In particular, an association between GD1 and Parkinson disease (PD) has been extensively reported. The first evidence of this association was published by Neudorfer et al in 1996, who reported a series of six GD 1 patients who developed PD. These findings were then confirmed in larger cohorts of GD patients, leading to the conclusion that the incidence of PD among GD patients is higher than in the general population (Halperin et al., 2006; Gan-Or et al., 2008; Neumann et al., 2009; Bultron et al., 2010; Lesage et al., 2011; Moraitou et al., 2012).

In addition, it has been found that PD occurs at an increased frequency in the relatives of GD patients who are carriers of *GBA* mutations (Goker-Alpan et al., 2004). In fact, being a carrier of a *GBA* mutation is considered to be the most common genetic risk factor for PD and related synucleinopathies, such as dementia with Lewy Bodies (DLB).

Although the exact mechanism linking mutant GCase with α-synuclein (α-syn) neuropathology is not known, results from many studies suggest that a loss of GCase enzymatic function as well as a toxic gain function of mutated GCase might be implicated in the accumulation of α-syn (Sardi et al., 2011; Xu et al., 2011; Mazzulli et al., 2011).

Type 2 GD: (acute) neuronopathic GD is a rare phenotype (1% of cases) associated with a neurodegenerative course leading to a rapid deterioration and death at a very early age, ranging from birth to the second year of life. It is associated with

homozygosity or compound heterozygosity for severe and/or null mutations. It is characterized by hypertrophic posturing, strabismus, trismus and retroflexion of the head shortly after birth. Massive hepatosplenomegaly and lung involvement are common (Zimran 2010).

Type 3 GD: is the most heterogeneous and attenuated neuronopathic form (2%-3% of cases) characterized by central nervous system involvement ranging from eye movement abnormalities (oculomotor apraxia and/or strabismus) to progressive mental deterioration and onset of myoclonic epilepsy. Visceral involvement is similar to type 1 GD. The age of onset is highly variable, the first symptoms are usually the results of visceral involvement, with neurologic findings developing in about one-half of the children during the first decade of life.

1.6.2 Diagnosis

The diagnosis of GD is based on clinical symptoms and confirmed first by the demonstration of reduced GCase activity in peripheral blood cells or skin fibroblasts compared to normal controls. The enzymatic diagnosis is then confirmed by the molecular analysis of *GBA* gene that also provides information regarding genotype-phenotype correlation and prognosis evaluation. In addition, molecular analysis allows the identification of carriers within the families and it is an important tool for prenatal diagnosis.

The plasma chitotriosidase activity is elevated in affected subjects, because macrophages are chronically activated (Hollak et al., 1994). In fact, plasma chitotriosidase activity has been used not only as a marker of the disease, but also to evaluate the response upon treatment. However, before evaluating this marker, it is necessary to exclude the presence of the 24 nucleotide duplication, a polymorphic variant which inactivates the enzyme (Boot et al., 1998).

1.6.3 Cellular pathology

GlcCer is a constituent of biological membranes and a key intermediate in the biosynthetic and degradative pathways of complex glicosphingolipids (GSLs). Therefore its accumulation in GD has severe pathological consequences. However, the molecular mechanism linking GlcCer accumulation to cellular damage in GD has not been fully elucidated.

In addition, the primary storage of GlcCer leads to secondary alterations of sphingolipids that have been reported to affect gangliosides in various tissues (Gornati et al, 2002; Boomkamp et al, 2008) and sphingomyelin in cell models of GD (Bodennec et al, 2002). Secondary storage of these substrates may also contribute to the celular pathology. However, the molecular mechanism linking GSL accumulation to cellular damage in GD has not been fully elucidated.

Although GlcCer levels are elevated, they are not enough to account for change in tissue mass and/or tissue pathology. Indeed, whereas the size of the spleen increases up to 25-fold in GD patients, GlcCer accounts for <2% of the additional tissue mass (Cox, 2001), suggesting that other biochemical pathways must be activated in GD and contribute to changes in tissue mass and to the development of pathology.

Macrophages

The macrophage origin of “Gaucher cells” has been demonstrated in many studies (Boven, et al., 2004; Pennelli, et al., 1969). All cells of the mononuclear phagocyte system, and especially tissue macrophages of the liver (Kupffer cells), bone (osteoclasts), the central nervous system (microglia, cerebrospinal fluid macrophages), lungs (alveolar macrophages), spleen, lymph nodes, bone marrow, and others can be affected in GD.

It has been demonstrated, that some pathological features in GD are caused not just by the burden of GlcCer storage, but by macrophage activation. The serum levels of many cytokines, such as IL-1β, IL-6 and TNFα are elevated in GD patients (Barak, et al., 1999). These changes might explain some of the pathological features, since they may contribute to osteopenia, activation of coagulation, hypermetabolism and hematological malignancies. However, on macrophages themselves, expression of pro-inflammatory mediators is not always apparent, although markers characteristic of

alternatively activated macrophages are found (Boven, et al., 2004). Finally, as mentioned above chitotriosidase produced by activated macrophages, is markedly elevated and commonly used to examine GD severity and improvement upon treatment (Hollak, et al., 1994).

Neurons

The acute neuronopathic form of GD (GD2) is characterized by severe neuronal loss (Sidransky et al., 1996) and by astrogliosis (Wong et al., 2004). A pathway involved in the pathology of a number of LSDs is altered calcium homeostasis (Ginzburg et al., 2004). Indeed, enhanced agonist-induced calcium release via the ryanodine receptor (RyaR) has been detected in both cellular models (Korkotian, et al., 1999) and in human brain tissue (Pelled, et al., 2000). In particular, upon incubation of neurons with conduritol B-epoxide, a specific GCase inhibitor (Legler and Bieberich, 1988), enhanced Ca^{2+} release was detected from intracellular stores in response to caffeine, an agonist of the RyaR, which resulted in increased sensitivity to neurotoxic agents, especially glutamate. This effect could be reversed either by inhibition of sphingolipids synthesis or by the addition of GCase. These mechanisms could be relevant in particular in brain areas with a significant glutaminergic input, such as hippocampal layers CA2 to CA4, which are subjected to neurodegeneration and gliosis in GD (Wong, et al., 2004).

Another major cellular pathway, the phospholipids metabolism, is altered in a neuronal model of GD (Bodennec, et al., 2002). Upon GlcCer accumulation, axonal growth is stimulated in a genetic model of GD and neuronal synthesis of phosphatidylcholine (PC), the major structural lipid of eukaryotic cells, is increased as a result of activation of phosphocholine cytidylyltransferase. PC synthesis might account, at least partly, for increased rates of cell growth.

1.6.4 Therapy

The goal of all treatment strategies for GD is to reduce the GlcCer storage, thus diminishing the deleterious direct or indirect effects caused by its accumulation.

Currently two different treatment modalities have been approved for GD: enzyme replacement therapy (ERT) and substrate reduction therapy (SRT).

ERT consists in the correction of the metabolic defect in patients with GD by the infusion of a purified or a recombinant human GCase enzyme (Bembi et al., 1994; Grabowski et al., 1995). The rationale of ERT for treatment LSDs is based on the observation that most cell types released small amounts of lysosomal enzymes and that these secreted forms could be internalized via M6PR present on the cell surface. In 1991, ERT for GD was approved by the Food and Drug Administration (FDA). The first commercially available formulation was aglucerase, a placental-derived enzyme. Until recently, two recombinant enzymes were available: the imiglucerase (Cerezyme®, Genzyme Corporation) produced in CHO cells, and Velaglucerase alfa (VPRIV™, Shire HGT), produced by Gene-Activation technology in a human cell line (Brumshtein et al., 2010). Recently, taliglucerase alfa, a plant-cell derived enzyme has been developed (Haddley et al., 2011).

ERT with the human recombinant form of GCase demonstrated to be effective in the treatment of type 1 GD (Grabowski et al 1998). However, due to its high molecular weight the enzyme does not cross the blood brain barrier, therefore patients with neurological features only benefit from the effect of ERT on visceral, haematological and skeletal features.

Substrate reduction therapy (SRT) is based on the use of the orally derived, glucose analogue iminosugar, N-butyl-deoxynojirimycin (NB-DNJ, Miglustat; Zavesca™, Actelion Pharmaceuticals Ltd). Miglustat is a reversible inhibitor of ceramide-specific glucosyltransferase, the first enzyme in the synthetic pathway of GlcCer. The inhibition of this enzyme leads to a reduction of the GlcCer biosynthesis. An important advantage of this therapeutic agent is its ability to cross the blood brain barrier. Therefore, it may impact the neuronopathic disease features. However, Miglustat is currently approved only for the treatment of type 1 GD and its possible effect on theneuronopathic forms of the disease is still controversial. (Schiffmann et al., 2008; Kraoua et al., 2011).

1.6.5 GBA mutations and genotype-phenotype correlation

To date, more than 300 GBA mutations have been identified in patients with GD distributed throughout the whole gene. These include all kinds of defects such as single base changes, splicing alterations, insertions, partial and total deletions, gene-pseudogene rearrangements (Stenson, et al., 2003) (**Figure 1.6**).

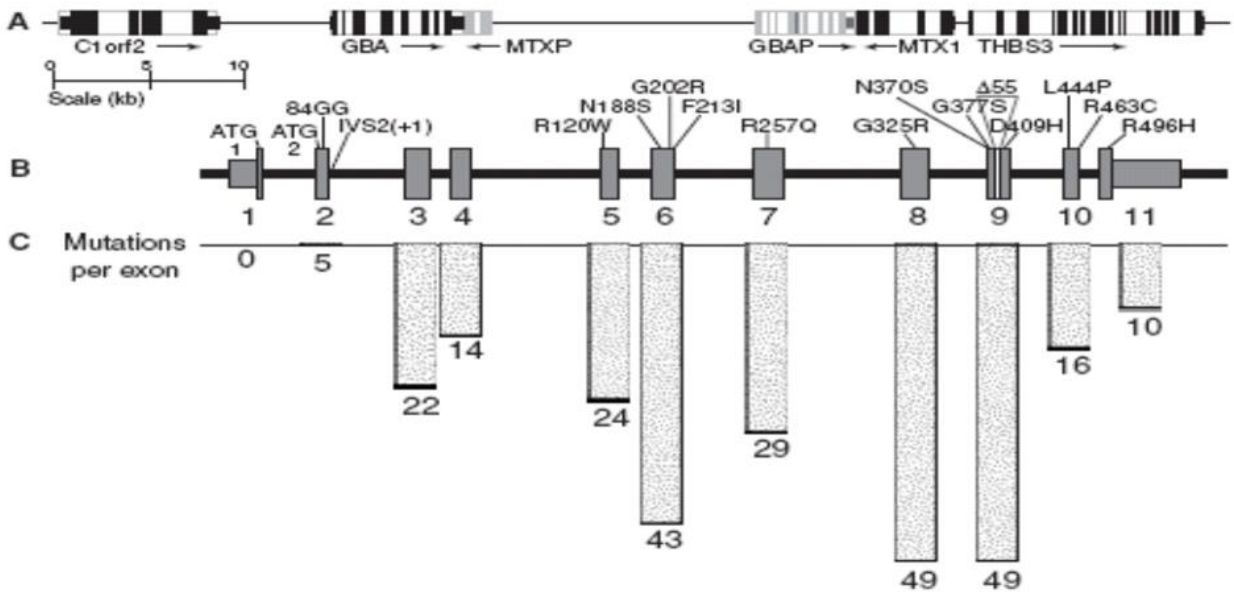

Figure 1.6 *GBA* structure and mutation distribution. **(A)** The 62-kb region surrounding the *GBA* along chromosome 1q showing the known genes and pseudogenes and their transcription direction. C1orf2, chromosome 1 open reading frame 2 (cote1); GBA, glucocerebrosidase; MTXP, metaxin1pseudogene; GBAP, glucocerebrosidase pseudogene; MTX1, metaxin1;THBS3, thrombospondin 3. **(B)** The exonic structure ofGBA, with the twoATGs and positions of15 commonmutations indicated. **(C)** Number of reported substitution, deletion, insertion, and splice-sitemutations per exon (from Hruska et al., 2008).

Recent studies, aimed to investigate *in vitro* the effect of mutant alleles on GCase synthesis, trafficking and function, demonstrated that many mutant proteins do not reach the lysosomes. In fact, many missense mutations lead to the synthesis of unfolded proteins, which are recognized by the cellular “quality control” system and retained in the ER where they become associate with the molecular chaperones (e.g. calnexin, Bip, etc) and eventually undergo rapid degradation by Endoplasmic Reticulum Associated Degradation (ERAD) via ubiquitin-proteosome system (Schmitz et al., 2005; Ron and Horowitz, 2005).

Numerous attempts have been done to explain the wide phenotype variability among GD patients since individuals with the same genotype, affected siblings and even monozygous twins can exhibit marked differences in disease severity and clinical outcomes.

Although, the expectations for a consistently close correlation between the mutant genotype and variant phenotype have been mostly disappointing some general conclusions can be drawn regarding the neuroprotective nature of the N370S mutation and the association of the L444P allele with the neuronopathic phenotype.

Indeed, the most common *GBA* mutation N370S, is associated with the non-neuronopathic GD (type 1) even in compound heterozygotes (Tsuji, et al., 1988). Patients who are homozygous for N370S tend to present a later onset of the disease than heterozygous individuals who carry the N370S mutation in combination with a different mutant allele. Furthermore, frequency studies in population with an high prevalence of GD reported that only 30% of Ashkenazy Jewish people who are homozygous for N370S mutation develop sufficient pathology to reach medical attention (Beutler et al., 1993; Grabowski and Horowitz, 1997), indicating that most of them have a normal or close normal phenotype.

The N370S mutation results from an A>G transition at position 1226 of the cDNA (c.1226A>G) that causes the substitution of an asparagine residue with a serine at position 370 at the interface between domains II and III of mature protein. The N370S mutation affects both the conformational stability and the catalytic activity of mutated protein. Mechanistic analyses of the catalytic cycle revealed that N370S substitution alters the enzymatic kinetics, even though this residue is located far from the active site (Dvir, et al., 2003). Further studies demonstrated that poor contact between N370S GCase and its activator Sap C contributes to reduce the residual enzymatic activity (Salvioli, et al., 2005). In addition, localization studies showed that N370S GCase distribution within the cells looks similar to that of WT GCase, being predominantly lysosomal. However, fibroblasts carrying N370S mutation express lower amount of total GCase protein probably as a consequence of a greater extent of ERAD (Schmitz et al., 2005; Sawkar et al., 2006).

A large number of mutations originate from recombination events between gene and pseudogene. Among them, the most common alteration is the second most frequent mutation in GD patients: the T to C transition at position 1448 of the cDNA

(c.1448T>C), leads to the substitution of a leucine residue with a proline in the 444 position of the mature polypeptide (L444P). Alleles containing the L444P substitution are strongly, although not exclusively, associated with neuronopathic GD. In type 2 GD the L444P allele is often found in association with a “complex allele” (an allele containing more than one *GBA* mutation) or it is itself within a complex allele. Moreover, homozygous L444P mutation is strongly associated with the type 3 GD (Tsuji, et al., 1987), even if the analysis of a series of 35 L444P/L444P patients demonstrated significant phenotypic variability among them (Goker-Alpan, et al., 2005).

L444P mutation is located in the Ig-like domain of GCase. Thus, this substitution does not directly affect the GCase catalytic site but destabilize the enzyme native conformation, thereby rendering the protein more susceptible to mistrafficking and degradation. As a consequence, in patient-derived fibroblast the L444P protein is largely degraded with a small fraction making it to the lysosome (Schmitz et al., 2005; Sawkar et al., 2006).

Data from the International Gaucher Registry have shown that while 72% of 122 GD3 patients included in the registry carry the p.L444P/p.L444P genotype, only one out of 16 GD3 patients with progressive myoclonic epilepsy (PME) present this genotype. These data suggest that the most frequent genotype found in GD3 patients would be underrepresented among GD3 patients with PME. In contrast, some rare mutants were encountered among GD3 patients with PME. In particular three point mutations seem to be associated with this phenotype, the V394L, N188S and G377S, suggesting that GD3 patients carrying one of these mutations in the absence of the N370S mutation should be carefully evaluated for PME (Park et al., 2003).

As mentioned above, besides these relatively common genotypes, no good correlation have been found between most GD genotypes and the clinical presentation and progression of the disease. Indeed, the wide phenotypic variability in GD, suggests that other factor might contribute to determine the disease severity (**Figure 1.7**).

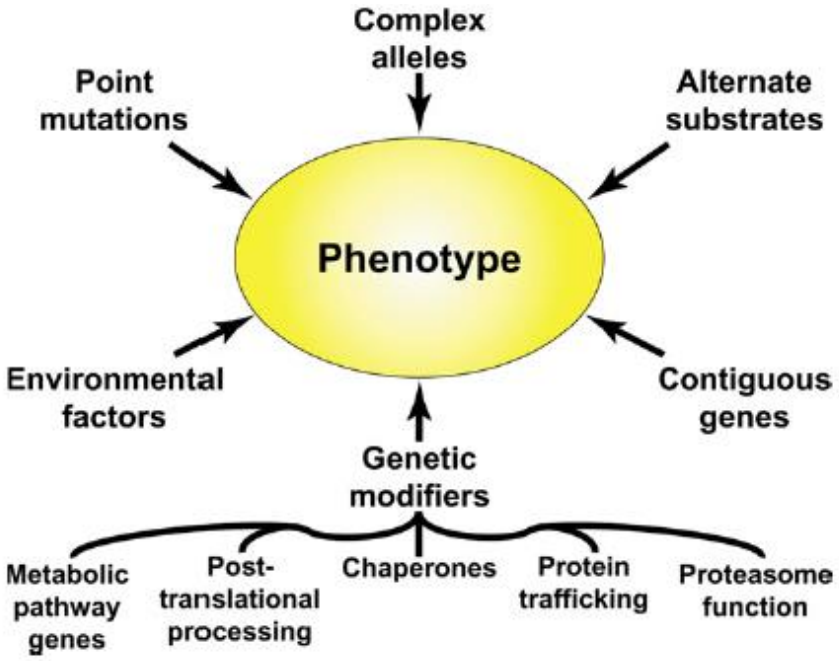

Figure 1.7 Multiple factors contribute to the phenotypes encountered in patients with Gaucher disease. These include several types of possible genetic modifiers (from Sidransky 2004).

1.7 LIMP-2 as modifier in GD

Understanding the genotype-phenotype correlation is one of the major challenge in the study of GD and patients with atypical presentations continue to be recognized.

In particular, a rare subgroup of patients with type 3 GD develop progressive myoclonic epilepsy. Even though some mutations have been associated to this particular phenotype (N188S, V394L, F213I, G202R, and G377S) (Kowarz et al., 2005; Park et al., 2003) these patients lack a common genotype. In addition, individuals sharing the same genotype may or may not develop myoclonic epilepsy, suggesting that other genes may modify the clinical presentation. Since it has been demonstrated that GCase protein is targeted to the lysosomal compartment by a M6P independent interaction with the lysosomal membrane receptor LIMP-2 (Reczek et al., 2007), it has recently been proposed that LIMP-2, may be a modifier in GD.

In fact, the analysis of SCARB2 in two siblings with GD, discordant for myoclonic seizure, showed the presence of a missense mutation [c.1412A>C (p.E471G)] only in the sibling affected by myoclonic epilepsy, suggesting that that mutations in SCARB2

might explain the rare cases of GD manifesting with myoclonic epilepsy (Velayati et al., 2011).

1.8 LIMP-2-GCase interaction

LIMP-2 is a type III transmembrane protein of 478 residues (Fujita et al., 1991) which comprise four domains: one cytoplasmic domain of 20 amino acids, two transmembrane domains and one lumenal domain of about 400 amino acid, required for physical association with GCase. Based on homology, LIMP-2 has been defined as a member of the CD36 family of scavenger receptor proteins (Febbraio et al., 2001; Krieger, 2001).

Recent studies have demonstrated that the LIMP-2 dependent sorting of GCase is pH dependent. The neutral pH of ER allows GCase to associate with LIMP-2, whereas the acidic pH of endosomal/lysosomal compartments leads to their dissociation. The region of LIMP-2 responsible for the interaction with GCase includes the luminal coiled-coil domain (Blanz et al., 2009) and a histidine within this region has been suggested as pH sensor which regulates the dissociation of the receptor-ligand complex in late endosomal/lysosomal compartment (Zachos et al., 2012) (**Figure 1.8**). Recently the crystal structure of LIMP-2 has been described and the residues 150-167 have been shown to be involved in LIMP-2-GCase interaction (Neculai et al., 2013).

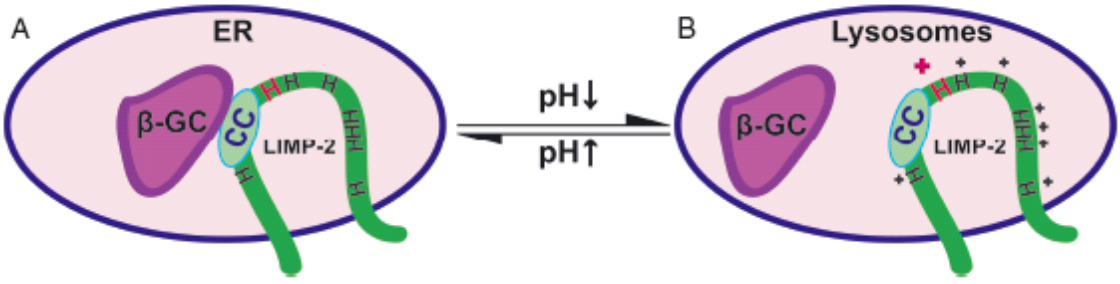

Figure 1.8 Model for pH-sensitive binding of LIMP-2 and GCase. LIMP-2 binds GCase at neutral pH in the ER (A), which involves a proposed coiled-coil domain. After progression of the receptor–ligand complex to prelysosmal compartments the histidine residue 171, which is located adjacent to the coiled-coil of LIMP-2, becomes protonated and positively charged (B). This leads finally to a dissociation of LIMP-2 and GCase (from Zachos et al., 2012).

Furthermore It has been reported an important role of two phosphatidylinositol 4-kinases (PI4Ks) in the proper trafficking of LIMP-2/GCase complex to the endosomal/lysosomal compartment. In particular, the catalytic activity of PI4IIIβ is important in the proper LIMP-2 sorting at the level of the Golgi and PI4IIα plays a key role in the trafficking step between the late endosomes and lysosomes (Jović et al., 2012) (**Figure 1.9**). Furthermore a depletion of PI4IIα leads to missorting of GCase away from the lysosomes, resulting in GCase secretion as previously shown in MEF and machrophages of LIMP-2 knock out mouse (Reczek et al., 2007).

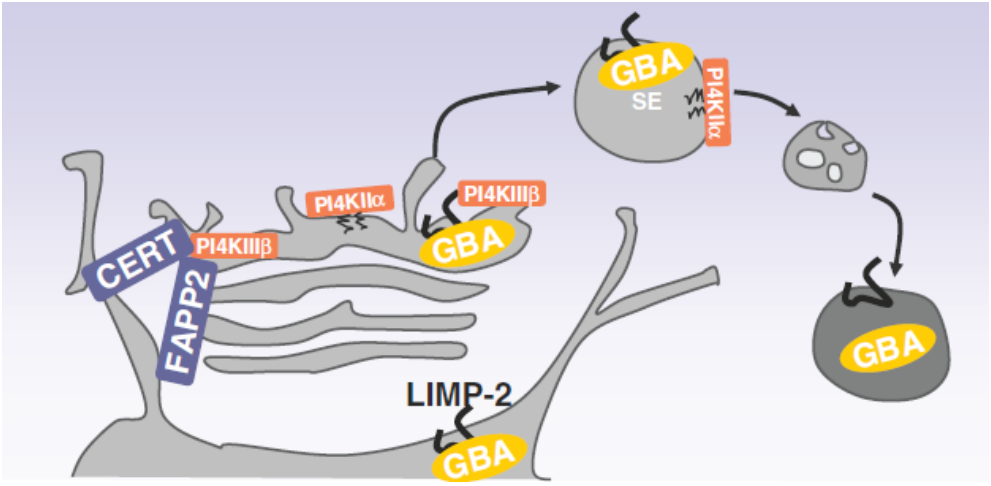

Figure 1.9 Model of PI4Ks regulation of LIMP-2-mediated GCase transport. Binding of GCase to LIMP-2 in the ER lumen results in trafficking of this complex to the Golgi. Efficient exit out of this compartment then depends on the catalytic activity of PI4KIIIβ. Once the GBA/LIMP-2 complex leaves the Golgi, PI4KIIα regulates its efficient transport from sorting endosome/late andosomes to lysosomes, such that depletion of PI4KIIα leads to missorting of GBA away from lysosomes, resulting in GBA secretion.

1.9 Deficit of LIMP-2 in human: Action myoclonus-renal failure (AMRF) syndrome

Action myoclonus-renal failure syndrome (AMRF, MIM# 254900) is an autosomal recessive disorder characterized by progressive myoclonus epilepsy (PME) associated with renal failure. The responsible gene was found studying 3 unrelated affected individuals and their relatives. Homozygosity mapping with single-nucleotide polymorphism (SNP) chips was used to localize AMRF to chromosome 4q13-q21. Using microarray expression analysis, *SCARB2* gene was identified as a likely site of

mutations causing AMRF within the critical region. Mutations in SCARB2 were found in all 3 families used for mapping and subsequently confirmed in 2 other unrelated AMRF families. The mutations were associated with lack of the protein codified by *SCARB2*: LIMP-2 (Berkovic et al., 2008).

Up to date only few mutations in *SCARB2* gene have been described responsible that for the AMRF (**Table 1.1**).

Table 1.1 AMRF-causing mutation.

Genomic location	Site of nucleotide substitution	Predicted effect on protein	References
Exon 1	c.111delC	Deletion and frameshift	Hopfner et al., 2011
Exon 2	c.296 delA	N99IfsX34	Berkovic et al., 2008
Exon 3	c.361C>T	R121X	Fu et al., 2013
Intron 3	c.424-2 A>C	Splice site change	Dibbens et al., 2009
Exon 4	c.435-436 insAG	W146fsX16	Berkovic et al., 2008
Exon 4	c.533 G>A	W178X	Balreira et al., 2008
Intron 5	c.704+5 G>A	Splice site	Berkovic etal., 2008
Exon 5	c.666 delCCTTA	Y222X	Dibbens et al., 2009; Hopfner et al., 2011
Intron 5	c.704+1 G>C	Splice site change	Dibbens et al., 2009
Intron 5	c.704+1 G>A	Splice site change	Perandones et al., 2012
Exon 7	c.862 C>T	Q288X	Berkovic et al., 2008
Exon 8	c.1087 C>A	H363N	Dardis et al., 2009; Dibbens et al., 2009
Intron 8	c.1116-2 A>C	Splice site change	Dibbens et al., 2009
Exon 8	c.1015insT	F339FfsX9	Guerrero-Lopez et al., 2012
Intron 9	c.1187+3ins T	Splice site change	Dibbens et al., 2011
Intron 10	c.1239+1 G>T	retention of intron 10, insertion of 20 aa (truncation at 433 aa)	Berkovic et al., 2008
Exon 11	c.1258 delG	E420RfsX5	Dibbens et al., 2009
Exon 11	c.1385_1390delins ATGCATGCACC	p.G462Dfs*34	Higashiyama et al., 2013
Exon 12	c.1412 A>G	E471G	Velayati et al. 2011

Among SCARB2 mutations, only few have been functionally characterized. It has been demonstrated that LIMP-2 mutants Q288X, W146SfsX16, and W178X are retained in the ER and do not reach the lysosome when expressed in COS7 cells.
Of these mutants, only Q288X is able to bind GCase as effectively as wild type, while W146SfsX16 and W178X are unable to bind GCase (Blanz et al., 2010).
A surprising effect on GCase binding was observed in COS7 cells expressing the H363N mutation. Indeed, co-immunoprecipitation experiments showed that the H363N mutant co-precipitated GCase more efficiently than the wild-type LIMP-2. However, in the presence of this mutation, LIMP-2 is retained in the ER. It is likely that the mutation generates a new glycosylation site that contributed to its ER retention and prolonged half-life, leading to increased GCase binding (Blanz et al., 2010).

1.10 The LIMP-2 deficient mouse

Most of the work aimed to characterize the role of LIMP-2 in the trafficking of GCase to lysosomes has been performed in LIMP-2 knockout mice (Reczek et al., 2007). In this model, both GCase activity and protein levels, were severely decreased in different tissues whereas they were increased in serum, clearly demonstrating a mistargeting of GCase. Moreover analysis of fibroblasts and macrophages isolated from these mice indicated that the majority of GCase was secreted.

1.11 Clinical features of AMRF

AMRF syndrome had never been recognized before the advent of dialysis and renal transplantation because of its rapidly fatal course if renal failure is not treated. It was first described in four French Canadian who presented with tremor of the upper limbs and proteinuria at 17–18 years of age. Severe progressive action myoclonus, dysarthria, ataxia, infrequent generalized seizures and renal failure ensued between 19 and 23 years of age. Intelligence remained normal in all four patients (Andermann et al., 1986).
A more complete characterization of this disease was performed in 2004, studying 15 patients with AMRF (Badhwar et al., 2004).

The renal pathology is characterized by focal glomerulosclerosis and sometimes with features of glomerular collapse.

Bilateral fine tremor of fingers and hands is often the first neurological symptom with age of onset from 17 to 26 years. Progression of the disease leads to progressive worsening of the tremor with involvement of head, trunk and sometimes the tongue. In the late stages of the disease, the tremor is replaced by severe multifocal action myoclonus.

Action myoclonus seems to be the most debilitating feature of the disease, with age of onset from 14 to 29 years. Convulsive seizures are also observed. Ataxia and dysarthria are observed as the disease progress. In most cases no cognitive impairment is observed.

Renal features are characterized by proteinuria that occur in all cases and is detected between ages 9 and 30 years and progress to renal failure. There is no visible storage in the kidney (Badhwar et al., 2004).

In most ARMF patients reported until recently, the neurological and renal features developed simultaneously or the renal symptoms appeared first. However, mutations in the SCARB2 gene have been demonstrated in a group of five AMRF patients who developed neurological symptoms before the appearance of the renal symptoms. When neurological symptoms develop first, the renal disease began after 3 to 11 years and always by the age of 30 years (Dardis et al, 2009; Dibbens et al., 2009; Dibbens et al., 2011; Rubboli et al., 2011; Guerrero-Lopez et al., 2012; Higashiyama et al., 2013).

1.12 AMRF and GD phenotype

PME, a main feature of AMRF, may be present in patients affected by several LSD, including GD3.

Since AMRF and GD affect the same metabolic pathway it is not unexpected that they share a common phenotype. However, they present several clinical and biochemical differences, suggesting that an alternative lysosomal targeting pathway may be active in different tissues.

In fact, while in GD patients GCase activity is absent or very low both in fibroblasts and leukocytes, AMRF patients show absent of very low GCase activity in fibroblast (less than 10% of controls) close to the values observed in fibroblasts of GD patients,

but normal or slightly reduced GCase activity in leukocytes, suggesting that even in absence of LIMP-2, at least part of GCase protein is still able to reach the lysosomes in these cells.

In addition, AMRF patients do not show the presence of lipid-laden machrophages in bone marrow, a hallmark of GD. Consistently, AMRF patients do not show elevated activity of chitotriosidase in plasma (Balreira et al. 2008, Dardis et al. 2009; Chaves et al., 2011).

These data suggest that in some tissues, in particular in blood cells, GCase may be transported to the lysosomes by a LIMP-2 independent mechanism.

Currently, no therapies are available for specific treatment of AMRF patients.

The therapeutic approaches currently available for GD (ERT and SRT) have been assessed in a AMRF patient (Chaves et al., 2011). ERT has no beneficial effects neither on PME or on the renal symptoms. Since the enzyme do not cross the Blood Brain Barrier, it is not surprising that it has no effects on the neurological signs. The lack of effects on peripheral symptoms suggests that LIMP-2 would be involved not only in the trafficking of the endogenous GCase to the lysosomes but also in the transport of the recombinant enzyme. However, the role of LIMP-2 in the uptake/transport of recombinant GCase to the lysosomes needs to be elucidated.

SRT seems to improve both PME and renal function. The rationale for the use of SRT in AMRF is based on the hypothesis that these patients, as a consequence of LIMP-2 deficiency, accumulate GSL. However, the nature of the accumulated material in the disease dtarget tissues is not known.

2. Aim of the study

Acid β-glucosidase (GCase) is a lysosomal enzyme defective in most cases of Gaucher disease (GD). GCase, encoded by the *GBA* gene, is synthesized in the endoplasmic reticulum (ER) and transported to the lysosomes in a mannose-6-phosphate independent manner through its interaction with the lysosomal integral membrane protein type 2 (LIMP-2). To date, more than 300 mutations of the *GBA* gene have been reported, most of them lead to the synthesis of misfolded proteins that are retained in the ER and rapidly degradated by ERAD. It has been proposed that mutations in the *SCARB2* gene, encoding LIMP-2, may modify the phenotypic expression of GD. However, the nature of the GCase-LIMP-2 interaction has not been characterized in detail and the impact of *GBA* mutations on this interaction has not been explored.

Recently, mutations in the human gene encoding for LIMP-2 (*SCARB2*) were found to be responsible for action myoclonus-renal failure syndrome (AMRF), a disorder characterized by a mistargeting of GCase. The main feature of AMRF is the presence of progressive myoclonus epilepsy, a frequent sign of patients affected by the chronic neuronophatic form of GD. However, even if AMRF and GD affect the same metabolic pathway and share some neurological features, they present with different clinical and biochemical phenotypes, suggesting that an alternative lysosomal targeting pathway may be active in different tissues.

Therefore the main aims of this study are:

1-To characterize *in vitro* the impact of different GBA mutations on enzymatic activity and binding capacity to LIMP-2.

2- To analyze the role of LIMP-2 in the trafficking of GCase in different human tissues.

3. Results

PART 1: *In vitro* characterization of enzymatic activity and LIMP-2 binding capacity of novel and frequent *GBA* alleles

It hase been demonstrated that GCase is targeted to the lysosomes by a mannose-6-phosphate (M6P) receptor independent mechanism through its interaction with the transmembrane receptor LIMP-2. However, the nature of the GCase-LIMP-2 interaction has not been characterized. Therefore, in the first section of this work, we analyzed *in vitro* the impact of different *GBA* mutations on the association between LIMP-2 and GCase. In addition, we characterized the effect on this interaction of a *SCARB2* mutation found to be associated with myoclonic epilepsy in a family affected by GD.

3.1 Molecular analysis of *GBA* gene in GD patients

Molecular analysis of the complete coding sequence and most intronic regions of *GBA* gene was performed in 8 unrelated patients clinically and biochemically diagnosed at two Italian laboratory reference centers (Udine and Genoa) during the routine molecular testing of GD patients. **Table 3.1** shows the 8 different genotypes and the phenotypes found in this group of patients.

Table 3.1. Phenotype-genotype correlation analysis

GENOTYPE*		PHENOTYPE
Allele 1	Allele 2	
[p.P284T (P245T)]	[p.N409S (N370S)]	1
[p.S405R (S366R)]		
[p.W420C (W381C)]		
[p.W351S (W312S)]	[p.L483P (L444P]	1
[p.N227I (N188I)]	[p.R170C (R131C)]	2
[p.E274K (E235K)]	[p.G241R (G202R)]	2
[p.E365K;p.D419N (E326K;D380N)]	**[p.P198S (P159S)]**	1
[p.N227S;p.G304R (N188S;G265R)]	unknown	3

*Traditional amino acid residue numbering, which excludes the first 39 aminoacids of the leader sequence, is provided in parentheses and designed without the prefix “p.” The novel mutations are indicated in bold.

Overall, 9 novel alleles were identified, among them, 7 alleles carried single point mutations and 2 alleles carried 2 *in cis* mutations on the same allele. In **Table 3.2** are reported the characteristic of the novel alleles.

Table 3.2. Characteristics of the *GBA* gene mutations identified in GD patients analyzed in this study.

Genomic location	Site of nucleotide substitution*	Predicted effect on protein	
		Amino acid change**	Traditional numbering
Exon 6	c.592C>T	p.P198S	P159S
Exon 6	c.680A>T	p.N227I	N188I
Exon 7	c.820G>A	p.E274K	E235K
Exon 7	c.850C>A	p.P284T	P245T
Exon 8	c.1052G>C	p.W351S	W312S
Exon 8	c.1215C>A	p.S405R	S366R
Exon 9	c.1260G>C	p.W420C	W381C
Exon 6 and Exon 7	c.680A>G;c.910G>C	p.N227S;p.G304R	N188S;G265R
Exon 8 and Exon 9	c.1093G>A;c.1255G>A	p.E365K;pD419N	E326K;D380N

* Reference sequence NM_000157.3; ** Reference sequence NP_000148.2

3.2 Functional analysis of novel *GBA* alleles

The impact of missense mutations on GCase activity and LIMP-2 association was evaluated by in vitro expression of constructs carrying the wild type or mutated *GBA* cDNA in Hek293 cells. As a negative control, Hek293 cells were transfected with empty pcDNA3 vector. The activity of proteins bearing the common p.N409S (N370S) and p.L483P (L444P) mutations were also analyzed. No changes in the viability of transfected cells were observed. Transfection of wild type *GBA* cDNA, resulted in a 5 to 6-fold increase of the basal GCase activity detected in Hek293 cells.

The residual activity of the different mutant construct is reported in **Table 3.3** and **Figure 3.1**.

Table 3.3. Novel mutations and residual activity of GBA constructs.

Mutant allele *	Residual activity (nmol/mg/h)
Negative control	131,2 ± 21,8
WT	577,2 ± 112,0
c.592C>T (P159S)	204,7 ± 23,1
c.680A>G (N188S)	244,8 ± 19,7
c.680A>T (N188I)	166,5 ± 4,9
c.820G>A (E235K)	118,0 ± 14,7
c.850C>A (P245T)	129,7 ± 16,6
c.910G>C (G265R)	143,5 ± 16,3
c.680A>G;c.910G>C (N188S;G265R)	137,5 ± 20,5
c.1052G>C (W312S)	126,3 ± 8,5
c.1215C>A (S366R)	134,7 ± 26,0
c.1260G>C (W381C)	84,5 ± 7,8
c.1093G>A (E326K)	360,1 ± 9,9
c.1255G>A (D380N)	45,7 ± 18,6
c.1093G>A;c.1255G>A (E326K;D380N)	48,3 ± 18,9
C.1226A>G (N370S)	360,0 ± 36,8
c.1448T>C (L444P)	171,0 ± 9,9

*The mutations in brackets are reported using the traditional amino acid residue numbering, which excludes the first 39 aminoacids of the leader sequence.

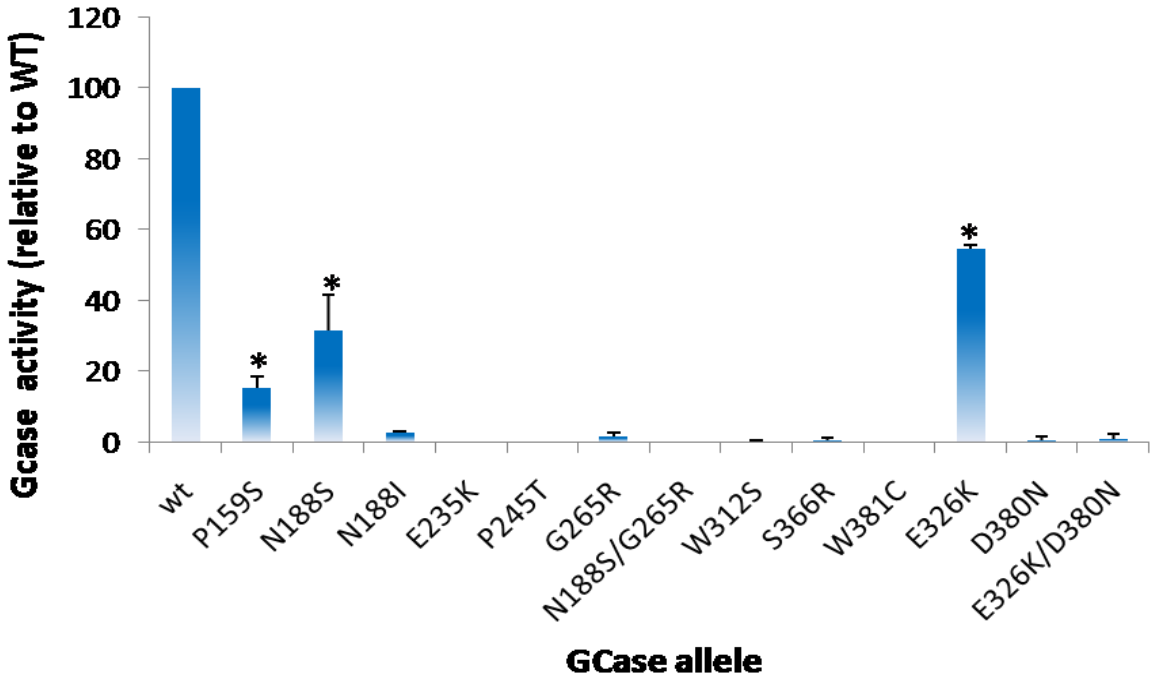

Figure 3.1. Functional analysis of novel missense *GBA* alleles. GCase activity in Hek293 cells transiently transfected with the wild type and mutant constructs was measured using the fluorogenic substrate 4-MU-D-glucopyranoside. Values are expressed as the percentages of wild type enzyme activity, after the subtraction of enzymatic activity of Hek293 cells transfected with the negative control. Data are mean±SD of 3 independent experiments. * $p<0.05$

As shown in **Table 3.3** and **Figure 3.1**, Gcase proteins carrying the changes p.N227I (N188I), p.E274K (E235K), p.P284T (P245T), p.W351S (W312S), p.S405R (S366R) and p.W420C (W381C) presented a very low or absent GCase activity as compared with the wild-type protein, while the p.P198S (P159S) mutant retained a residual activity of 15% of wild type. Both alleles carrying two in cis mutations [p.N227S;p.G304R (N188S;G265R)] and [p.E365K;p.D419N (E326K;D380N)] led to the expression of completely inactive proteins. To further characterize these alleles, each mutation was expressed *in vitro* and analyzed for the enzymatic activity. Although the G265R and D380N mutants expressed no activity, both N188S and E326K mutants retained a residual activity of 25% and 54%, respectively. Our data are in line with previous in vitro studies, which described the N188S as a modifier variant (Montfort et al., 2004) and the E326K as a very mild mutation (Horowitz et al., 2011). However, while the N188S has been found as a single mutation in GD patients, the E326K has always appeared in association with another mutation on the

same allele. As previously reported, mutants N370S and L444P retained a residual activity of 38% and 13% of WT, respectively (Alfonso et al., 2004)

3.3 Analysis of LIMP-2 and novel mutant GCase binding

LIMP-2 has been well defined as the transporter of the GCase to the lysosomes (Reczek et al., 2007). While the region of LIMP-2 responsible for the interaction with GCase has been characterized (Zachos et al., 2012), the regions of GCase protein which may be important for the binding to LIMP-2 are completely unknown.

To further investigate the nature of GCase-LIMP-2 binding, the ability of the respective GCase mutants to directly bind LIMP-2 receptor was evaluated by a co-immunoprecipitation assay performed in Hek293 cells transfected with constructs bearing the wild type or mutated GCase. The panethnic N370S and L444P mutant proteins were analyzed as well. As shown in **Figure 3.2**, all GCase mutants retained at least some LIMP-2 binding capacity.

However, while most GCase mutants co-precipitate with LIMP-2 as efficiently as the wild type GCase, a reduction of the levels of GCase proteins bearing the p.N227I (N188I), [p.N227S (N188S); p.G304R (G265R)] and p.W420C (W381C) mutations was detected in the immunocomplex, suggesting that they impaired the ability of GCase to associate with LIMP-2.

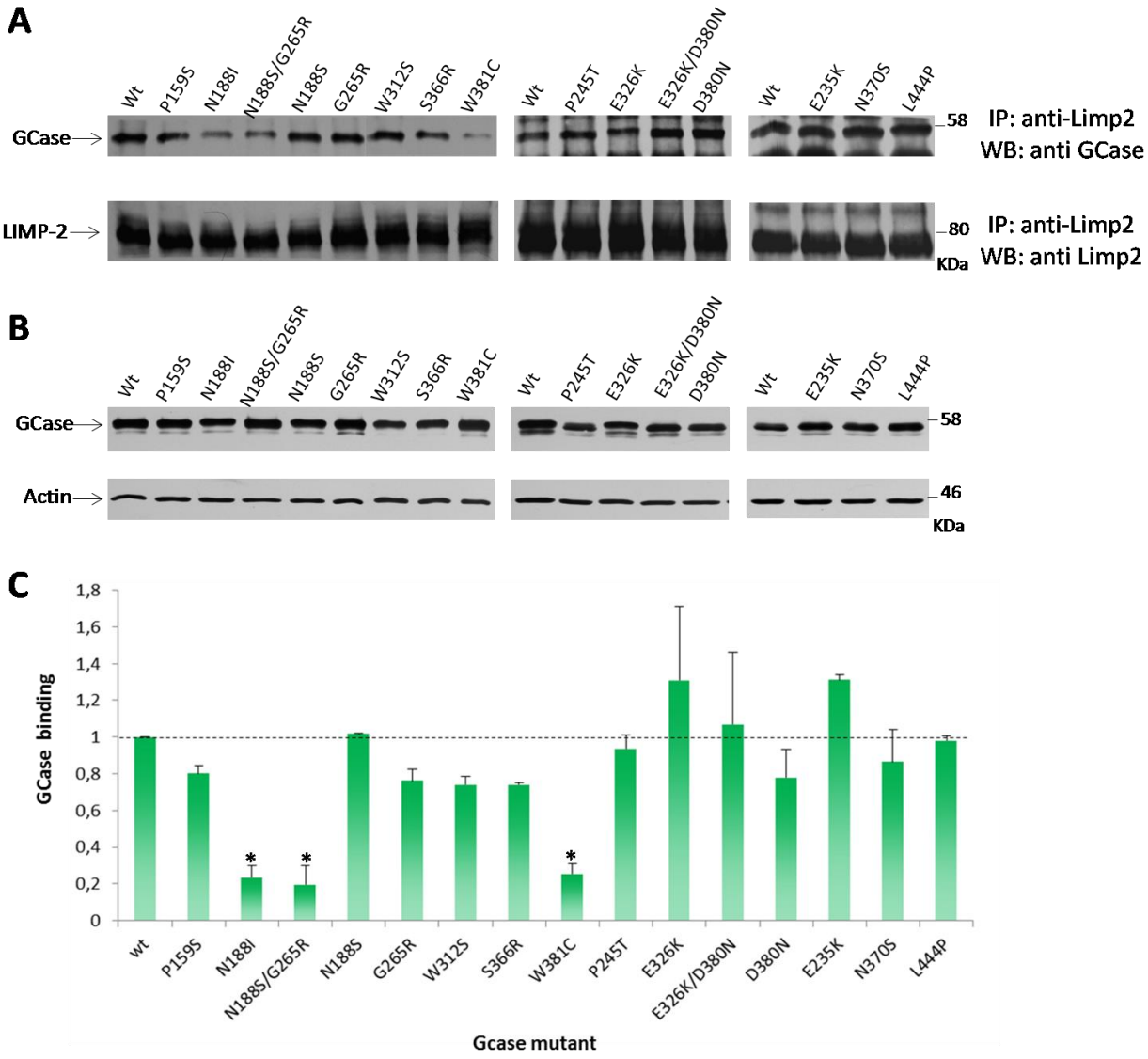

Figure 3.2. Co-immunoprecipitation of the LIMP-2 with wild type or mutated GCase.
(A) Representative experiment of Co-IP. Protein complexes obtained from Hek293 cells expressing various *GBA* constructs were immunoprecipitated with the anti-LIMP-2 antibody, separated by SDS–PAGE and detected by western blot using anti GCase or anti LIMP-2 antibodies. A reduction of the levels of GCase proteins bearing the p.N227I (N188I), [p.N227S (N188S); p.G304R (G265R)] and p.W420C (W381C) mutations was detec ted in the immunocomplex.
(B) Western blot analysis of GCase expression in Hek293 cells transiently transfected with wild type *GBA* and mutant constructs. All constructs expressed similar levels of GCase protein when transfected in Hek293 cells.
(C) Relative quantification of the GCase in the immunocomplexes. The corresponding western blots (showed in panel a) were analyzed using densitometry. The band intensities of CCase were divided by the band intensities of the corresponding LIMP-2. These ratios were expressed as percentage of the GCaseWT/LIMP-2 value in each experiment. The data are shown as mean±SD of three different experiments. (*p<0.05).

3.4 Structural analysis of N188I, [N188S; G265R] and W381C mutations

To shed further light on the possible consequences of these aminoacid changes at protein level, we performed a structural protein analysis based on the 3D model of GCase.

As shown in **Figure 3.3**, both residues N188 and G265 are located on the protein surface. In the case of the substitution of a polar residue (N) by a big hydrophobic one (I) in position 188 on the protein surface is predicted to cause a local misfolding that in turn could lead to the partial disruption of the interaction between GCase and LIMP-2, as demonstrated by the co-immunoprecipitation assay. Instead, the substitution of N188 by another polar residue S would be probably not enough to affect the ability of GCase to interact with LIMP-2. However, the concomitant presence of both N188S and G265R mutations would destabilize the binding of GCase to LIMP-2. It is worth noting that residues N188 and G265 are located on the same region of the protein surface separated by ca. 20 Å (**Figure 3.3**). Taking together these results, it is possible to hypothesize that a region of GCase, including residues 188 and 265, might be important for the binding to LIMP-2 and that mutations in this region could disrupt the formation of GCase-LIMP-2 complexes.

Interestingly, the replacement p.W420C (W381C), introducing a cysteine not only might affect catalytic activity, but also might cause a conformational change by creating a new disulphide bridges. In fact, the *in silico* analysis predicted that the newly introduced C in position 381 could form a disulphide bridge with C18. In this case the 3D structure of the mutated GCase would be completely destroyed and a protein with such severe structural changes would not only be catalytically inactive but also no longer able to interact with its partners, including LIMP-2.

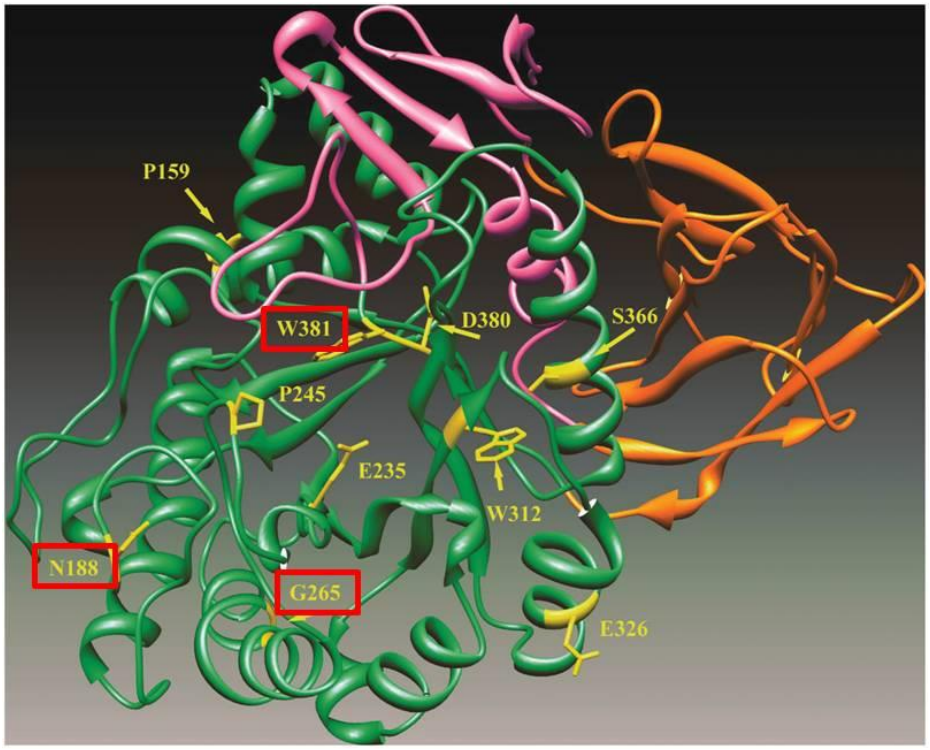

Figure 3.3. Location of GBA mutations on the X-ray structural model. Catalytic domain is represented in green while the N terminal and C terminal domains are drawn in orange and red, respectively. Positions of the mutations analyzed in this study are indicated in yellow. Aminoacid changes that affect the GCase-LIMP-2 interaction are underlined in red.

3.5 LIMP-2 as a modifier in GD: impact of the *SCARB2* mutation, c.1412A>G E471G, on GCase binding

It has been demonstrated that patients affected by AMRF (Action Myoclonous Renal Failure) (Berkovic et al., 2008; Balreira et al., 2008) as well as LIMP-2 knockout mice (Gamp et al., 2003) present neurological symptoms including epileptic seizures and ataxia. Interestingly, a rare subgroup of GD 3 patients also present myoclonic epilepsy (Park et al., 2003), suggesting that mutations in *SCARB2* could contribute to the GD phenotype. Indeed, it has been recently shown that the presence of a mutation in *SCARB2* gene, c.1412A>G (p.E471G), was associated with the presence of myoclonic epilepsy in a family affected with GD [genotype: c.535G>C (p.D140H)/c.10936G>A (p.E326K); c.586A>C (p.K157Q)] (Velayati et al., 2011). In fact, this genotype was found in two siblings discordant for myoclonic seizures. The *SCARB2* mutation, c.1412A>G (p.E471G) was found in the brother with GD and myoclonic epilepsy, and was absent in his sibling and controls. Furthermore, in cells from the GD patient carrying the p.E471G *SCARB2* mutation, GCase was found to be secreted to the culture medium, suggesting that this *SCARB2* mutation leads to the mistargetting of GCase. Based on these results, LIMP-2 has been proposed as a modifier in GD. However, the impact of the LIMP-2 mutation on wild type and the patient's mutant GCase interaction has not been assessed. Therefore, we decided to investigate whether this mutation affects the binding of LIMP-2 to GCase.

In order to analyze the ability of the E471G mutant to interact with wild type and mutant GCase, we performed a co-immunoprecipitation assay in Hek293 cells co transfected with *SCARB2* and GBA constructs.

As shown in **Figure 3.4 A**, co-immunoprecipitation experiments showed that the mutated LIMP-2, co-precipitated GCase (both wild type and mutants) as efficiently as wild-type LIMP-2.

This data suggests that the E471G mutation does not affect the binding capacity of LIMP-2 to GCase. Therefore, the mistargeting of GCase observed in the patient's fibroblasts is not due to a lack of interaction between GCase and LIMP-2. This result is quite expected, since the putative region of LIMP-2 involved in binding to GCase has been well described and located in luminal domain of LIMP-2 (involving the

region between residues 150-167), far from its COOH-terminal cytoplasmic tail where the E471G is located.

However, cells transfected with the E471G mutant express very low levels of LIMP-2 protein **(Figure 3.4 B**). This result strongly suggests that the E471G mutation would impair LIMP-2 protein expression and/or increase protein degradation. Therefore, in the presence of the E471G mutant, the mistargeting of GCase would be the result of insufficient expression of LIMP-2 rather than to an imparment of interaction between these to proteins. In addition, we have measured the residual enzymatic activity of the two GBA mutants found in this family. The impact of mutations on GCase activity was evaluated by in vitro expression of constructs carrying the wild type or mutated *GBA* cDNA in Hek293 cells. As shown in **Figure 3.4 C** only the double mutant D140H/E326K retained a residual activity of 15% of wild type. It is likely that in the sibling not affected by myoclonic epilepsy the D140H/E326K GCase mutant protein reachs the lysosome where it is partially active, while in the more severe affected sibling carrying the E471G mutation in the SCARB-2 gene, the amount of LIMP-2 expressed by the cells would not be enough to assure the correct trafficking of the GCase to the lysosomes. Thus, the D140H/E326K mutant, even if partially active, would not reach the lysosomes, leading to a more severe phenotype.

Taken together our data confirm the previous observation reported about *SCARB2* mutation E471G and suggest that the mistargeting of GCase observed in the GD patient carrying this mutation is probably due to lower stability of mutated LIMP-2 with consequent early degradation.

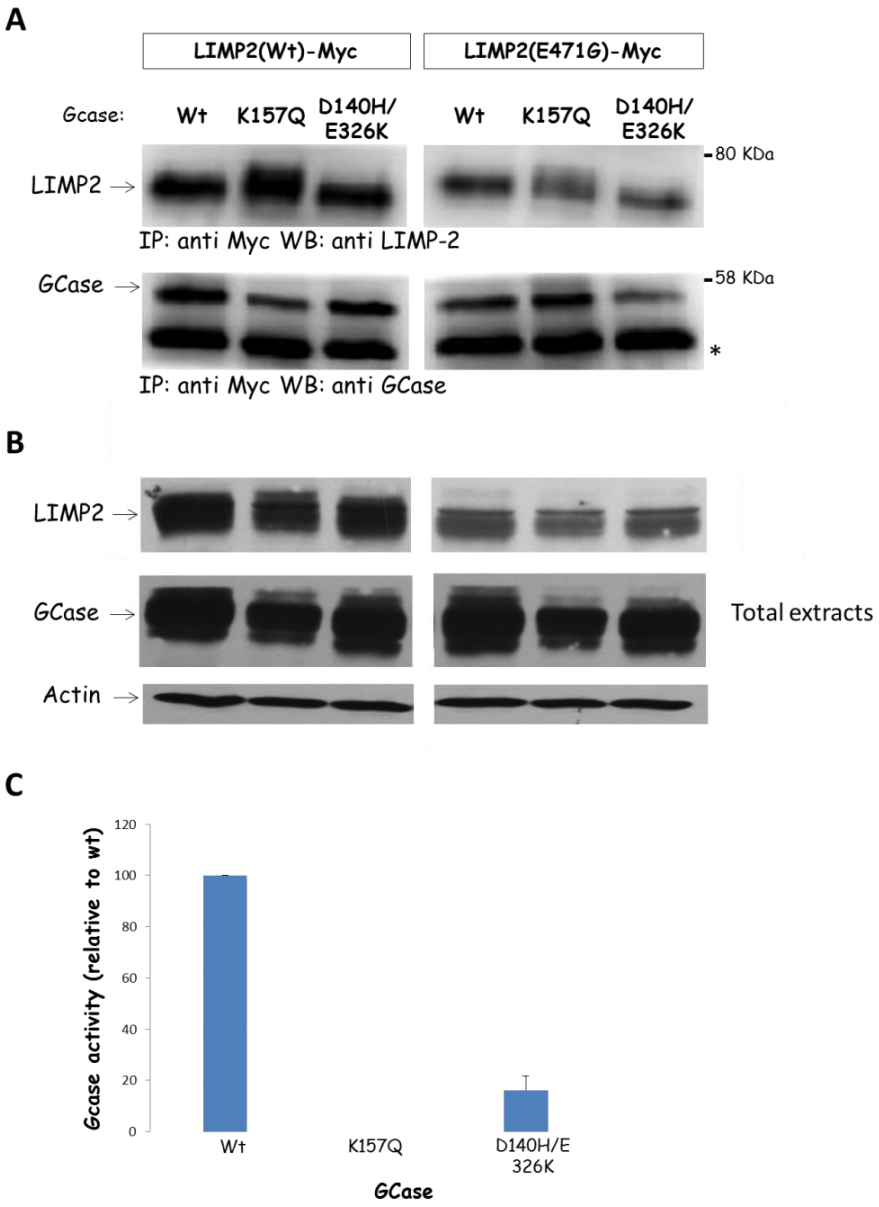

Figure 3.4. Co-immunoprecipitation of the myc-tagged LIMP-2 together with GCase. (A) Protein complexes obtained from Hek293 cells expressing myc-tagged LIMP-2 constructs together with GCase were immunoprecipitated with anti-myc antibody, separated by SDS-PAGE and detected by western blot analysis using anti-GCase and anti-LIMP-2 antibodies. The asterisks show the heavy chains of anti-myc antibody. (B) Western blot analysis of GCase expression in Hek293 cells transiently co-transfected with *SCARB2* and *GBA* constructs. (C) Functional analysis of missense *GBA* alleles found in two siblings affected by GD. GCase activity in Hek293 cells transiently transfected with the wild type and mutant constructs was measured using the fluorogenic substrate 4-MU-D-glucopyranoside. Values are expressed as the percentages of wild type enzyme activity, after the subtraction of enzymatic activity of Hek293 cells transfected with negative control. Data are mean±SD of 3 independent experiments.

3.6 Analysis of *SCARB2* in GD patients with myoclonic epilepsy

Since LIMP-2 may be a modifier in GD, we performed a molecular analysis of *SCARB2* gene in a group of 2 GD2 and 3 GD3 patients who presented myoclonic epilepsy. **Table 3.4** shows the different genotypes identified in these patients

Table 3.4. Patients genotype

Patients	GBA gene		SCARB2 gene	
	Allele 1	Allele 2	Allele 1	Allele 2
# 1 GD3	F213I	L444P	wt	wt
# 2 GD2	R131C	R131C	wt	wt
# 3 GD3	F213I	L444P	c.705 -74 A>G	wt
# 4 GD3	F213I	L444P	wt	wt
# 5 GD2	R463H	L444P	wt	wt

No alterations were detected in the coding region of *SCARB2* gene, while a single nucleotide change (c.705 -74 A>G) in intron 5 was detected in patient 3. This nucleotide change might create a putative acceptor splice site. Therefore, we analyzed the c.705 -74 A>G mutation using two different splice site prediction programs: ME: Maximum Entropy available at: http://genes.mit.edu/burgelab/maxent/Xmaxentscan_scoreseq_acc.html and NN: Neural Network available at http:// www.fruitfly.org/seq_tools/splice.html (Yeo et al., 2004; Reese et al., 1997) (see **Table 3.5**). Both programs predicted that the new putative splicing site would be recognized with a lower score than the wild type sequence, suggesting that it would probably not be used by the splicing machinery.

Thus, in this small series of GD patients affected by myoclonic epilepsy we did not identify *SCARB2* mutations.

Table 3.5. Predicted effects of the novel 3' splicing site

Mutation	Splicing site	
	ME	**NN**
c.705 -74 A>G	WT 3' ss 8,89	WT 3' ss 0,89
	New 3' ss 3,39	New 3' ss 0,28

PART 2: Role of LIMP-2 in the trafficking of GCase in different human tissues

Even if AMRF syndrome (LIMP-2 deficiency) and GD (GCase deficiency) affect the same metabolic pathway and share some neurological features such us myoclonic epilepsy, they present with different clinical and biochemical phenotypes, suggesting that an alternative lysosomal targeting pathway may be active in different tissues. Therefore, to better understand the role of LIMP-2 in the trafficking of GCase, we decided to compare GCase expression, intracellular localization and enzymatic activity of different cells from GD and from a patient affected by AMRF syndrome.

3.7 Characterization of an AMRF patient

We have recently reported the biochemical and molecular findings in a patient diagnosed with myoclonic epilepsy due to LIMP-2 deficiency (Dardis et al., 2009). The molecular analysis of the *SCARB2* gene showed the presence of two different mutations. One in intron 3; c.424-2 A>C, resulting in the loss of the 3' splicing site and one in exon 8 c.1087 C>A, which results in the amino acid change H363N.

In order to clarify the potential significance of these two mutations, *SCARB2* mRNA and protein expression were analyzed in the patient's fibroblasts. In addition, the possible effect of the c.424-2 A>C mutation on the splicing process was analyzed in silico using splicing prediction programs ME (Maximum Entropy) and NN (Neural Network).

Both programs predicted that in the presence of the mutation, the canonical 3' splice site would no longer be recognized. In addition, in the presence of the c.424-2 A>C substitution a new 3' ss located 10 nucleotides downstream of the canonical site was recognized by both programs. As shown in **Table 3.6**, similar scores were obtained for the WT 3'ss and for new 3'ss in the presence of the mutation.

Table 3.6. Predicted effects of the novel 3' splicing site

Mutation	Splicing site	
	ME	**NN**
c.424-2 A>C	WT 3' ss 7,61	WT 3' ss 0,47
	Mut: NR *	Mut: NR *
	New 3' ss 4,56	New 3' ss 0,47

*NR: not recognized because below the threshold.

The recognition of the new 3' ss in the presence of c.424-2 A>C mutation, would lead to the synthesis of an aberrant transcript lacking the first 10 nucleotide of exon 4, causing a shifting in the reading frame and the generation of a premature stop codon. However, the RT-PCR analysis of *SCARB2* mRNA resulted in the amplification of a unique product of a normal size (**Figure 3.5**).

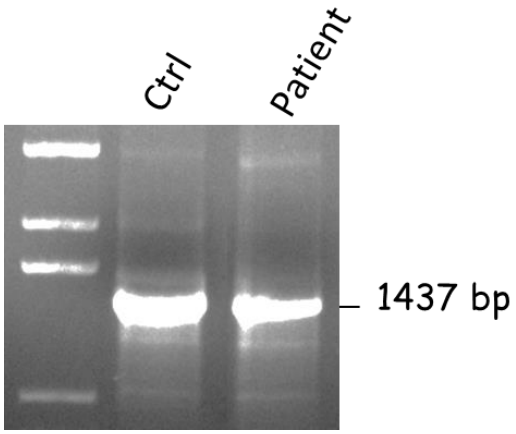

Figure 3.5. RT-PCR analysis of *SCARB2* mRNA of a healthy control and AMRF patient. Molecular Weight Mrkers: 1 kb Plus DNA Ladder.

As shown in **Figure 3.6**, the sequence analysis of the RT-PCR product derived from patient's fibroblasts showed that only the allele carrying the c.1087 C>A was transcribed, suggesting that the c.424-2 A>C substitution leads to the expression of an aberrant mRNA which is probably rapidly degradated.

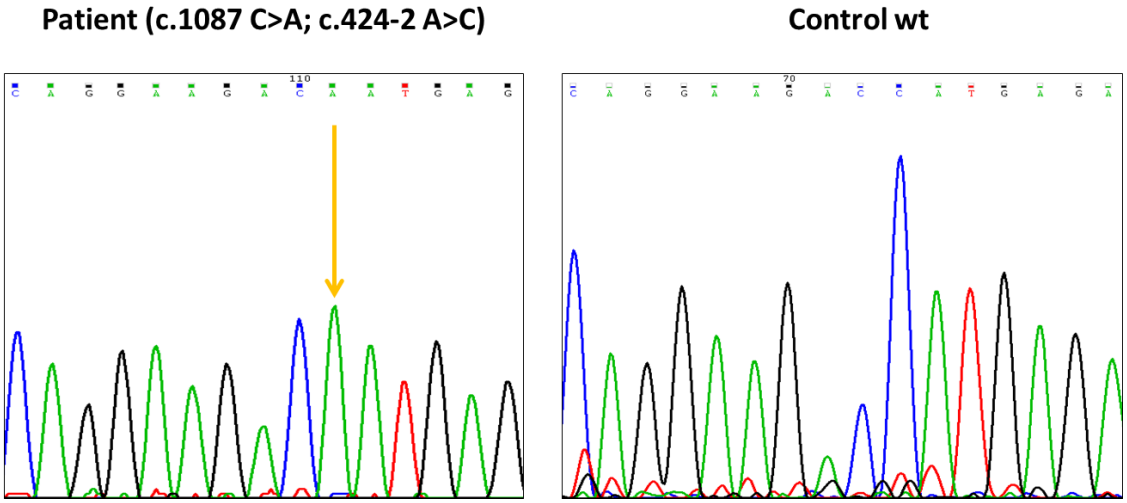

Figure 3.6. Sequence analysis of the *SCARB2* mRNA RT-PCR product obtained in a AMRF patient and a healthy control. The arrow indicates the nucleotide substitution c.1087 C>A in patient. At mRNA level the mutation (found in hyeterozygosis in the genomic DNA) results in homozygosis.

To better characterize the impact of the missense H363N mutation on the protein expression a western blot analysis of LIMP-2 protein extracted from the patient's fibroblasts was carried out. In addition, the intracellular localization of the mutant LIMP-2 was analyzed by treating the samples with endoglycosidase H (endo-H). Endo-H is a specific endoglycosidase that distinguish between glycoproteins with a high mannose content that have not reached the mid-Golgi (endo-H sensitive) and mature glycoproteins with less than four mannose residues which have reached lysosomes (endo-H resistant) (Maley et al., 1989; Trimble et al., 1991; Ron et al., 2005).

As shown **in Figure 3.7**, the expression of the mutant LIMP-2 was reduced with respect to wild type and it was entirely sensitive to Endo-H, indicating that LIMP-2 is almost completely retained in the ER.

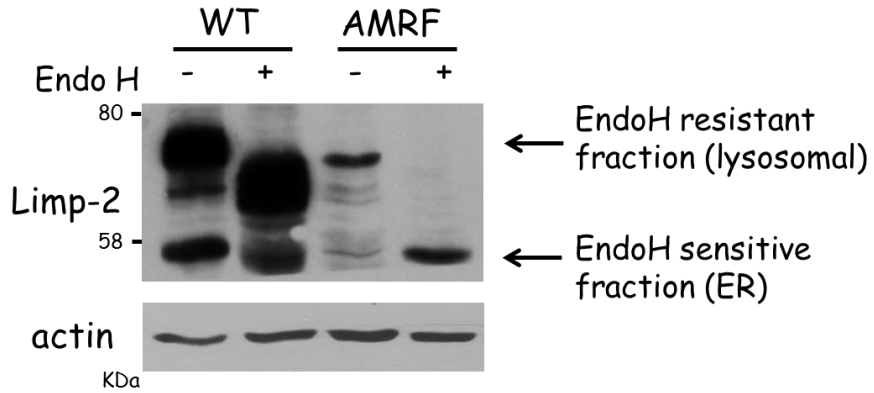

Figure 3.7. Endo H assay. Cell lysates containing the same amount of protein prepared from skin fibroblasts of a AMRF patient and a normal control were subjected to a overnight endo-H digestion and subjected to western blot analysis with anti-LIMP-2 and anti-actin antibodies.

Taken together, these data demonstrated that in the patient affected by AMRF, both mutations c.424-2 A>C and c.1087 C>A (H363N), are in fact pathogenic and cause a severe impairement of mRNA and/or protein expression.

3.8 Trafficking of GCase in human fibroblasts

3.8.1 Analysis of GCase enzymatic activity and localization

Cultured fibroblasts derived from skin biopsies of a GD type 2 patient [genotype: c.508 C>T (p.R131C); c.508 C>T (p.R131C)] and the AMRF patient mentioned above were used to determine GCase enzymatic activity and cellular localization.
As shown in **Table 3.7**, both patients retained a very low GCase activity in fibroblasts.

Table 3.7. Gcase enzymatic activity in fibroblasts.

Patient	Genotype	Residual activity (% of WT)
AMRF	c.1087 C>A (p. H363N) / c.424-2 A>C	2,27 ± 0,55
GD type 2	c.508 C>T (p.R131C) / c.508 C>T (p.R131C)	1,75 ± 0,91

To understand whether the impairment of the enzymatic activity was due to the mislocalization of GCase, an analysis of the glycosilation pattern of the protein was evaluated. The samples were treated with endoglycosidase H (endo-H) and analyzed by western blot.

As shown in **Figure 3.8**, GCase protein levels were reduced in AMRF and GD type 2 patients compared to healthy control. In normal cells, most of GCase was endo-H resistant, indicating that most of the protein already passed the mid-Golgi and it was probably within the lysosome. In contrast, in fibroblasts from the GD2 patient GCase was entirely endo H sensitive, indicating that the protein was completely retained in the ER

The analysis of GCase in fibroblasts from the AMRF patient showed that in these cells GCase was also entirely endo H sensitive, suggesting that LIMP-2 deficiency leads to the retention of GCase in the ER. Furthermore, the reduced levels of GCase protein detected in fibroblasts from the GD2 patient as well as the AMRF patient, suggest that the ER retention of GCase leads to an increase of protein degradation.

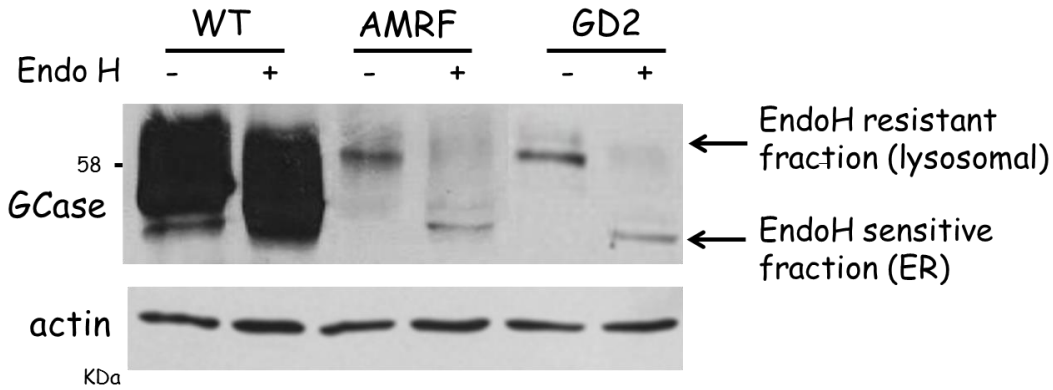

Figure 3.8. Endo H assay. Cell lysates containing the same amount of protein prepared from skin fibroblasts of patients and from a normal control were subjected to overnight endo-H digestion and western blot analysis with anti-GCase and anti-actin antibodies was then performed.

To confirm the results obtained from Endo H digestion, which revealed a high ER retention of GCase both in GD type 2 and AMRF fibrobalsts, the intracellular localization of GCase was analyzed by immunofluorescence. As shown in **Figure 3.9**, in normal cells, GCase accumulated in punctuate lysosomal structures and colocalized with the lysosomal marker LAMP-1. In contrast, only a negligible fraction

of GCase colocalized with LAMP-1 in fibroblasts from the GD type 2 and AMRF patients.

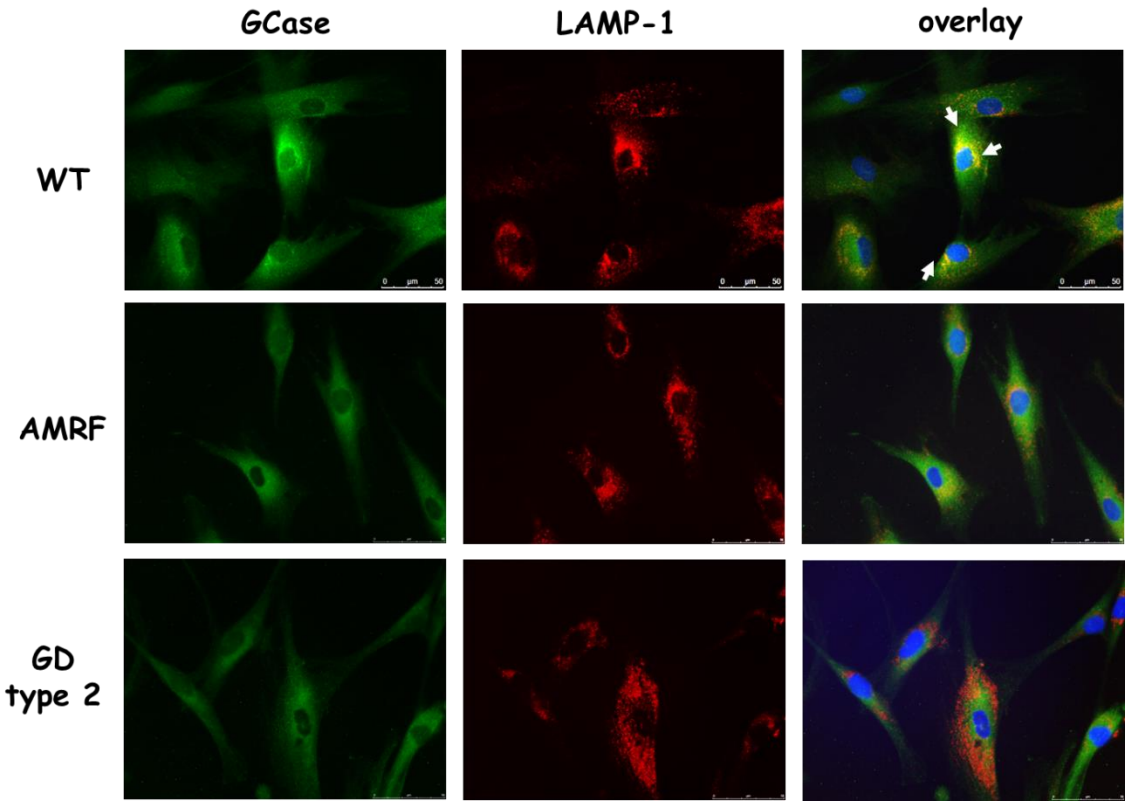

Figure 3.9. Intracellular localization of GCase in AMRF and GD type 2 fibroblast cells. Cells were grown on cover-slips, fixed, permeabilized with 0.1% Triton X-100 and incubated with anti-GCase and anti-LAMP1 antibodies. The overlay images represent the merge of GCase and LAMP-1 signals. Arrows indicates the colocalization of GCase and LAMP-1. The results were visualized with a fluorescence microscope. Magnification 63x.

Taken together, these results indicate that, LIMP-2 is critical for the lysosomal targeting of GCase in human fibroblasts. In these cells LIMP-2 deficiency leads to the retention of GCase in the ER and its degradation, which in turn causes a severe impairment in GCase activity.

3.8.2 Trafficking of hrGCase in human fibroblasts

It has been demonstrated the ERT (Enzyme Replacement Therapy) with the human recombinant form of GCase is effective in the treatment of peripheral symptoms of GD. Recombinant GCase enters the cells via mannose receptor (Mistry et al., 1996; Friedman et al., 1999) that is primarily distributed on the surface of macrophages and dendritic cells, but it is also expressed in skin cells such as human dermal fibroblasts and keratinocyte.

To analyzed whether LIMP-2 is involved not only in the trafficking of the endogenous GCase but also in the lysosomal targeting of the exogenous GCase, we evaluated the uptake of hrGCase in cultured fibroblast of a GD type 2 patient [genotype: c.508 C>T (p.R131C); c.508 C>T (p.R131C)] and a AMRF patient [genotype: c.1087 C>A (p. H363N); c.424-2 A>C].

Currently, two recombinant enzyme are commercialized, recombinant GCase produced in CHO cells, imiglucerase (Cerezyme®) (Jmoudiak and Futerman, 2005) and Gene-Activated human GCase, Velaglucerase alfa (VIPRIN™) (Brumshtein et al., 2010). We first compared the internalization of both of them in fibroblasts from healthy controls. Cells were treated for 4 hours with different amount of Imiglucerase or Velaglucerase alfa (50nM – 2000 nM). As shown in **Figure 3.10**, both preparations were internalized by a saturable mechanism and the maximal uptake was observed when cells were treated with 500 - 1000nM of enzyme.

Since both enzymes were internalized in a similar manner, further experiments were carried out using Velaglucerase alfa.

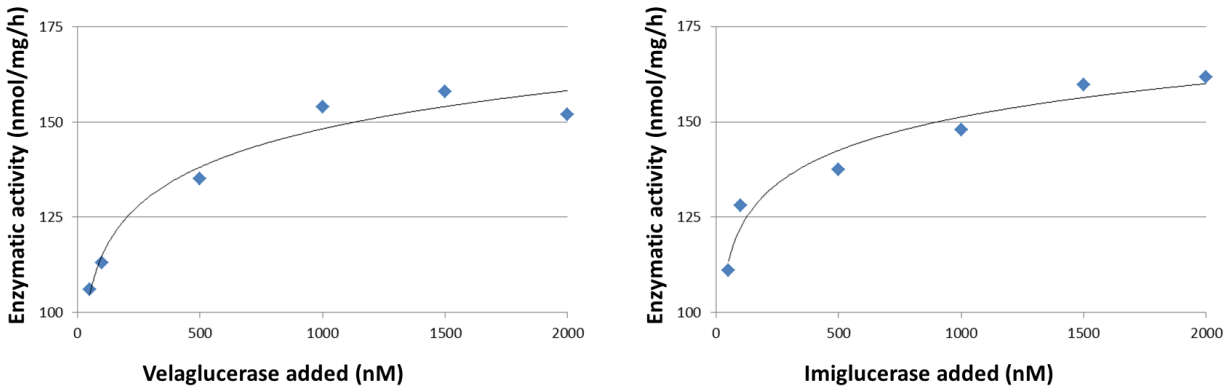

Figure 3.10. Enzymatic activity measured in fibroblast protein extract after the treatment with two recombinant enzymes, Velaglucerase and Imiglucerase. Equimolar amounts of protein were added at increasing concentration to the cells for 4 hours. The cells were washed and collected to measure the GCase anzymatic activity using the fluorogenic substrate 4-MU-D-glucopyranoside.

Then, to evaluate whether the hrGCase uptake was dependent of functional LIMP-2, fibroblast cells from a GD type 2 patient and an AMRF patient were cultured in the presence of 200 nM to 1,6 µM of hrGCase for 4 hours.

The amount of internalized protein was measured through western blot after treating the cells with 1.6 µM of hrGCase. This concentration was chosen to ensure the saturation of mannose receptor (see **Figure 3.10**). As shown in **Figure 3.11 A**, the recombinant enzyme is internalized both by AMRF and GD type 2 fibroblasts.

When the enzymatic activity was measured in cells treated with 200 nM to 1.6 µM of hrGCase, a dose dependent rescue of GCase activity was observed both in GD2 and in AMRF cells. However, while the maximum correction of enzyme activity in AMRF cells barely reached a 20% of the activity detected in normal fibroblasts, in GD2 cells it reached 80% of the activity of control fibroblasts (**Figure 3.11 B**).

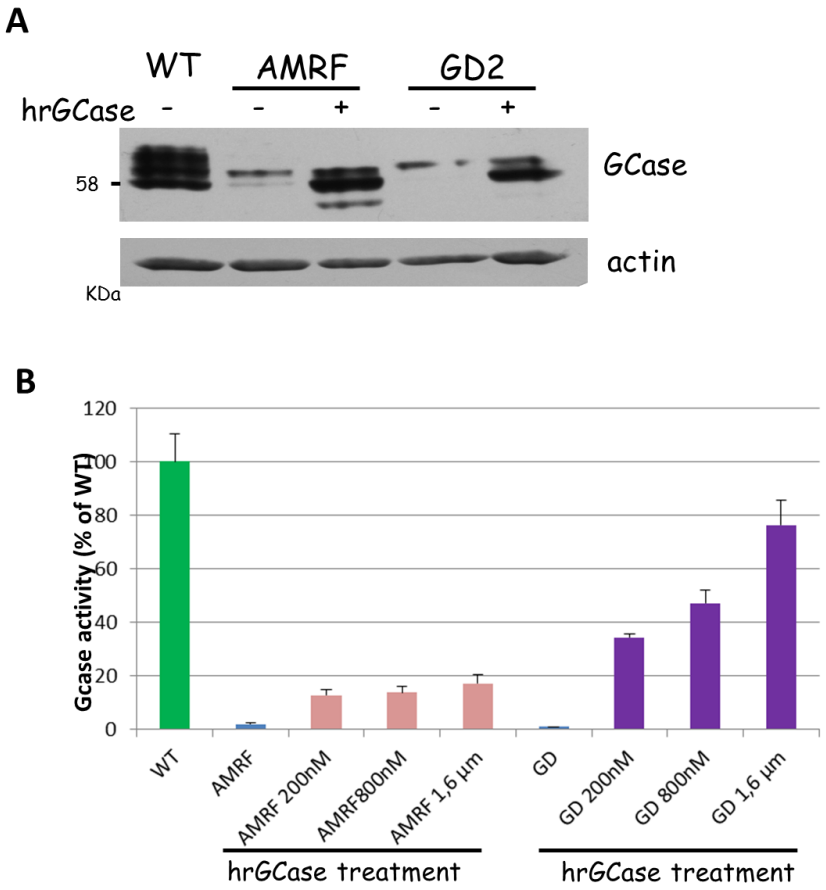

Figure 11. Uptake of hrGCase in fibroblast cells. (A) Level of GCase protein internalized after treatment with 1.6µM hrGCase for 4 hours of fibroblasts from an AMRF patient and fibroblasts from a GD type 2 patient. Protein extracts from fibroblasts of a healthy control were loaded as control. The multiband pattern recognized by the anti-GCase antibody correspond to the three differently glycosylated forms of GCase. The lower band represents the mature form of GCase. (B) GCase activity measured after uptake of hrGCase, the mean of three independent experiment is reported. The enzymatic activity was measured using the fluorogenic substrate 4-MU-D-glucopyranoside. Values are expressed as the percentages of endogenous wild type enzyme activity detected in normal fibroblasts.

These data suggest that hrGCase enters the cells via mannose receptor exclusively and that LIMP-2 might not be necessary for the GCase uptake. However, LIMP-2 might be important in the endocytic pathway to transport internalized hrGCase to the lysosomes.

To confirm this hypothesis, the fate of internalized hrGCase in AMRF and GD2 fibroblasts was also investigated by analyzing the internalization and intracellular localization of Alexa Fluor 555-labelled rhGCase. Fibroblasts were incubated with

fluorescent rhGCase for different periods of time (0, 30, 60 and 120 minutes) fixed and examined by fluorescence microscopy. **Figure 3.12** shows the results obtained after 60 min. of treatment of GD2 and AMRF fibroblast. Recombinant GCase was efficiently taken up by both AMRF and GD2 fibroblasts, but while in GD2 cells the recombinant enzyme presented a lysosomal localization, as shown by its colocalization with the lysosomal marker (LysoTracker®), in AMRF cells the Alexa Fluor 555 signal did not colocalized with LysoTracker®.

These results clearly show that in the presence of mutant LIMP-2 the targeting of hrGCase to lysosomes is impaired. Therefore, LIMP-2 is a key player for the targeting of hrGCase to the lysosomes in human fibroblasts.

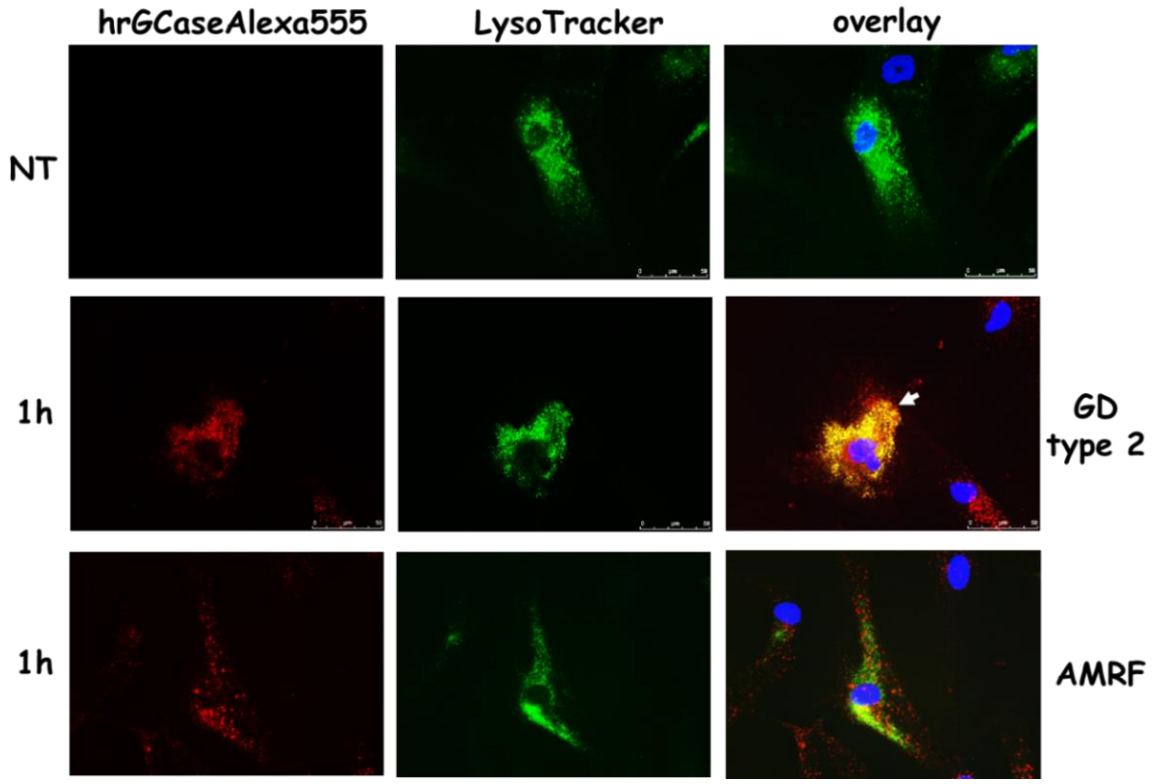

Figure 3.12. Uptake of Alexa Fluor 555-labeled hrGCase. The cells were grown on coverslips and incubated with fluorescent rhGCase (15nM) for 1 h, Lysotracker-Green (75 nM) was added for the last 30 min. Then, cells were washed, fixed and visualized by fluorescence microscopy. Arrows indicates the colocalization of hrGCase and LysoTracker.

3.9 Trafficking of GCase in blood cells

Macrophages are the main affected cells in GD and they accumulate massive amount of GlcCer. Consequently, GD is characterized by the presence of lipid-laden macrophages (Gaucher cells) in the liver, spleen, bone, and lungs.

The absence of “Gaucher cells” in bone marrow of AMRF patients and the presence of residual GCase activity in peripheral leukocytes suggest that in these cells, GCase might still reach the lysosome even in the absence of LIMP-2.

To investigate the role of LIMP-2 in the trafficking of GCase in blood cells, human peripheral blood mononuclear cells (PBMCs) were obtained from an AMRF patient, 6 GD patients and healthy donors. Monocytes were isolated from PBMCs by magnetic separation of $CD14^+$ cells using microbeads. After separation, 90 % of cells were CD14+ as shown by flow cytometry analysis (**Figure 3.13 A**). $CD14^+$ cells were induced to differentiate to machrophages by treating them with human macrophage colony stimulating factor (m-CSF). The adherence of cells with a characteristic fibroblast-like shape to the culture plate was observed after 7 days (**Figure 3.13 B**).

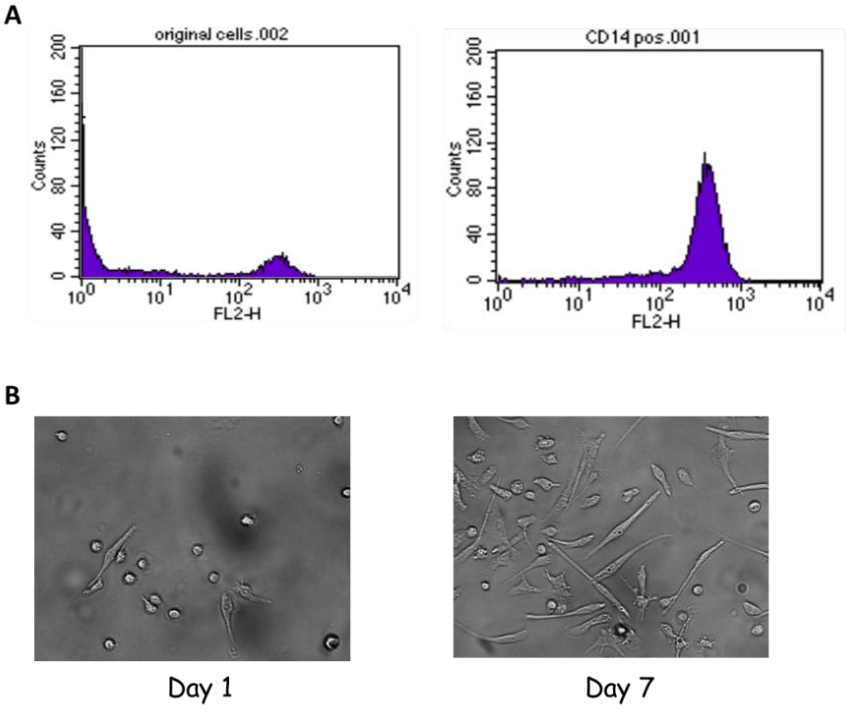

Figure 3.13. Macrophagic differentiation of monocytes isolated from PBMCs. (A) Acquisition on flow cytometry. Histogram profile of cells separated through CD14+ microbeads and analysed using anti CD14-FITC, after magnetic separation (right) compared to total PBMCs (left). (B) Light microscopy images of monocytes induced to machrophagic differentiation one day and seven days after induction by m-CSF (100 ng/mL).

Macrophages derived from an AMRF patient, 5 GD type 1 and 1 GD type 3 patient were tested for GCase enzymatic activity. In **Table 3.8** are reported the obtained residual enzymatic activity expressed as % of the activity measured in healthy controls. Macrophages obtained from GD patients displayed a very low enzymatic activity, below 16% of wild type. Furthermore, macrophages from the patient affected by the chronic neurophatic form of GD (GD3) presented a residual activity of 3.6% of wild type. Instead, macrophages derived from an AMRF patient showed a quite high residual enzymatic activity, reaching approximately 30% of the activity detected in normal controls. These data indicate that GCase is partially functional in AMRF machrophages.

Table 3.8. Enzymatic activity of macrophages.

Patient	Genotype	Residual activity (% of WT)
AMRF	c.1087 C>A (p.H363N) / c.424-2 A>C	31,5
GD type 1	c.1226 A>G (p.N370S) / c.1226 A>G (p.N370S)	11,6
GD type 1	c.882 T>G;c.1342G>C (p.H255Q;D409H) / c.1226 A>G (p.N370S)	15,9
GD type 1	c.1226 A>G (p.N370S) / c.508 C>T (p.R131C);	13
GD type 1	c.259 C>T (p.R48W) / c.1448 T>C (p.L444P)	12,5
GD type 1	c.259 C>T (p.R48W) / c.1448 T>C (p.L444P)	14,1
GD type 3	c.1448 T>C (p.L444P) / c.1448 T>C (p.L444P)	3,6

To obtain further insight into the GCase trafficking in blood cells, lymphoblastic cells were prepared immortalizing lymphocytes isolated from PBMCs of an AMRF and from three GD type 3 patients. As shown in **Table 3.9**, in lymphoblastic cells the activity of AMRF patient resulted to be again approximately 30% of the activity detected in normal controls.

Table 3.9. Enzymatic activity in immortalized lymphocytes.

Patient	Genotype	Residual activity (% of WT)
AMRF	c.1087 C>A (p.H363N) / c.424-2 A>C	28,23 ± 1,1
GD type3	c.1342G>C (p.D409H) / c.971G>C (p.R285P)	0,97 ± 0,44
GD type3	c.882T>G;c.1342G>C (p.H255Q;D409H)/ c.754T>A (p.F213I)	3,54 ± 0,87
GD type3	c.1448 T>C (p.L444P) / c.1448 T>C (p.L444P)	0,68 ± 0,29

These data suggest a partial LIMP-2 independent targeting of GCase to lysosomes in these cells.

Therefore, we then evaluated the impact of LIMP-2 on GCase trafficking in blood cells by analyzing the glycosilation pattern of GCase in AMRF immortalized lymphocytes.

As shown in **Figure 3.14**, GCase protein levels were reduced in AMRF immortalized lymphocytes when compared to normal cells. In the normal control, after Endo H treatment approximately 90% of GCase was endo H resistant, indicating that most protein was already leaved the ER. In contrast, about 50% of GCase was EndoH resistant in AMRF cells, indicating that in these cells even in the absence of LIMP-2 about 50% of the protein reaches the lysosomes.

These results correlate with data of enzymatic activity in AMRF macrophages and immortalized lymphocytes, providing further evidences supporting the presence of a potential alternative mechanism of GCase targeting to the lysosomes in these cells.

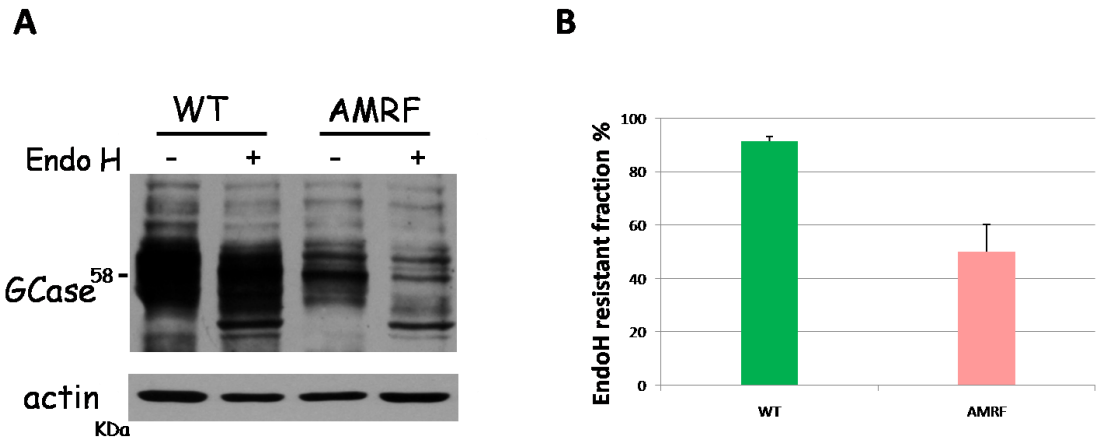

Figure 3.14. Endo H digestion of GCase in immortalized lymphocytes. (A) Cell lysates containing the same amount of protein prepared from immortalized lymphocytes of an AMRF patient and from a healthy control were subjected to a overnight endo-H digestion and western blot analysis with anti-GCase, and anti-actin antibodies. (B) To determine the endo-H resistant fraction, the blots were scanned and the intensity of each band was measured. GCase resistant fraction was calculated by subtracting the intensity of the endo-H sensitive fraction (in the endo-H + lane) to the intensity of the entire amount of the GCase in the same lane.

3.10 Trafficking of GCase in human neuronal cells obtained by differentiation of hSKIN-MASC

In order to analyze the role of LIMP-2 in the trafficking of GCase in neuronal cells, we developed a neuronal model of AMRF and GD type 2 by inducing neuronal differentiation of multipotent adult stem cells isolated from patient's cultured fibroblast (hSKIN-MASC) as previously described (Bergamin et al, 2013).

3.10.1 Stem cell characterization

Using a protocol previously developed in our laboratory, early passages (P1-P3) of cultured fibroblasts obtained from patients and a healthy control, were exposed to a selective medium enabling the growth of hSKIN-MASC. After three passages in the selective medium, the cells acquired a homogeneous morphology.
In order to investigate whether these cells retained the pathologic phenotype, GCase enzymatic activity was measured. As shown in **Table 3.10**, hSKIN-MASC isolated from both GD2 and AMRF patients presented an extremely low enzymatic activity, similar to the activity observed in fibroblast cells.

Table 3.10. Enzymatic activity in hSKIN-MASC.

Patient	Genotype	Residual activity (% of WT)
AMRF	c.1087 C>A (p. H363N) / c.424-2 A>C	1,73 ± 0,66
GD type 2	c.508 C>T (p.R131C) / c.508 C>T (p.R131C)	2,79 ± 0,72

3.10.2 Neural differentiation

hSKIN-MASC were then induced to neuronal differentiation by growing them in selective medium (see Material and Methods). After differentiation, they showed remarkable morphological changes; in particular the enlargement of the cellular bodies and the presence of long projections, closely resembling the morphology of neuronal cell (**Figure 3.15**).

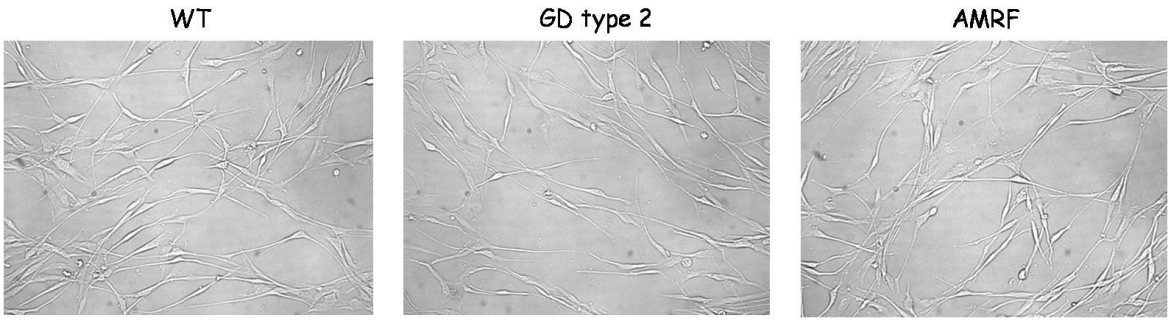

Figure 3.15. Light microscopy images of differentiated cells of healthy control, GD type 2 and AMRF patients.

After differentiation a large fraction of cells became positive for markers of the neuronal lineage. They expressed MAP2, a structural protein specifically present in neuronal cells (**Figure 3.16 A**) and NeuN, a neuronal specific nuclear protein (**Figure 3.16 B**). To better characterize the type of neuronal cells obtained, mRNA expression of specific markers of dopaminergic (tyrosine hydroxylase TH and dopamine transporter, DAT), cholinergic (choline acetyltransferase, CHAT) and GABAergic (glutamic acid decarboxylase, GAD) neurons were analyzed by real time PCR. While none of these markers were detected in undifferentiated cells, the differentiated cells expressed only CHAT (**Figure 3.16 C**), suggesting that the protocol used for neuronal differentiation promote the differentiation of hSKIN-MASC to cholinergic neurons (as previously described).

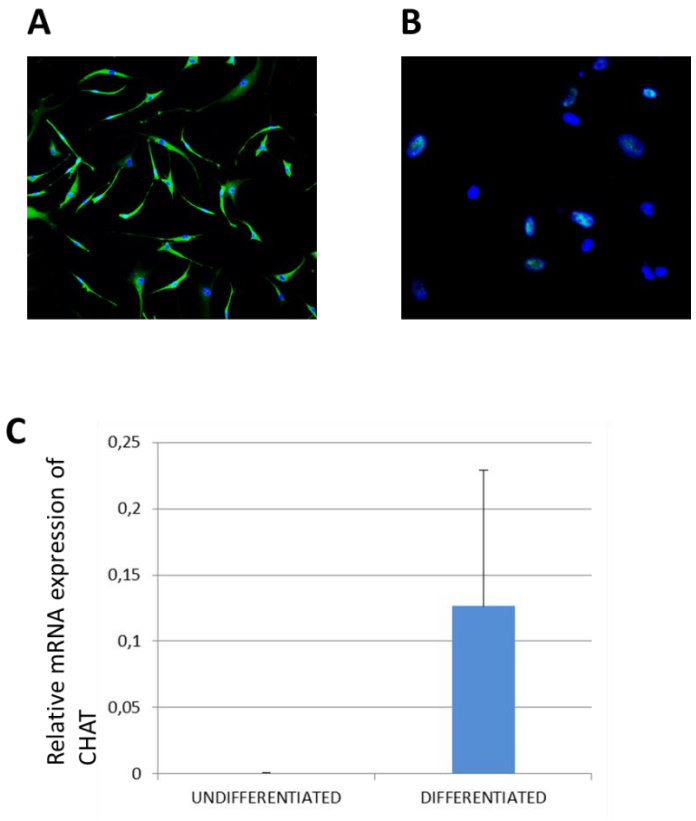

Figure 3.16. Neural differentiation of hSKIN-MASC obtained from cultured fibroblasts. Expression of neuronal markers, MAP-2 (A) and NeuN (B) as green fluorescence. Nuclei are depicted by the blue fluorescence of DAPI staining. (C) Relative expression of CHAT mRNA in hSKIN-MASC and differentiated cells. The relative abundance of CHAT mRNA were analyzed by real time PCR before (UNDIFFERENTIATED) and after neuronal differentiation (DIFFERENTIATED). Data were normalized by the expression of GAPDH and expressed as mean ± SD of 3 independent experiments.

3.10.3 Characterization of GCase trafficking in neuronal cells

To evaluate the role of LIMP-2 in the trafficking of GCase in neuronal cells, GCase enzymatic activity and cellular localization was analyzed in neuronal cells derived from the AMRF patient and compared with cells derived from a GD type 2 patient and healthy controls. As shown in **Table 3.11**, GCase activity resulted severely impaired in cells derived from both AMRF and GD2 patients.

Table 3.11. Enzymatic activity in neuronal cells.

Patient	Genotype	Residual activity (% of WT)
AMRF	c.1087 C>A (p. H363N) / c.424-2 A>C	2,88 ± 0,09
GD type 2	c.508 C>T (p.R131C) / c.508 C>T (p.R131C)	1,64 ± 0,33

To investigate the localization of GCase in neuronal cells, an Endo H assay was carried out. The results presented in **Figure 3.17** show that GCase is almost completely retained in the ER both in GD and AMRF neuronal cells.

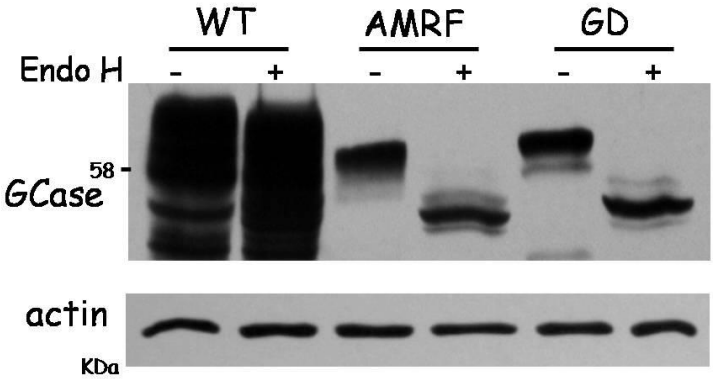

Figure 3.17. Endo H assay. Cell lysates containing the same amount of protein prepared from neural derived cells of patients and a healthy control were subjected to a overnight endo-H digestion and western blot analysis with anti-GCase and anti-actin antibodies.

The subcellular localization of GCase in neuronal cells was further confirmed by immunofluorescence. As expected, while in cells derived from a healthy control GCase colocalized with the lysosomal marker LAMP-1, in GD2 and AMRF cells GCase showed a reticular distribution and did not colocalize with LAMP-1(**Figure 3.18**).

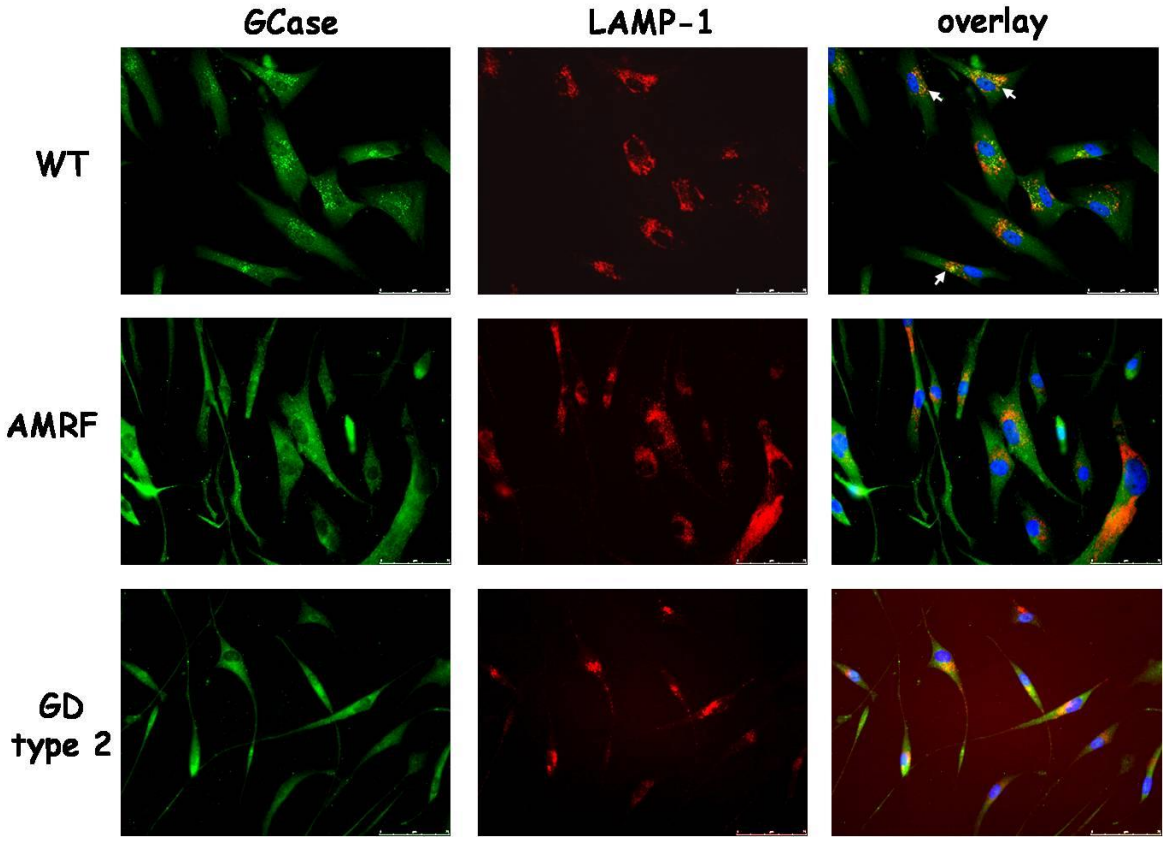

Figure 3.18. Intracellular localization of GCase in AMRF, GD and normal differentiated neuronal cells. Cells were grown on cover-slips, fixed, permeabilized with 0.1% Triton X-100 and incubated with anti-GCase and anti-LAMP1 antibodies. The overlay images represent the merge of GCase and LAMP-1. The results were visualized with a fluorescence microscope. Arrows indicates the colocalization of GCase and LAMP-1. Magnification 40x.

Our results showed that in LIMP-2 deficient neuronal cells, GCase protein levels are reduced and GCase does not reach the lysosomes, leading to a severe impairment of GCase activity. These observations support the hypothesis that the neurological signs present in AMRF patients are caused by the lack of functional GCase within the lysosomes that in turn, would likely cause a storage of undigested glycosphingolipids (GSL) within this organelle.

3.10.4 Analysis of intracellular storage in neuronal differentiated cells

In order to gain insight into the effects of LIMP-2 deficiency in neuronal cells, the number/size of lysosomes and the intracellular accumulation of gangliosides and cholesterol were analyzed.

To compare the lysosomes distribution, the neuronal derived cells from AMRF and GD2 patients and from a healthy control were incubated with Lysotracker and analyzed by FACS. **Figure 3.19** shows the flow cytometry analysis of stained cells. Cells derived from GD type 2 and AMRF patients showed an increased mean fluorescence compared to healthy control, specially the AMRF cells, suggesting an enlargement of endo-lysosomal compartments probably due to the massive accumulation of storage material.

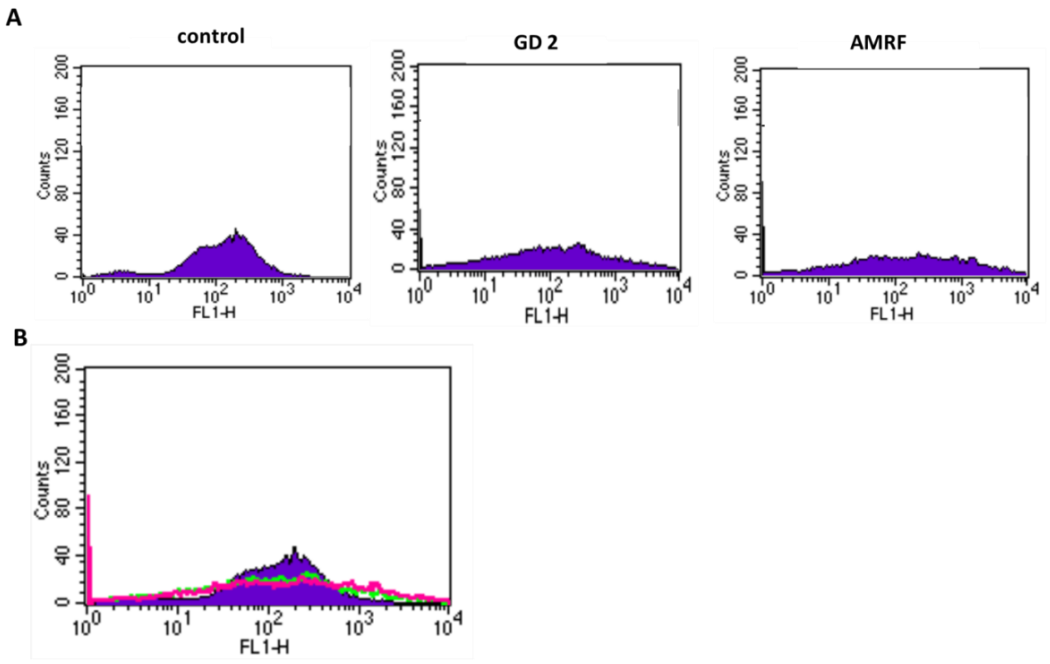

Figure 3.19. Flow cytometry analysis detecting green fluorescence of Lysotracker. (A) Single histogram profile of neuronal cells obtained from a healthy control, GD type 2 and AMRF patients respectively. (B) Overlay of the three independent histogram profile. Filled profile correspond to green fluorescence of control cells, pink and green profile correspond to AMRF and GD type 2 cells respectively.

Storage of gangliosides, sialic acid containing GSL, mostly found in the central nervous system, is a hallmark of neuronopathic forms of many lysosomal storage diseases, including GM1 and GM2 gangliosidoses, GD2 and GD3 and Niemann-Pick type C (Boomkamp et al., 2008).

Therefore, the intracellular storage of gangliosides was evaluated by immunofluorescence in fibroblasts and neuronal cells derived from the ARMF and GD2 patients and healthy controls. No accumulation of gangliosides was observed in cultured fibroblasts (data not shown). As shown in **Figure 3.20 A**, a storage of GM2 ganglioside was found in neuronal cells derived from both GD type 2 and AMRF patients, in contrast no accumulation of GM1 and GM3 ganglioside was detected in normal, GD type 2 and AMRF cells.

Since LDL derived unesterified cholesterol accumulates in late endosomes/lysosomes in several sphingolipid storage disorders (Puri et al., 1999), including GD (Salvioli et al., 2005), we analyzed the intracellular accumulation of free cholesterol in fibroblasts and in neuronal derived cells from the ARMF and GD2 patients and healthy controls by filipin staining. As shown in **Figure 3.20 B**, increased filipin fluorescence relative to control cells was observed in fibroblasts of GD2 and AMRF patients. In addition, cholesterol accumulation was analyzed in cells derived from a patient affected by Niemann Pick Type C (NPC), which accumulate massive quantities of cholesterol within the lysosomes as a control. The intensity of the fluorescence observed in GD and AMRF fibroblast was weaker than that observed in NPC1 cells, but the cholesterol distribution in vesicular structures was identical. On the contrary, no accumulation of cholesterol was observed in neuronal differentiated cells of GD type 2 and AMRF patients.

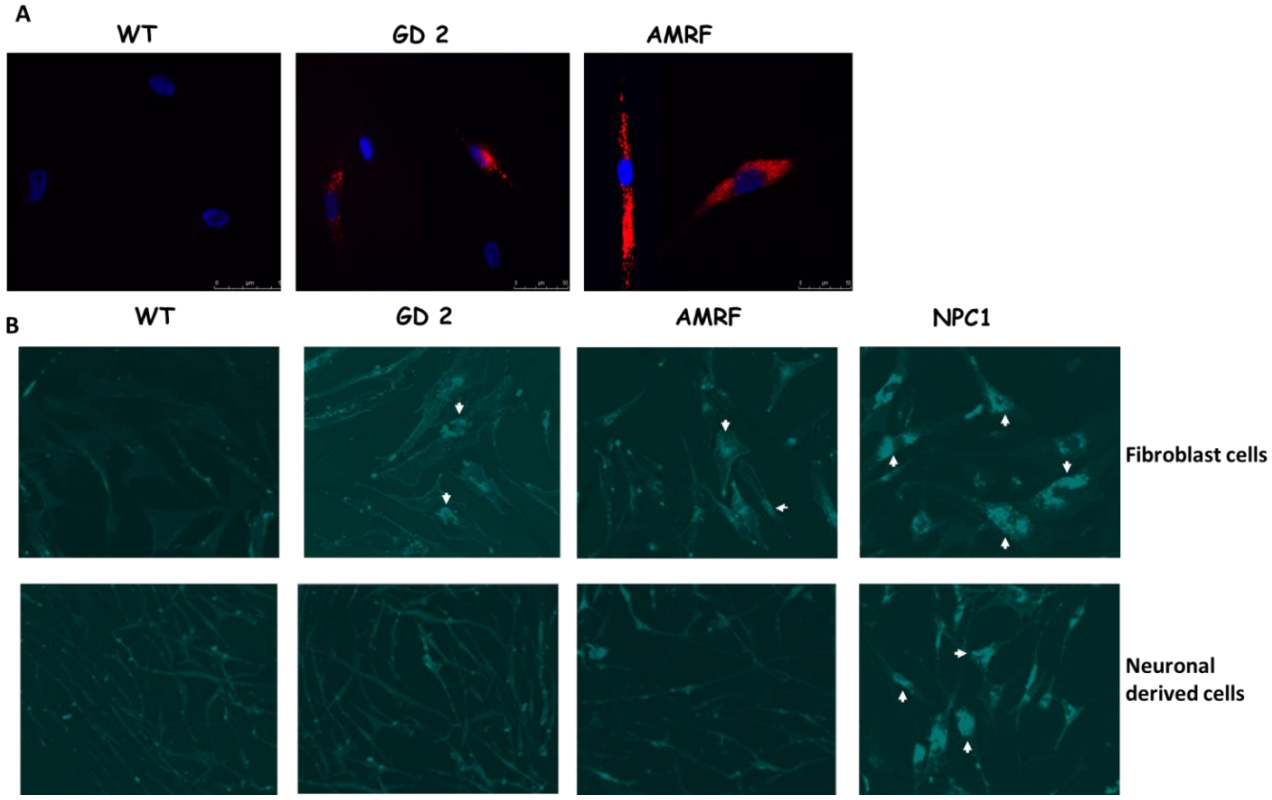

Figure 3.20. Storage of GM2 and unesterified cholesterol cells from GD 2 and AMRF patients. (A) Expression of GM2 was analyzed by immunofluorescence (red) in a healthy donor (WT), GD2 and AMRF after neuronal differentiation. (B) Filipin staining of fibroblast cells and differentiated cells obtained from healthy donor, GD2 and AMRF patients. NPC1 fibroblasts and NPC1 neuronal derived cells was used as positive control. Arrows indicates accumulation of cholesterol within the lysosomes.

4. Discussion

Acid β-Glucosidase (GCase) is the enzyme defective in most cases of Gaucher Disease (GD). This rare lysosomal storage disease (LSD) is characterized by the accumulation of glucosylceramide (GlcCer) and other sphingolipids in several tissues and organs.

GCase enzyme is synthesized in the ER and targeted to the lysosomes through a mannose 6-phosphate (M6P) receptor independent mechanism. It has been shown that the lysosomal integral membrane protein type 2 (LIMP-2), an ubiquitously expressed transmembrane protein mainly found in the lysosomes and late endosomes, is a receptor for lysosomal mannose 6-phosphate-independent targeting of the GCase (Reczek et al., 2007).

LIMP-2 dependent sorting of GCase is pH dependent. The neutral pH of ER allows GCase to associate with LIMP-2, whereas the acidic pH of endosomal/lysosomal compartements leads to their dissociation. Recently, the crystal structure of LIMP-2 has been described and a coiled-coil domain between residues 150-167 has been shown to be involved in LIMP-2-GCase interaction (Neculai et al., 2013). A critical histidine located at position 171 has been suggested as pH sensor which regulates the dissociation of the receptor-ligand complex in late endosomal/lysosomal compartement (Zachos et al., 2012).

To date, more than 300 mutations of the *GBA* gene have been reported in patients affected by GD, most of them lead to the synthesis of misfolded proteins that are retained in the ER and rapidly degradated by ERAD. Considering that LIMP-2 is a key player in the targeting of GCase to the lysosomes, it has been proposed that mutations/polymorphisms in the *SCARB2* gene, encoding LIMP-2, may modify the phenotypic expression of GD.

However, the nature of the GCase-LIMP-2 interaction has not been characterized in detail and the impact of *GBA* mutations on this interaction has not been explored.

Recently, mutations in the *SCARB2* were found to be responsible for action

myoclonus-renal failure syndrome (AMRF), a disorder characterized, by a mistargeting of GCase. The main feature of AMRF is the presence of progressive myoclonus epilepsy, a frequent sign of patients affected by the chronic neurological form of GD. However, even if AMRF and GD affect the same metabolic pathway and share some neurological features, they present with different clinical and biochemical phenotypes, suggesting that an alternative lysosomal targeting pathway may be active in different tissues.

Therefore, in this study we characterized the impact of different *GBA* mutations on the LIMP-2-GCase interaction and the role of LIMP-2 in the trafficking of GCase to the lysosomes in different tissues.

The region of GCase protein directly involved in the interaction with LIMP-2 is completely unknown and the impact of *GBA* mutations on the LIMP-2-GCase interaction has not been studied. Therefore, in the first part of the study, we analyzed the impact of the most frequent *GBA* mutations (N370S and L444P) and 9 novel mutations identified during the routine molecular testing of GD patients on the GCase-LIMP-2 of association. Among new alleles, 7 carried single point mutations and 2 carried 2 *in cis* mutations on the same allele.

The pathogenic nature of novel *GBA* mutations was first established by in vitro expression of the mutated alleles. In fact, all mutants were inactive except the P159S, which retained 15% of wild type activity. To further characterize the alleles carrying 2 *in cis* mutations, we expressed constructs bearing singly each mutation. The presence of G265R or D380N mutations completely abolished enzyme activity, while N188S and E326K mutants retained 25% and 54% of wild type activity, respectively.

Considering these data a quite good correlation between the genotype and the phenotype was found in most studied patients. Indeed, all patients affected by GD2 (the most severe phenotype) carried *GBA* mutations that completely abolish GCase enzymatic activity in both alleles. Among patients affected by GD1 (the less severe form of the disease) 3 out of 5 carried mutations that completely abolish GCase enzymatic activity in association with the N370S mutation, which leads to the synthesis of a protein that retains 40% of residual activity. One patient carried the severe complex allele [(E326K;D380N)] in heterozygosis with the P159S allele, leading to the synthesis of a mutant protein that 15% of activity, which may be enough to prevent the severe phenotype. Much less expected was the GD type 1 phenotype

in the patient compound heterozygous for the new W312S mutation, which completely abrogates the GCase activity, in association with the severe mutation L444P. This patient, who was diagnosed as having GD and treated with ERT at the age of 9 years, is indeed a 22-year-old woman with no evidence of clinical or subclinical neurological involvement. In an attempt to exclude the theoretical possibility of additional in *cis* mutations, both the alleles of this patient have been entirely sequenced. In circumstances like these, it is particularly difficult to evaluate how the therapy, on one hand, and other modifying genetic or non genetic factors, on the other hand, might have contributed to such an unexpected clinical course of the disease.

Finally, the only patient affected by GD3, carried 2 in cis mutations [N188S;G265R] in one allele, while the mutation in the second allele remained unidentified . Even in the absence of a complete genotype, some important considerations can be made in this patient based on the presented results.

Results of the '*in vitro'* expression of each single mutation showed that while the enzymatic activity of G265R mutant was nearly absent, the N188S mutant retained a quite high residual activity, as also reported in previous studies (Montfort et al., 2004). Conversely, the cumulative effect of the double mutant seemed to be highly deleterious as the in vitro expressed activity was almost undetectable. Interestingly, this patient developed myoclonic epilepsy, previously reported as associated with the N188S mutation (Filocamo et al., 2004; Kowarz et al., 2005). It is therefore likely that myoclonic epilepsy is always determined by the N188S both as single mutation and as part of a double-mutant allele.

The fact that the N188S mutant, which retains such a high residual activity, has been found strongly associated with myoclonic epilepsy is quite intriguing. A possible explanation might be that the mutation affects the binding of the protein to LIMP-2 and therefore the mutant, even if partially active, would not be able to reach the lysosomes.

However, our data do not support this hypothesis, since when we analyzed the ability of the N188S mutant to associate with LIMP-2, we found that the mutant binds to the receptor as efficiently as the wild type protein.

Discrepancies between the *in vitro* residual enzymatic activity and the clinical phenotype have been described in LSD (Yoshizawa et al., 2002; Montfort et al., 2004). These discrepancies may be caused by the fact that the results obtained *in*

vitro may not reflect exactly how the mutated protein functions in *vivo*, when it is expressed in a certain level, in a particular cell type and organelle and interacting with other proteins (such as Saposin C).

In addition, the analysis of LIMP-2-GCase association showed that all Gcase mutants included in this study, retained at least some LIMP-2 binding capacity.

However, while most GCase mutants co-precipitate with LIMP-2 as efficiently as the wild type GCase, a reduction of the levels of GCase proteins bearing the p.N227I (N188I), [p.N227S (N188S); p.G304R (G265R)] and p.W420C (W381C) mutations was detected in the immunocomplex, suggesting that they impaired the ability of GCase to associate with LIMP-2.

It is worth noting that, as shown by a 3D structural analysis, N188 is located at the surface and substitution of the polar residue (N) by a big hydrophobic one (I) may cause a local misfolding that in turn could lead to the disruption of the interaction between GCase and its protein partners.

Interestingly the substitution of N188 by another polar residue (S), a very similar aminoacid in terms of polarity and size, would have a mild impact on GCase structure. However, when the N188S is associated with the G265R, another mutation located on the same region of the protein surface, the interaction with LIMP-2 might be destabilized. The G265R mutation introduces a long, ramified and charged side chain in place of an hydrogen atom, probably inducing a steric hindrance and the loss of local main chain plasticity.

The last aminoacid change that affects the interaction of GCase with LIMP-2 is W381C. The introduction of a cysteine in this position not only might affect catalytic activity, but also might cause a dramatic conformational change by creating a new disulphide bridge leading to a loss of interaction of GCase with its partners.

Even if our results shed some light into the LIMP-2-GCase interaction, further studies need to be conducted in order to identify the regions of GCase directly involved in the interaction with LIMP-2.

Although, as described above, a quite good correlation between the genotype and the phenotype has been found in our series of patients, a wide phenotypic variability has been reported in GD, even among siblings. Given the key role of LIMP-2 in the trafficking of GCase, the gene encoding for LIMP-2 (*SCARB2*) has been proposed as a modifier in GD.

This hypothesis has been recently explored by Velayati and co-workers (Velayati et al., 2011). The authors studied two siblings affected by GD and sharing the same genotype [c.535G>C (p.D140H)/c.10936G>A (p.E326K)]; c.586A>C (p.K157Q), but displaying very different phenotypes. Sibling 1 was diagnosed with GD type 3 presenting with progressive myoclonic epilepsy and dementia while sibling 2 was found to have asymptomatic GD. In cultured fibroblasts, P1 showed a lower GCase expression and activity with respect to P2 and the analyses of *SCARB2* showed the presence a mutation in LIMP-2 COOH-terminal tail, c.1412A>G (p.E471G) only in sibling 1. Thus the authors proposed that the presence of this aminoacid variation may lead to an impairment of the ability of LIMP-2 to bind GCase, which would in turn be unable to reach the lysosomes. This is a very interesting finding. However, whether the differences in GCase expression and enzymatic activity between these siblings are due to an impairment of LIMP-2-GCase association was not established. In fact, other factors such us differences in the abundance and/or activity of components of the ubiquitine- proteasome system may account for a different level of degradation of GCase in both siblings (Horowitz et al., 2008).

In fact, in our work we demonstrated that the E471G mutation does not impair the binding capacity of LIMP-2 to GCase. However, we have shown lower levels of LIMP-2 protein in cells transfected with the *SCARB2* mutant constructs with respect to the expression in cells transfected with the *SCARB2* wild type.

It has been well described the role of COOH-terminal cytoplasmic tail of LIMP-2 in the proper localization of LIMP-2 in the endo-lysosomal compartment through the interaction with the adaptor-like complex AP3. The interaction is dependent on the Leucine-Isoleucine (LI) motif and two acidic amino acid residues, D470 and E471 in positions –4 and –5 to the LI motif are crucial for this binding (Le Borgne et al., 1998; Honing et al., 1998). Furthermore it has also been demonstrated that residue D470 and E471 are implicated in the lysosomal localization of LIMP-2, in the presence of D470A or E471A mutations LIMP-2 shows a significant early endosomal localization (Tabuchi et al., 2000).

In light of these data, it is likely that the aminoacid change at position 471 leads also to an improper localization of LIMP-2 with the consequent reduction of protein levels. Therefore, even if the interaction between GCase and LIMP-2 would be preserved in patients carrying the *SCARB2* E471G mutation, the amount of LIMP-2 generated from

this allele would not be enough to allow a partially active GCase mutant protein to reach the lysosomes.

To shed further light on the possible role of LIMP-2 as modifier in GD, the entire coding region of *SCARB2* gene was analyzed in a group of 5 patients affected by GD3 with myoclonic epilepsy. It is worth noting that these patients presented, in all cases, a genotype associated with the neuronopathic forms of GD (GD2 and GD3), but not always associated with myoclonic epilepsy. Therefore, the presence of other genetic or non genetic factors that modify the phenotype has been hypothesized.

Our screening identified only a single nucleotide change localized in intron 5 with no predicted pathological effect. This result suggests that factors other than SCARB2 mutations, would modify the GD phenotype at least in the small group of patients included in this study.

Few years after the identification of LIMP-2 as the receptor of GCase, mutations in *SCARB2* gene, encoding LIMP-2 were found to cause action myoclonus-renal failure (AMRF) syndrome, characterized by progressive myoclonic epilepsy with associated renal failure. It typically presents with neurological symptoms including tremor, seizures, ataxia and action myoclonous, which overlap with those frequently observed in GD type 3. These phenotypic similarities are not unexpected considering that LIMP-2 deficiency leads to a mistargeting of GCase and the consequent lack of GCase protein within the lysosomes. Conversely AMRF patients do not show the massive occurrence of lipid laden macrophages and consistently they do not show elevated plasma chitotriosidase activity (a marker of macrophage activation). In addition, they present normal or slightly reduced GCase activity in leucocytes but absent or reduced GCase activity in fibroblasts (Blanz et al., 2008; Dardis et al., 2009).

These differences at the biochemical and clinical level suggest that the role of LIMP-2 in the transport of GCase to the lysosomes would not be the same in all tissues and probably alternative lysosomal targeting pathways may be active in different tissues.

In line with this idea, it has been shown that LIMP-2 deficient mice display different levels of GlcCer accumulation in different tissues. Liver and lung presented elevated level of GlcCer, conversely kidney, spleen and brain were apparently unaffected (Reczeck et al., 2007). In fact, such tissue specific differences in mice may result from

differences in the amount of GCase that is transported to the lysosomes in different tissues even in the absence of LIMP-2, even if they may also account for differences in substrate availability or utilization in each tissue.

However, until now a characterization of the role of LIMP-2 in the trafficking of GCase to the lysosomes in human tissues has not been performed. Therefore, different cell types from an AMRF patient were analyzed and the results compared with those obtained in GD patients in which GCase activity is deficient in all tissues.

Our data demonstrated that in machrophages, and generally in white blood cells, of LIMP-2 deficient individuals, at least part of GCase protein can still reach the lysosomes. These finding may explain why patients affected by AMRF do not present “gaucher cells” in bone marrow an show normal levels of chitotriosidase activity. It is possible to hypothesize that these cells express membrane proteins other than LIMP-2 that mediates the intracellular transport of GCase from ER to lysosomes. It will be interesting to look at other receptors involved in the sorting of lysosomal proteins that might be active in different tissues.

In fact, many aspects of lysosomal targeting pathways still need to be elucidated. It is likely that M6P-dependent and independent routes collaborate in the targeting of lysosomal enzymes and the relative contribution of each mechanism may be different in different tissues. Regarding the M6P-independent trafficking of lysosomal proteins, sortilin has been implicated in the binding of different ligands and in the transport to lysosomes of several proteins, both hydrolytic and non-hydrolytic such as the sphingolipid activator protein, prosaposin and GM2 activator protein, acid sphingomyelinase and cathepsin D and H (Petersen et al., 1997; Mazella et al., 1998; Lefrancois et al., 2003; Ni and Morales 2006; Canuel et al., 2008). Considering the multifunctional role of sortilin in the trafficking of lysosomal proteins, it is a good candidate to mediate the LIMP-2 indipendent targeting of GCase in blood cells and further studies should be performed in order to address this issue.

We have also studied the trafficking of exogenous GCase in order to elucidate the role of LIMP-2 in the uptake of recombinant GCase used for enzyme replacement therapy (ERT) in GD patients. We demonstrated that while GCase enters the cells using a LIMP-2 indipendent mechanism, probably via mannose receptor as thoroughly described (Mistry et al., 1996; Friedman et al., 1999), LIMP-2 is necessary for the intracellular trafficking between endocytic compartments. However, even if we

have demonstrated that LIMP-2 is involved in the trafficking of recombinant GCase to the lysosomes in fibrobalsts, alternative mechanisms in cells of mononuclear phagocyte origin, the main target tissue of ERT in GD cannot be ruled out. Further studies to address this issue are still ongoing.

Neuronal disfunction is a typical feature of GD2/GD3. It has been demonstrated that the increase of GlcCer correlates with the severe neurodegeneration and loss of neurons observed in neuronopathic forms of GD (Pelled et al., 2000). On the other hand, AMRF patients present several neurological symptoms and the accumulation of undefined storage material in the brain has been described. The nature of this material and the molecular events leading to neurodegeneration in these patients are unknown.

The study of neurodegenerative diseases results difficult due to the unavailability of human samples. Although murine models of neuronopatic GD (Enquist et al., 2007) and of LIMP-2 deficiency (Gamp et al., 2003) have been developed, they present a phenotype that does not completely overlap the phenotype observed in human patients. Indeed, LIMP-2 knockout mice show no evidence of action myoclonus or seizures (Gamp et al., 2003; Berkovic et al., 2008).

Recently, we described a method to develop a human neuronal model of Niemann Pick C disease, a severe neurodegenerative lysosomal storage disorder, by differentiation of multipotent adult stem cells obtained from skin biopsies (hSKIN-MASC) of affected patients (Bergamin et al., 2013).

In order to study the role of LIMP-2 in the neuronal pathology of AMRF, we developed a human neuronal model of AMRF by inducing neuronal differentiation of hSKIN-MASC isolated from an affected patient. In addition, using the same method, a neuronal model of GD2 was generated for comparison. Cells obtained both from GD2 and AMRF patients showed similar levels of residual GCase activity, suggesting that LIMP-2 might be the main receptor for the lysosomal trafficking of GCase in neuronal cells.

Considering that in neuronal cells the deficit of LIMP-2 leads to a severe impairment of enzymatic activity, we hypothesized that in these cells undigested glycosphingolipids would accumulate within lysosomes.

Indeed, we observed an enlargement of endo-lysosomal compartment in cells derived from patients compared to healthy control cells.

It is likely that lysosomal enlargement is caused by accumulation of undigested glycosphingolipids. In fact, the analysis of the acidic compartment volume has been recently proposed as a universal marker for LSD (Te Vruchte et al., 2014).

However, an alteration in lysosomal biogenesis cannot be excluded. In fact, it has been previously reported that cells over-expressing LIMP-2 show an enlargement of early endosomes and late/endosomes/lysosomes, and a role of this protein in the biogenesis and maintenance of the endo-lysosomal system has been proposed (Kuronita et al., 2002).

It has been demonstrated that in addition to the primary substrate, cells from patients affected by different LSD accumulate a wide variety of macromolecules. This is not surprising, given that the main role of the endosomal/lysosomal system is to degrade and recycle substrates derived from the cell surface by endocytosis and from inside the cell by autophagy. Therefore, it would be logical that single lysosomal protein defects might lead to overall dysfunction of this system and therefore to the storage of multiple substrates. In particular, storage of gangliosides, sialic acid containing glycosphingolipids, mostly found in the central nervous system, has been described as a hallmark of neuronopathic forms of LSD, including GM1 and GM2 gangliosidoses, GD type 2 and 3 and Niemann-Pick C (Boomkamp et al, 2008). Since in human brain GM2 and GM3 are normally very minor components and constitute no more than 1-2% of the total gangliosides, it is likely that a little increase of these gangliosides may lead to pathological effects.

Differentiated cells from GD type 2 patients accumulate GM2 gangliosides. Interestingly, differentiated cells from the AMRF patients accumulate GM2 ganglioside to a similar extent. No accumulation of GM1 and GM3 ganglioside was in GD or in AMRF cells.

Cholesterol accumulation has also been demonstrated to occur as a secondary event in several LSD such us Niemann pick C (Sleat et al., 2004; Zervas et al., 2001; Reid et al., 2004) GM1 and GM2 gangliosidosis, α-mannosidosis (Crawley et al., 2007) as well as MPS I, II, IIIA, and VI diseases (McGlynn et al., 2004; Walkley et al., 2005). While total cholesterol levels in brain are apparently not increased, in situ labeling

using filipin staining reveals the presence of conspicuous sequestration of unesterified cholesterol in individual brain cells (Walkley and Vanier 2009).

We confirmed that cholesterol accumulates in fibroblasts from GD patients as previously reported (Salvioli et al., 2005) and demonstrated that it also accumulates in fibroblasts from an AMRF patient. Conversely in neuronal derived cells of GD and AMRF patients, no cholesterol storage was observed.

Accumulation of glycosphingolipids (GSL) has been linked to signal transduction derangements (Walkley et al., 2009). "Lipid rafts" [also referred to as membrane rafts and detergent-resistant membranes (DRM)] are low-density membrane domains enriched in cholesterol, GSL, and phospholipids. They play a role in many cellular functions, facilitating interactions among the lipid and protein components of signaling pathways, thereby regulating these processes (Simons et al., 2000). The lipid composition of the membrane rafts is highly specialized, and it is this unique composition that enables them to carry out their signaling role (Brown et al., 1998). Therefore, to ensure their function the composition of the lipid rafts must be tightly regulated by mechamisms involved in the control of GSL synthesis and degradation and in the transport to and from the cell surface. It has been extensively shown that the composition of lipid rafts is altered in several disorders affecting proteins involved in the GSL degradative pathways, suggesting key role of these membrane microdomains in the developing of pathological phenotype (Hein et al., 2008; Dawson et al., 2012; McGlynn et al., 2004).

In addition, altered trafficking of gangliosides out of the endosomal/lysosomal system to other sites in the cell (e.g.: the endoplasmic reticulum) cause consequences on neuron function. It has been proposed, that in GM1 gangliosidosis the GM1 ganglioside mislocalizes to membrane domains normally containing little or no ganglioside, like the ER, resulting in depletion of Ca++ stores, activation of the ER stress response and eventually apoptosis and neuron death (d'Azzo et al., 2006). Similarly, in GM2 gangliosidosis it has been shown that GM2 ganglioside increases in microsomal membranes and inhibits the activity of SERCA (Sarco/Endoplasmatic Reticulum Calcium ATPasi), which in turn has the capacity to cause ER stress and apoptosis (Ginzburg et al., 2004).

Whether this cascade of events is triggered by GLS accumulation also in LIMP-2 deficient neurons needs to be investigated.

However, the human neuronal model presented here, offers a interesting source for the study of neuronal pathology in this and other neurodegenerative diseases.

In conclusion, this work provides new insight into the nature of GCase-LIMP-2 interaction and the GCase intracellular trafficking.

5. Material and Methods

5.1 Patients

Novel *GBA* mutations were found in 10 patients diagnosed with GD disease based on the demonstration of reduced GCase activity in white blood cells or fibroblast and lymphoblast cell lines. According to clinical parameters including onset, visceromegaly, bone disease and neurological signs, 5 patients were classified as GD1, 2 as GD2 and 1 as GD3 (Beutler and Grabowski, 2001).

5.2 Patients' cell lines

Fibroblasts were cultured and maintained in Dulbecco's modified Eagle's medium (DMEM) (EuroClone, Gibco) containing 10% of fetal calf serum (FCS) and penicillin/streptomycin, in a humidified atmosphere containing 5% CO2 at 37°C.

Lymphoblasts cells were cultured in RPMI medium (EuroClone, Gibco) containing 15% of fetal calf serum (FCS) and penicillin/streptomycin, in a humidified atmosphere containing 5% CO2 at 37°C.

5.3 GCase enzymatic activity determination

To measure GCase enzymatic activity, cells were lysed in H_2O containing a complete protease inhibitor cocktail and sonicated for 15sec. Protein concentration of samples was determined using the Bradford reagent (Biorad).

GCase activity was determined using the fluorogenic substrate 4-methylumbelliferyl-β-D-glucopyranoside (Sigma). Ten µl containing 6-7 µg of proteins obtained from cell lysates were incubated with 10 µl of 5mM 4-metylumbellyferil-β-D-glucopyranoside (Sigma) in 0.1M acetate buffer pH 4.2 at 37°C for 3 hrs. The reaction was stopped adding 2ml of 0.5M carbonate buffer pH10.7 and the fluorescent product quantified using a Spectra MAX GEMINI XPS fluorimeter (Molecular Devices) at excitation

wavelength of 335nm and emission of 495nm. The nanomoles of substrate hydrolyzed of unknown samples were calculated using a standard calibration curve and enzymatic activity was expressed as nanomoles of substrate hydrolyzed per milligram of total protein per hour.

For blood cells and Hek293 cell lines, GCase activity was determined using 10-50 µg of protein in the presence of 7,5mM 4-metylumbellyferil-β-D-glucopyranoside (Sigma-Aldrich) in 0.1M citrate/0,2Mphosphate buffer pH 5.2, containing 0,15% taurocholate (w/v, Calbiochem) at 37°C for 2 hrs. The reaction was stopped adding 2ml of 0.5M carbonate buffer pH10.7 and the fluorescent product quantified.

5.4 DNA extraction

Genomic DNA for molecular analysis was obtained from different samples such as peripheral blood leukocytes, fibroblasts, immortalized lymphoblasts and purified using the QIAampDNA Blood mini Kit (Qiagen GmbH) following the manufacturing instructions.

5.5 RNA extraction

Total RNA was extracted from peripheral blood leukocytes, fibroblasts and cell lines using Rneasy mini Kit (Qiagen) following the manufacturing instructions. RNA obtained was stored at -80°C.

5.6 Nucleic acids quantification

Nucleic acids were quantified by spectrophotometry measuring the absorbance (A) at 260nm. The nucleic acid concentration was calculated according to the following equation: 1OD = 50 µg/µl DNA and 1OD = 40 µg/µl RNA. Protein content was calculated by measuring the absorbance at 280 nm and the sample was considered to be well purified when the 260/280 ratio was between 1.6 and 2.

5.7 GBA gene amplification

GBA gene was amplified from genomic DNA by PCR. To discriminate the gene from the highly homologous pseudogene it is important to design the oligonucleotides in region with the lowest homology. The 11 exons of GBA gene and flanking intronic regions were amplified in 3 fragment as described by Koprovica et al. (2000). The reaction was carried out in a mixture containing the Platinum DNA Polymerase High Fidelity (Invitrogen), 10 pmol of each primer and 10 nmol of dNTPs at the following conditions:

- 94°C 2'
- *10 cycles:* 94°C 10" ; (T ann) 30"; 68°C 4'
- *20 cycles:* 94°C 10"; (T ann) 30"; 68°C 4' (+20'' on each cycle)
- 68°C 7'

Table 5.1: *GB*A gene amplification

FRAGMENT	PRIMERS	ANNEALING TEMPERATURE (°C)	SIZE (bp)
1-5	CCTAAAGTTGTCACCCATAC AGCAGACCTACCCTACAGTTT	57	2970
5-7	GACCTCAAATGATATACCTG AGTTTGGGAGCCAGTCATTT	58.5	2050
8-11	TGTGTGCAAGGTCCAGGATCAG ACCACCTAGAGGGGAAAGTG	61	1681

5.8 SCARB2 gene amplification

The reaction was carried out in a mixture containing *GoTaq DNA Polymerase* (Promega) 10 pmol of each primer and 10 nmol of dNTPs at the following conditions:

- 95°C 5'
- *35 cycles:* 95°C 30" ; (T°C annealing) 30"; 72°C 1'
- 72°C 7'

Table 5.2: *SCARB2* gene amplification

EXON	PRIMERS	ANNEALING TEMPERATURE (°C)	SIZE (bp)
1	CTGCACTCTCCCGAGCTG AGATGTAGCAGCAGGGATGG	61	473
2	GCGTCCCTTCCTCTGCTTCT TGGGAAGAGGCAAGGACTCA	63	313
3	ACTTGGATGCTGAAAGAAAG TGGCTCCTAAATGTAAAATC	58	320
4	CCCCTTTGCTATGGGGTAGT AGTTAATCTGGCTTGGGGTG	60	347
5	GCACCATAGTCTAGCCAAGTT GCAATGTAGAAGTAGACATGT	62	236
6	CTGTGGATAGACAGCTCCAG CATGCTTTTGGTGGTCTTGC	63	283
7	GTTGTACCTGAGAACTGTTG AACTCCAATCCTTCTGCATT	62	311
8	GAACTAGGAGGTAAAGGATGGTG GCTCAGGACTAAACTGGTGAACA	58	281
9	GACTACACACAGAAATGGTGCT GAAGTAGGCTGTACTCCTCC	63	340
10	TATAAATGTGTCTGTCCGGG TCTTTTGCCCTTCTGTCATA	61	236
11	CTAACAGGAGGACATTCCCA ATAAGCCAGCTGACAGCCCT	63	360
12	GTGAGTGAGATGAGCCACCT TCTGGCCAGAATGTTCCTAT	63	319

5.9 Reverse transcription and cDNA amplification

For RT-PCR analysis, the first strand cDNA was synthesized with random primers (Invitrogen) using the SuperScript™ II Reverse Transcriptase (Invitrogen) following manufacturer instructions.

In the first step (cDNA synthesis), 1 µg of total RNA was incubated with 50-250ng of random primers and 10nmol dNTPmix in a volume of 12 µl at 65°C for 5 min, then 4µl buffer 5X, 1µl DTT 0.1M, 40U RNAse OUT and SuperscriptIII (Invitrogen) were added and the sample was maintained for 10 min at 25°C, at 42°C for 50 min, followed by the inactivation at 70°C for 15 min.

The cDNA obtained in first step was used as template for the second step: to 2µl cDNA was added the PCR mix containing the enzyme buffer (Tris-HCl pH8.3, 1.5mM

$MgCl_2$, 50mM KCl), 10nmol dNTPs mix (Invitrogen), Platinum DNA Polymerase High Fidelity (Invitrogen), 10pmol of each primer in a volume of 50µl.
The cDNA of LIMP-2 was amplified in one fragments. In Table 2 are reported primers, optimal annealing temperature and size of the RT-PCR fragment. The PCR reaction was composed of three cycles (denaturation at 95°C for 1 min, annealing for 1 min and extension at 72°C for 1' 30'') repeated 45 times.

Table 5.3: RT-PCR for SCARB2 cDNA amplification

PRIMERS	ANNEALING TEMPERATURE (°C)	SIZE (bp)
CCCAAGCTTATGGGCCGATGCTGCTTCT CCGGAATTCTTAGGTTCGAATGAGGGGT	63	1437

5.10 Nucleic acids electrophoresis

To evaluate the yield of an amplification reaction, the PCR or RT-PCR product was loaded on an agarose gel (Sigma). This method was also useful to purify fragment obtained from non-optimized amplifications and enzymatic reactions.
The agarose concentration varied from 0.8% to 2% in TBE buffer (50mM Tris, 50mM boric acid, 1mM EDTA pH8) depending on the fragment length. Fragments were visualized using an intercalating molecule, ethidium bromide (Sigma-Aldrch) 1µg/ml, which is fluorescent when put on an UV transilluminator (Euroclone).
Samples were loaded on the gel with Loading Buffer 6X (7 volumes glycerol, 3 volumes H_2O, 0.25% bromophenol blue, 0.25% xylene cyanol) and their molecular weight was compared with 1kb Plus DNA Ladder (Invitrogen).

5.11 Gel extraction of DNA fragments

To isolate PCR fragments, the DNA was loaded on an agarose gel and the band of interest was excised and purified using the QIAquick gel extraction kit (Qiagen GmbH).

5.12 Automatic sequencing

The samples were analyzed by automated sequencing (ABI Prism 3500xl genetic analyzer). The reaction synthesized a mixture of DNA fragments using the BigDye® terminator cycle sequencing kit (Applied Biosystems) which contains the DNA polymerase, the dNTPs mix and the four ddNTPs modified with four different fluorochromes. The samples loaded on a 96-well plate were separated by electrophoresis through the POP 7 polymer (Applied Biosystems). The result was visualized as electropherogram where four different colors represented the four nucleotides.

Briefly, purified PCR product were sequenced adding 5pmol of the sequencing primer, BigDye® and 5X sequencing Buffer (Applied Biosystems) to a final volume of 20µl at the following conditions: 25 cycles (denaturation at 95°C for 10 sec, annealing at 50°C for 15 sec, extension at 72° C for 2 min).

It was necessary to remove the reaction components to prevent the presence of a background signal on the electropherogram. Therefore, the sequence product was precipitated with 2 volumes of ethanol and 1/10 CH_3COONa 3M pH5.2. The pellet was then washed with ethanol 70%, dried and resuspended in 15µl of formamide Hi-Di™ (Applied Biosystems) and denatured for 2 min at 95°C.

5.13 Mutation nomenclature

All mutations are described according to current mutation nomenclature guidelines (http://www.hgvs.org/mutnomen).

For GBA the A of the first ATG translation initiation codon as nucleotide +1 (GenBank NM_000157.3). Traditional amino acid residue numbering, which excludes the first 39 aminoacids of the leader sequence, has nevertheless also been provided in parentheses and designed without the prefix “p”.

5.14 Splicing Prediction

To predict the potential effect of the novel mutant alleles on splicing process, the following programs were used:

- ME: Maximum Entropy available at http://genes.mit.edu/burgelab/maxent/Xmaxentscan_scoreseq_acc.html
- NN: Neural Network available at http:// www.fruitfly.org/seq_tools/splice.html

5.15 GBA constructs

Novel *GBA* missense mutations found in this study and the two common N370S and L444P mutations were expressed *in vitro* to establish their effect on GCase function. The mutations were introduced in the wild type full length cDNA cloned in pcDNA3 already described (Miocić et al., 2005) by site directed mutagenesis using the Quikchange Site-directed Mutagenesis Kit (Stratagene) according to manufacturer's instructions. The sequence of primers used for mutagenesis are listed in **Table 5.4**.

Table 5.4. Primers for mutagenesis

Point Mutations	Primers used for site directed mutagenesis
c.592C>T p.P198C (P159S)	ATACCAAGCTCAAGATA**t**CCCTGATTCACCGAGCC GGCTCGGTGAATCAGGG**a**TATCTTGAGCTTGGTAT
c.680A>T p.N227I (N188I)	CCACTTGGCTCAAGACCA**t**TGGAGCGGTGAA TTCACCGCTCCA**a**TGGTCTTGAGCCAAGTGG
c.680A>G p.N227S (N188S)	CCACTTGGCTCAAGACCA**g**TGGAGCGGTGAA TTCACCGCTCCA**c**TGGTCTTGAGCCAAGTGG
c.820G>A p.E274K (E235K)	AGTGACAGCTGAAAAT**a**AGCCTTCTGCTGGGCT AGCCCAGCAGAAGGCT**t**ATTTTCAGCTGTCACT
c.850C>A p.P284T (P245T)	TGTTGAGTGGATAC**a**CCTTCCAGTGCCTGG CCAGGCACTGGAAGG**t**GTATCCACTCAACA
c.910G>C p.G304R (G265R)	CATTGCCCGTGACCTA**c**GTCCTACCCTCGCCA TGGCGAGGGTAGGAC**g**TAGGTCACGGGCAATG
c.1052G>C p.W351S (W312S)	TGGCATTGCTGTACATT**c**GTACCTGGACTTTCTGG CCAGAAAGTCCAGGTAC**g**AATGTACAGCAATGCCA
c.1093G>A p.E365K (E326K)	CACCCTAGGGGA**g**ACACACCGCCTG CAGGCGGTGTGT**c**TCCCCTAGGGTG

c.1015C>A p.S405R (S366R)	ATGCAGTACAGCCACAG**a**ATCATCACGAACCTCCT AGGAGGTTCGTGATGAT**t**CTGTGGCTGTACTGCAT
c.1226A>G p.N409S (N370S)	GCCACAGCATCATCACGA**g**CCTCCTGTACCATGT ACATGGTACAGGAGG**c**TCGTGATGATGCTGTGGC
c.1255G>A p.D419N (D380N)	GTCGGCTGGACC**a**ACTGGAACCTTGCCCTGAA TTCAGGGCAAGGTTCCAGTT**t**GTCCAGCCGAC
c.1260G>C p.W420C (W381C)	GGTCGGCTGGACCGACTG**c**AACCTTGCCCTGA TCAGGGCAAGGTT**g**CAGTCGGTCCAGCCGACC
c.1448T>C p.L483P (L444P)	GCCAGTCAGAAGAACGACC**c**GGACGCAGTG CACTGCGTCC**g**GGTCGTTCTTCTGACTGGC
c.481G>C p.D179H (D140H)	TGCAGACACCCCT**c**ATGATTTCCAGTTGCA TGCAACTGGAAATCAT**g**AGGGGTGTCTGCA
c.586A>C p.K196Q (K157Q)	AAGATACCAAGCTC**c**AGATACCCCTGATTC GAATCAGGGGTATCT**g**GAGCTTGGTATCTT

5.16 SCARB2 cloning

cDNA of SCARB2 was clonend into pcDNA4-myc/His (Invitrogen). Briefly pcDNA4-myc and SCARB2 cDNA (obtained by RT-PCR) were digested with *Eco*RI and *Hind*III. The ligation reaction was performed using T4 DNA ligase (New England Biolabs) following the manufacturer instruction. The E471G mutation was introduced in the wild type full length cDNA by site directed mutagenesis using the Quikchange Site-directed Mutagenesis Kit (Stratagene) according to manufacturer's instructions. The sequence of primers used for mutagenesis are listed in **Table 5.5**.

Table 5.5. Primers for mutagenesis

Point Mutations	Primers used for site directed mutagenesis
c.1412A>C (E471G)	GGGAACAGCGGATG**g**AAGAGCACCCCTCAT ATGAGGGGTGCTCTT**c**CATCCGCTGTTCCC

5.17 Competent cells preparation

For the transformation the *E.Coli* strain DH5α was used. One DH5α colony was grown in 3ml LB medium (Luria-Bertani medium: 1 liter: Bactotryptone 10g, Yeast extract 5g, NaCl 10g; pH 7.5) at 37°C for 16-18 hrs. Then, 400µl of bacterial culture were grown in 200 ml LB at 37°C until the absorbance at 600nm was between 0.3 and 0.4. The bacteria were centrifuged and the pellet was resuspended in 1/10 volume of TSS (10% PEG, 5% DMSO, 20-50mM $MgSO_4$ or $MgCl_2$ in LB medium) and stored at -80°C in aliquots.

5.18 Transformation

80µl DH5α were added to the ligation mix and incubated 30 min on ice. Permeability of bacterial membrane was obtained by heat shock at 42°C for 90". After incubation for 1 hour at 37°C in 300µl LB medium, bacteria were plated on LB-agar containing the selection antibiotic (Ampicillin 75µg/ml) and grown o/n at 37°C.

5.19 Plasmid preparation

Plasmid Miniprep

Ampicillin-resistant colonies were grown in 3ml LB medium with Ampicillin 20µg/ml at 37°C for 16-18hrs. For the plasmid DNA extraction the "QIA PREP SPIN MINIPREP" kit (Qiagen GmbH) was used following the manufacturer's instructions.

Plasmid Maxiprep

Positive colonies were grown in 200ml LB medium with Ampicillin 20µg/ml at 37°C for 16-18hrs. For the purification of plasmid DNA the "Purelink hipure plasmid filter maxiprep kit" (Invitrogen) was used following manufacturer's instructions.

5.20 Transient transfection

Human Hek293 cells were grown in Dulbecco's modified Eagle's medium (DMEM) supplemented with 10% FCS, 2mM glutamine, 100 U/ml penicillin and 100 mg/ml streptomycin (Gibco) at 37°C in a humidified atmosphere enriched with 5% (v/v) CO_2. Cells were transfected with the 4 µg of constructs using Lipofectammine^{TM} 2000 (Invitrogen) according to manufacturer's instructions. After 48 h cells were harvested

and the cellular extracts were analyzed for GCase activity and for GCase-LIMP-2 interaction.

5.21 SDS PAGE and Western Blot

Cell were washed three times with ice-cold phosphate-buffered saline (PBS) and lysed at 4°C in Cell Lysis Buffer TNN (Tris-HCl 100mM pH 8, NaCl 250mM, NP40 0.5%). Lysates were incubated on ice for 30 min and centrifuged at 10000g for 15 min at 4°C. Samples containing the same amount of protein were electrophoresed through 10% SDS–PAGE and blotted onto a nitrocellulose membrane (Biorad).
Membranes were blocked with 5 % non-fat milk in TBS (0.01M Tris HCl, 0.15M NaCl) containing 0.1% Tween (TBST) and incubated with the primary antibody. The membranes were then washed three times in 0.1% Tween-20 in TBS and incubated with the appropriate secondary antibody for 1 h at RT. After washing, membranes were reacted with ECL detection reagents (Santa Cruz Biotechnology, Inc.).

5.22 Immunoprecipitation of LIMP-2 and Myc tagged LIMP-2

Hek293 cells transfected with wild type and mutated GBA constructs or co-transfected with GBA constructs and Myc tagged LIMP-2 construct were lysed in Co-IP buffer (100 mM NaCl, 10 mM Hepes pH 8, 1 mM $MgCl_2$, 0.5% NP40 (v/v) supplemented with protease inhibitor cocktail containing PMSF, NaF, Na_3VO_4, and Iodoacetamide. The lysates were incubated on ice for 30’ and then centrifugated at 10,000 g for 15sec. Protein concentration was determined by Bradford using Bio-Rad Protein Assay (Biorad, Hercules, CA, USA).
For immunoprecipitation of endogenous LIMP-2, for each samples 650 µg of cell lysate were precleared with 30 µl of protein A/G (Santa Cruz Biotechnology Inc) for 2 h at 4°C. The supernatant was then incubated over night at 4°C with a rabbit polyclonal α-LIMP-2 antibody (Novus Biologicals). Then 30 µl of protein A/G were added and incubated for 3 h. After 3 washes with Co-IP buffer, proteins were eluted for 10 min at 100°C in SDS sample buffer, separated by 10% SDS PAGE and transferred onto nitrocellulose membranes (Biorad, Hercules).

For immunoprecipitation of Myc tagged LIMP-2 or mutated LIMP-2, 200 µg of protein were incubated overnight at 4°C with sepharose immobilized mouse anti-Myc antibody (Cell Signaling Technology Inc) followed by three washes with Co-IP buffer, proteins were eluted for 10 min at 100°C in SDS sample buffer, separated by 10% SDS PAGE and transferred onto nitrocellulose membranes (Biorad, Hercules).

5.23 Antibodies

Anti GCase antibody (2E2 clone, Abnova), anti- human LIMP-2 antibody (Novus Biologicals) or anti-human β Actin antibody (Sigma-Aldrich).
Secondary antibodies: Anti-rabbit HRP conjugated antibody and Anti-mouse HRP conjugated antibody (DAKO).

5.24 Structural 3D analysis

Visual inspection of GCase three dimensional structure (PDB code 1OGS) and amino acid substitutions were carried out using the program Coot (Emsley et al., 2004), energy minimization using the program DISCOVER3 from the InsightII program suite (Accelrys, Inc.). Figures were drawn using the program Chimera (Pettersen et al., 2004). The possible disulfide bridges were predicted using the program http://clavius.bc.edu/~clotelab/DiANNA/

5.25 Endoglycosidase-H digestion

To evaluate the endo-H resistant and endo-H sensitive fractions, variable amounts of total cellular extracts were subjected to overnight incubation with 10mU of endoglycosidase-H (Boehringer Mannheim GmbH) in 20µl of 50mM sodium citrate buffer pH5.2 containing 0.5mM PMSF, 0.1% SDS, 0.5%, 0.1M 2-ME and 0.5% Triton-X. After digestion, samples were subjected to Western Blot.

5.26 Uptake of rhGCase and correction of GCase activity

To study rhGCase uptake and correction of GCase activity, control fibroblasts were incubated with different concentrations (50nM - 2µM) of imiglucerase (Cerezyme®)

and Velaglucerase alfa (VIPRIN™) for 4 hours to determine the working concentration for further assays. The cells were then harvested and cell pellets were washed twice with PBS, resuspended in water and disrupted by sonication. GCase activity was assayed as already described (5.3). Protein concentrations were determined in total homogenates by the Bradford assay (Bio-Rad).

GD, AMRF and control fibroblasts were incubated with 200 nM -1,6 µM of Velaglucerase. The cells were washed and analyzed by western blot and for enzymatic activity.

To study the uptake of fluorescent rhGCase, Velaglucerase was labelled and purified using the Alexa Fluor 555 Protein labelling kit (Invitrogen), according to the manufacturer's instructions. Fibroblasts were incubated with Alexa Fluor 555-labeled hrGCase (15nM) for different times 0, 30minutes, 1 and 2 hours. Lysotracker-Green (75 nM) was added for the last 30 min. The cells were fixed in 4% paraformaldehyde in PBS for 15 minutes and examined on a fluorescence microscope.

5.27 Monocyte isolation and differentiation

Peripheral blood mononuclear cells (PBMCs) were obtained from buffy coats by density centrifugation using Ficoll (GE Healthcare). Briefly, the buffy coats were mixed with an equal volume of phosphate buffered saline (PBS), pH = 7.4, layered over on a volume of Ficoll equal to the volume of blood, centrifuged 15’ 700 x g and washed three times with PBS, pH = 7.4. The monocytes were then isolated by magnetic separation, using the CD14+ microbeads following the customer instruction (Miltenyi Biotech). Purified cells were stained for CD14 (Miltenyi Biotech), and the purity of monocytes was determined by flow cytometry to be >90%. The CD14 positive cells were treated with human macrophage colony stimulating factor (m-CSF) (Miltenyi Biotech) for seven days.

5.28 Lymphocyte Transformation

1×10^6 lymphocytes were grown in 500 µL of RPMI medium (EuroClone, Gibco) containing 15% of fetal calf serum (FCS) and penicillin/streptomycin added with 300µl of EBV (Epstein-Barr virus) supernatant, previously prepared from marmoset cell line

B95-8 and with cyclosporine A (0.1µg/ml, Sigma-Aldrich). After 10-15 days the typical outgrowths are clearly visible.

5.29 Stem cell selection and culture

Stem cell enriched cultures were obtained, both from already established skin fibroblast cultures at early passages (P1, P2, P3), adapting the methods previously described (Beltrami et al., 2007; Cesselli et al., 2009). 1×10^6 cells obtained from confluent primary skin fibroblast cultures were seeded onto 100 mm plates coated with fibronectin and expanded at least for three passages in a selective media composed of 60% Dulbecco's Modified Eagle medium (DMEM Low Glucose, Euroclone)/40% MCDB-201 (Sigma-Aldrich) supplemented with 1 mg/ml Linoleic Acid-BSA (Sigma-Aldrich); 10-9 M dexamethasone (Sigma-Aldrich); 10-4 M Ascorbic acid-2 phosphate (Sigma-Aldrich); 1X Insulintransferrin-sodium selenite (Sigma-Aldrich); 2% fetal bovine serum (FBS), (STEMCELL Technologies), 10 ng/ml human PDGF-BB (Peprotech EC); 10 ng/ml human EGF (Peprotech EC). Medium was replaced every 4 days and cells were split when they reached 70-80% confluence.

5.30 Neuronal differentiation

For neurogenic differentiation, stem cells obtained after 3 passages in selective medium, were seeded at a density of 40.000 cells/plate into 100 mm plates or on coverslips coated with fibronectin. Cells were plated in medium containing DMEM High Glucose (Euroclone, Gibco)/Nutrient mix HamF12(Sigma Aldrich) (1/1) medium with 10% FBS (called N1 medium). After 24 hours the medium was replaced with fresh medium supplemented with 1% of B27 (Invitrogen), 10 ng/ml EGF (Peprotech) and 20 ng/ml bFGF (Peprotech) (called N2 medium) for 5 days. Thereafter, cells were incubated for 24/48 hours in DMEM supplemented with 5 µg/ml insulin, 200 µM of indomethacin and 0.5 mM IBMX (all from Sigma-Aldrich) without FBS (called N3 medium).

5.31 Immunofluorescence microscopy

Cells were fixed for 20 min with 4% paraformaldehyde in PBS and permeabilized for 5 min with 0.1% Triton X-100 in PBS. Slides were incubated over night at 4°C with primary antibody. The primary antibody was the revealed by Alexa-Fluor 555 or 488 labeled secondary antibodies (Molecular Probes) at 1:600 dilution. Images were obtained with a live cell imaging dedicated system consisting of a Leica DMI 6000B microscope connected to a Leica DFC350FX camera (Leica Microsystems).

Primary antibodies: anti-LAMP1 (Santa Cruz, 1:100), anti-LIMP-2(Novus Biological, 1:100), anti-GBA clone 2E2 (Abnova, 1:50), anti-NeuN, (Millipore, 1:50) and anti-MAP2 (Millipore, 1:50).

GM1 analysis: cells were grown on coverslips then fixed in 3% paraformaldehyde for 30 minutes at room temperature. Cells were then incubated at room temperature for 1 hour in blocking buffer: PBS with 2% albumin bovine serum (BSA) and 0.1% triton. Then the cells were stained 1 h at RT with 3µg/ml of cholera toxin B (Sigma Aldrich) in 0.2% BSA in PBS. Cells were washed and visualized on microscope.

GM2 and GM3 analysis: For the analysis of GM2 and GM3 gangliosides: cells were grown on coverslips then fixed in 4% paraformaldehyde for 20 minutes at room temperature. Cells were then incubated at room temperature for 1 hour in blocking buffer PBS with 10% normal goat serum (NGS) and 0.02% saponin (Sigma-Aldrich) and stained overnight at 4°C with mouse IgM anti-GM2 (1:20 in blocking buffer) or mouse IgM anti-GM3 (1:20 in blocking buffer). Cells were washed 3 times with PBS with 0.02% saponin. Cells were then incubated with a TRITC conjugated donkey anti-mouse IgM (1:80 in PBS with 2% NGS and 0.02% saponin).

In all cases, cell nuclei were stained by Vectashield Mountain Medium with DAPI (Vector Laboratories, Inc).

5.32 Lysotracker FACS analysis

Neuronal differentiated cells were incubated with Lysotracker green 100Mm (Invitrogen) for 20 minutes in the dark. The cells were washed, collected, resuspended in PBS and analyzed by Flow Citometry (BD FACS Calibur). We count 10.000 single events. Sample were acquired and subjected to SSC-H versus FL1-H gating on singlets eliminating double events.

5.33 Filipin staining

Filipin staining was performed using the method previously described (Blanchette-Mackie et al., 1988). Briefly, cells grown on coverslips, were incubated in serum free medium for 24 hours and then treated for 24 hours with Low Densit Lipoprotein LDL (Sigma-Aldrich) enriched medium. Cells were rinsed with PBS and fixed with 3% paraformaldehyde. After washing them with PBS, the cells were incubated with glycine 1.5 mg/ml of PBS for 10 minutes, stained with filipin complex (Sigma-Aldrich) (0.05 mg/ml, in PBS 10% FCS) for 2 hours and examined.

5.34 Real time PCR

Total RNA was extracted from both non-confluent cultures of undifferentiated and differentiated cells at P3. After treatment with DNase I (Ambion), first strand cDNA synthesis was performed with 1 μg total RNA using random hexanucleotides and the SuperScript™ III Reverse Transcriptase (Invitrogen) following manufacturer instructions. Primers were designed from available human sequences using the primer analysis software Primer3 (**Table 5.6**). Quantitative RT-PCR was performed using Roche LightCycler 480 Real-Time PCR System and the LightCycler 480 SYBR Green I Master (Roche), following manufacturer's instructions. GAPDH was used as internal control for normalization. LightCycler 480 Basic software (Roche) utilized the second derivative maximum method to identify the crossing point (Cp).

Table 5.6. Primers for Real time PCR

Gene	Primers	T°C melting
OCT-4	TCAGGTTGGACTGGGCCTAGT GGAGGTTCCCTCTGAGTTGCTT	63
NANOG	AATACCTCAGCCTCCAGCAGATG CTGCGTCACACCATTGCTATTCT	62
SOX2	TTGCTGCCTCTTTAAGACTAGGA CTGGGGCTCAAACTTCTCTC	59
ChAT	CCCTGATGCCTTCATCCA GTAGGTGGGCACCAGTCTTC	60
GAD	TCAAGTAAAGATGGTGATGGGATA GCCATGATGCTGTACATGTTG	60
TH	TTGAGGAGAAGGAGGGGAAG GGATTTTGGCTTCAAACGTC	60

DAT	CCAGCTACAACAAGTTCACCAA AGAAGCTCGTCAGGGAGTTG	60

5.35 Statistical analysis

Statistical analysis was performed using the Microsoft Excel data analysis program for Student's *t*-test analysis. P<0.05 was considered as statistically significant.

6. References

Abrahamov A, Elstein D, Gross-Tsur V, Farber B, Glaser Y, Hadas-Halpern I, Ronen S, Tafakjdi M, Horowitz M, Zimran A. Gaucher's disease variant characterised by progressive calcification of heart valves and unique genotype. Lancet. 1995; 346(8981):1000-1003.

Alberts B, Johnson A, Lewis J, Raff M, Roberts K, Walter P. Molecular Biology of the Cell (4th edition)2002: pp739-756. Garland Science, New York, USA.

Alfonso P, Rodrıguez-Rey JC, Ganan A, Pérez-Calvo JI, Giralt M, Giraldo P, Pocoví M. Expression and functional characterization of mutated glucocerebrosidase alleles causing Gaucher disease in Spanish patients. Blood Cells Mol Dis 2004; 32(1):218–225.

Andermann E, Andermann F, Carpenter S, Wolfe LS, Nelson R, Patry G., Boileau J. Action myoclonus–renal failure syndrome: a previously unrecognized neurological disorder unmasked by advances in nephrology. Adv Neurol 1986; 43: 87–103.

Badhwar A, Berkovic SF, Dowling JP, Gonzales M, Narayanan S, Brodtmann A, Berzen L, Caviness J, Trenkwalder C, Winkelmann, J, et al. Action myoclonus-renal failure syndrome: Characterization of a unique cerebro-renal disorder. Brain 2004; 127(10): 2173–2182.

Balreira A, Gaspar P, Caiola D, Chaves J, Beirao I, Lima JL, Azevedo JE and Miranda, MC. A nonsense mutation in the LIMP-2 gene associated with progressive myoclonic epilepsy and nephrotic syndrome. Hum. Mol. Genet. 2008; 17(14):2238–2243.

Barak V, Acker M, Nisman B, Kalickman I, Abrahamov A, Zimran A, Yatziv S.. Cytokines in Gaucher's disease. Eur Cytokine Netw 1999; 10(2):205-210.

Beltrami AP, Cesselli D, Bergamin N, Marcon P, Rigo S, Puppato E, D'Aurizio F, Verardo R, Piazza S, Pignatelli A et al. Multipotent cells can be generated in vitro from several adult human organs (heart, liver and bone marrow). Blood 2007; 110(9):3438–3446.

Beutler E, Nguyen NJ, Henneberger MW, Smolec JM, McPherson RA, West C, Gelbart T. Gaucher disease: gene frequencies in the Ashkenazi Jewish population. Am J Hum Genet. 1993; 52(1):85-88.

Bembi B, Zambito Marsala S, Sidransky E, Ciana G, Carrozzi M, Zorzon M, Martini C, Gioulis M, Pittis MG, Capus L. Gaucher's disease with Parkinson's disease: clinical and pathological aspects. Neurology 2003; 61(1):99-101.

Bembi B, Zanatta M, Carrozzi M, Baralle F, Gornati R, Berra B, Agosti E. Enzyme replacement treatment in type 1 and type 3 Gaucher's disease. Lancet 1994; 344(8938):1679-1682.

Berg-Fussman A, Grace ME, Ioannou Y, Grabowski GA.. Human acid beta-glucosidase. N-glycosylation site occupancy and the effect of glycosylation on enzymatic activity. J Biol Chem 1993; 268(20):14861-14866.

Bergamin N, Dardis A, Beltrami A, Cesselli D, Rigo S, Zampieri S, Domenis R, Bembi B, Beltrami CA.A human neuronal model of Niemann Pick C disease developed from stem cells isolated from patient's skin. Orphanet J Rare Dis. 2013; 8:34.

Berkovic SF, Dibbens LM, Oshlack A, Silver JD, Katerelos M, Vears DF, Lullmann-Rauch R, Blanz J, Zhang KK, Stankovich, J. Array-based gene discovery with three unrelated subjects shows SCARB2/LIMP-2 deficiency causes myoclonus epilepsy and glomerulosclerosis. Am. J. Hum. Genet. 2008; 82(3):673–684.

Beutler E and Grabowski GA: Gaucher disease; in: Scriver CR, Beaudet AL, Sly WS, Valle D (eds): The Metabolic and Molecular Basis of Inherited Disease. New York: McGraw-Hill, 2001, Vol 3, 3635-3668.

Blanchette-Mackie EJ, Dwyer NK, Amende LM, Kruth HS, Butler JD, Sokol J, Comly ME, Vanier MT, August JT, Brady RO: Type-C Niemann-Pick disease: low density lipoprotein uptake is associated with premature cholesterol accumulation in the Golgi complex and excessive cholesterol storage in lysosomes. Proc Natl Acad Sci U S A 1988; 85(21):8022–8026.

Bodennec J, Pelled D, Riebeling C, Trajkovic S, Futerman AH. Phosphatidylcholine synthesis is elevated in neuronal models of Gaucher disease due to direct activation of CTP:phosphocholine cytidylyltransferase by glucosylceramide. FASEB J. 2002; 16(13):1814-1816.

Boomkamp SD, Butters TD. Glycosphingolipid disorders of the brain. Subcell Biochem. 2008; 49:441-467.

Boot RG, Renkema GH, Verhoek M, Strijland A, Bliek J, de Meulemeester TM, Mannens MM, Aerts JM. The human chitotriosidase gene. Nature of inherited enzyme deficiency. J Biol Chem 1998; 273(40):25680-25685.

Boven LA, van Meurs M, Boot RG, Mehta A, Boon L, Aerts JM, Laman JD. Gaucher cells demonstrate a distinct macrophage phenotype and resemble alternatively activated macrophages. Am J Clin Pathol 2004; 122(3):359-369.

Brown D and London E. Functions of lipid rafts in biological membranes. Annu. Rev. Cell Dev. Biol. 1998; 14:111–136.

Brumshtein B, Salinas P, Peterson B, Chan V, Silman I, Sussman JL, Savickas PJ, Robinson GS, Futerman AH. Characterization of gene-activated human acid-beta-glucosidase: crystal structure, glycan composition, and internalization into macrophages. Glycobiology. 2010; 20(1):24-32.

Bultron G, Kacena K, Pearson D, Boxer M, Yang R, Sathe S, Pastores G, Mistry PK. The risk of Parkinson's disease in type 1 Gaucher disease. J Inherit Metab Dis. 2010; 33(2):167-173.

Canuel M, Korkidakis A, Konnyu K, Morale CR. Sortilinmediates the lysosomal targeting of cathepsins D and H, Biochem. Biophys. Res. Commun. 2008; 373(2): 292–297.

Cesselli D, Beltrami AP, Rigo S, Bergamin N, D'Aurizio F, Verardo R, Piazza S, Klaric E, Fanin R, Toffoletto B et al. Multipotent progenitor cells are present in human peripheral blood. Circ Res 2009; 104(10):1225–1234.

Chabas A, Cormand B, Grinberg D, Burguera JM, Balcells S, Merino JL, Mate I, Sobrino JA, Gonzalez-Duarte R, Vilageliu L. Unusual expression of Gaucher's disease: cardiovascular calcifications in three sibs homozygous for the D409H mutation. J Med Genet 1995; 32(9):740–742.

Chaves J, Beirão I, Balreira A, Gaspar P, Caiola D, Sá-Miranda MC, Lima JL. Progressive myoclonus epilepsy with nephropathy C1q due to SCARB2/LIMP-2 deficiency: Clinical report of two siblings. Seizure. 2011; 20(9):738-740.

Chen S, Zhang Y, Chen W, Wang Y, Liu J, Rong TY, Ma JF, Wang G, Zhang J, Pan J, Xiao Q, Chen SD. Association study of SCARB2 rs6812193 polymorphism with Parkinson's disease in Han Chinese. Neurosci Lett. 2012; 516(1):21-23.

Christomanou H, Aignesberger A, Linke RP. Immunochemical characterization of two activator proteins stimulating enzymic sphingomyelin degradation in vitro. Absence of one of them in human Gaucher disease variant. Biol Chem Hoppe Seyler. 1986; 367(9):879–890.

Christomanou H, Chabas A, Pampols T, Guardiola A. Activator protein deficient Gaucher's disease. A second patient with the newly identified lipid storage disorder. Klin Wochenschr. 1989; 67(19):999–1003.

Crawley AC, Walkley SU. Developmental analysis of CNS pathology in the lysosomal storage disease alpha-mannosidosis. J Neuropathol Exp Neurol. 2007; 66(8):687-697.

d'Azzo A, Tessitore A, Sano R. Cell Death Differ. Gangliosides as apoptotic signals in ER stress response. 2006;13(3):404-14

Dardis A, Filocamo M, Grossi S, Ciana G, Franceschetti S, Dominissini S, Rubboli G, Di Rocco M, Bembi B. Biochemical and molecular findings in a patient with myoclonic epilepsy due to a mistarget of the beta-glucosidase enzyme. Mol Genet Metab. 2009; 97(4):309-311.

Dibbens LM, Karakis I, Bayly MA, Costello DJ, Cole AJ, Berkovic SF. Mutation of SCARB2 in a patient with progressive myoclonus epilepsy and demyelinating peripheral neuropathy. Arch Neurol. 2011; 68(6):812-813.

Dibbens LM, Michelucci R, Gambardella A, Andermann F, Rubboli G, Bayly MA, Joensuu T, Vears DF, Franceschetti S, Canafoglia L et al. SCARB2 mutations in progressive myoclonus epilepsy (PME) without renal failure Ann Neurol. 2009; 66(4):532-536.

Dittmer FD, Ulbrich EJ, Hafner A, Schmahl W, Meister T, Pohlmann R, and von Figura K. Alternative mechanisms for trafficking of lysosomal enzymes in mannose 6-phosphate receptordeficient mice are cell type-specific. J. Cell Sci. 1999; 112(10):1591–1597.

Do CB, Tung JY, Dorfman E, Kiefer AK, Drabant EM, Francke U, Mountain JL, Goldman SM, Tanner CM, Langston JW et al. Web-based genome-wide association study identifies two novel loci and a substantial genetic component for Parkinson's disease. PLoS Genet. 2011; 7(6):e1002141.

Dvir H, Harel M, McCarthy AA, Toker L, Silman I, Futerman AH, Sussman JL. X-ray structure of human acid-beta-glucosidase, the defective enzyme in Gaucher disease. EMBO Rep. 2003; 4(7):704-709.

Dittmer, FD, Ulbrich, EJ, Hafner A, Schmahl W, Meister T, Pohlmann R, and von Figura K. Alternative mechanisms for trafficking of lysosomal enzymes in mannose 6-phosphate receptordeficient mice are cell type-specific. J. Cell Sci. 1999; 112(10):1591–1597.

Dawson G, Fuller M, Helmsley KM, Hopwood JJ . Abnormal gangliosides are localized in lipid rafts in Sanfilippo (MPS3a) mouse brain. Neurochem Res. 2012 Jun;37(6):1372-80

Emsley P, Cowtan K: Coot: model-building tools for molecular graphics. Acta Crystallogr D Biol Crystallogr 2004; 60(12):2126–2132.

Enquist IB, Lo Bianco C, Ooka A, Nilsson E, Mansson J-E, Ehinger M, Richter J, Brady RO, Kirik D. and Karlsson S. Murine models of acute neuronopathic Gaucher disease. Proc. Natl Acad. Sci. USA 2007; 104(44):17483–17488.

Febbraio M, Hajjar DP, and Silverstein RL. CD36: a class B scavenger receptor involved in angiogenesis, atherosclerosis, inflammation, and lipid metabolism. J. Clin. Invest. 2001; 108(6):785–791.

Filocamo M, Mazzotti R, Stroppiano M, Seri M, Giona F, Parenti G, Regis S, Corsolini F, Zoboli S, Gatti R.. Analysis of the glucocerebrosidase gene and mutation profile in 144 Italian Gaucher patients. Hum Mutat 2002; 20(30):234–235.

Friedman B, Vaddi K, Preston C, Mahon E, Cataldo JR, and McPherson JM. A comparison of the pharmacological properties of carbohydrate remodeled recombinant and placental-derived β-glucocerebrosidase: implications for clinical efficacy in treatment of Gaucher disease. Blood 1999; 93(9):2807–2816.

Fu YJ, Aida I, Tada M, Tada M, Toyoshima Y, Takeda S, Nakajima T, Naito H, Nishizawa M, Onodera O. et al. Progressive myoclonus epilepsy: extraneuronal brown pigment deposition and system neurodegeneration in the brains of Japanese patients with novel SCARB2 mutations. Neuropathol Appl Neurobiol. 2013. [Epub ahead of print]

Fujita H, Ezaki J, Noguchi Y, Kono A, Himeno M, and Kato, K. Isolation and sequencing of a cDNA clone encoding 85kDa sialoglycoprotein in rat liver lysosomal membranes. Biochem. Biophys. Res. Commun. 1991; 178(2):444–452.

Gamp AC, Tanaka Y, Lullmann-Rauch R, Wittke D, D'Hooge R, De Deyn PP, Moser T, Maier H, Hartmann D, Reiss K. LIMP-2/LGP85 deficiency causes ureteric pelvic junction obstruction, deafness and peripheral neuropathy in mice. Hum. Mol. Genet. 2003; 12(6):631–646.

Gan-Or Z, Giladi N, Rozovski U, Shifrin C, Rosner S, Gurevich T, Bar-Shira A, Orr-Urtreger A. Genotype-phenotype correlations between GBA mutations and Parkinson disease risk and onset. Neurology. 2008; 70(24):2277-2283.

Germain DP, Kaneski CR, Brady RO. Mutation analysis of the acid beta-glucosidase gene in a patient with type 3 Gaucher disease and neutralizing antibody to alglucerase. Mutat Res 2001; 483(1-2):89–94.

Ginns EI, Choudary PV, Martin BM, Winfield S, Stubblefield B, Grabowski GA, Horowitz M. Gaucher's disease: molecular, genetic and enzymological aspects. Baillieres Clin Haematol 1997; 10(4):635-656.

Ginsel LA and Fransen JA. Mannose 6-phosphate receptor independent targeting of lysosomal enzymes. Cell Biol. Int. Rep. 1991; 15(12):1167–1173.

Ginzburg L, Kacher Y and Futerman AH. The pathogenesis of glycosphingolipid storage disorders. Semin. Cell Dev. Biol. 2004; 15(4):417–431.

Glickman JN and Kornfeld S. Mannose 6-phosphate-independent targeting of lysosomal enzymes in I-cell disease B lymphoblasts. J. Cell Biol. 1993; 123(1):99–108.

Goker-Alpan O, Hruska KS, Orvisky E, Kishnani PS, Stubblefield BK, Schiffmann R, Sidransky E. Divergent phenotypes in Gaucher disease implicate the role of modifiers. J Med Genet 2005; 42(6):e37.

Goker-Alpan O, Schiffmann R, LaMarca ME, Nussbaum RL, McInerney-Leo A and Sidransky E. Parkinsonism among, Gaucher disease carriers. J. Med. Genet. 2004; 41(12):937-940.

Gornati R, Berra B, Montorfano G, Martini C, Ciana G, Ferrari P, Romano M, Bembi B. Glycolipid analysis of different tissues and cerebrospinal fluid in type II Gaucher disease. J Inherit Metab Dis. 2002; 25(1):47-55.

Grabowski GA.. Phenotype, diagnosis, and treatment of Gaucher's disease. Lancet 2008; 372(9645):1263-1271.

Grabowski GA. Gaucher disease and other storage disorders. Hematology Am Soc Hematol Educ Program. 2012; 13-18.

Grabowski GA, Barton NW, Pastores G, Dambrosia JM, Banerjee TK, McKee MA, Parker C, Schiffmann R, Hill SC, Brady RO. Enzyme therapy in type 1 Gaucher disease: comparative efficacy of mannose-terminated glucocerebrosidase from natural and recombinant sources. Ann Intern Med 1995; 122(1):33-39.

Grabowski GA, Horowitz M. Gaucher's disease: molecular, genetic and enzymological aspects. Baillieres Clin Haematol. 1997; 10(4):635-656.

Grace ME, Grabowski GA. Human acid beta-glucosidase: glycosylation is required for catalytic activity. Biochem Biophys Res Commun 1990; 168(2):771-777.

Graves PN, Grabowski GA, Eisner R, Palese P, Smith FI.. Gaucher disease type 1: cloning and characterization of a cDNA encoding acid beta-glucosidase from an Ashkenazi Jewish patient. DNA 1988; 7(8):521-528.

Guerrero-López R, García-Ruiz PJ, Giráldez BG, Durán-Herrera C, Querol-Pascual MR, Ramírez-Moreno JM, Más S, Serratosa JM. A new SCARB2 mutation in a patient with progressive myoclonus ataxia without renal failure. Mov Disord. 2012; 27(14):1826-1827.

Haddley K. Taliglucerase alfa for the treatment of Gaucher's disease. Drugs Today (Barc). 2012; 48(8):525-532.

Halperin A, Elstein D, Zimran A. Increased incidence of Parkinson disease among relatives of patients with Gaucher disease. Blood Cells Mol Dis. 2006; 36(3):426-428.

Hein LK, Duplock S, Hopwood JJ, Fuller M. Lipid composition of microdomains is altered in a cell model of Gaucher disease. J Lipid Res. 2008; 49(8):1725-1734.

Higashiyama Y, Doi H, Wakabayashi M, Tsurusaki Y, Miyake N, Saitsu H, Ohba C, Fukai R, Miyatake S, Joki H et al. A novel SCARB2 mutation causing late-onset progressive myoclonus epilepsy. Mov Disord. 2013; 28(4):552-553.

Ho MW, O'Brien JS. Gaucher's disease: deficiency of 'acid' -glucosidase and reconstitution of enzyme activity in vitro. Proc Natl Acad Sci USA 1971; 68(11):2810-2813.

Hollak CE, van Weely S, van Oers MH, Aerts JM. Marked elevation of plasma chitotriosidase activity. A novel hallmark of Gaucher disease. J Clin Invest 1994; 93(3):1288-1292.

Höning S, Sandoval IV, von Figura K. A di-leucine-based motif in the cytoplasmic tail of LIMP-II and tyrosinase mediates selective binding of AP-3. EMBO J. 1998; 17(5):1304-1314.

Hopfner F, Schormair B, Knauf F, Berthele A, Tölle TR, Baron R, Maier C, Treede RD, Binder A, Sommer C et al. Novel SCARB2 mutation in action myoclonus-renal failure syndrome and evaluation of SCARB2 mutations in isolated AMRF features. BMC Neurol. 2011; 11:134.

Hopfner F, Schulte EC, Mollenhauer B, Bereznai B, Knauf F, Lichtner P, Zimprich A, Haubenberger D, Pirker W, Brücke T et al. The role of SCARB2 as susceptibility factor in Parkinson's disease. Mov Disord. 2013; 28(4):538-540.

Horowitz M, Wilder S, Horowitz Z, Reiner O, Gelbart T, Beutler E. The human glucocerebrosidase gene and pseudogene: structure and evolution. Genomics 1989; 4(1):87-96.

Horowitz M, Pasmanik-Chor M, Borochowitz Z, Falik-Zaccai T, Heldmann K, Carmi R, Parvari R, Beit-Or H, Goldman B, Peleg L et al. Prevalence of glucocerebrosidase mutations in the israeli ashkenazi jewish population. Hum Mutat. 1998; 12(4):240–244.

Horowitz M, Pasmanik-Chor M, Ron I, Kolodny EH. The enigma of the E326K mutation in acid β-glucocerebrosidase. Mol Genet Metab.2011; 104(1-2): 35-38.

Hruska KS, LaMarca ME, Scott CR, Sidransky E. Gaucher disease: mutation and polymorphism spectrum in the glucocerebrosidase gene (GBA). Hum Mutat. 2008; 29(5):567-583.

Jeyakumar M, Dwek RA, Butters TD, Platt FM. Storage solutions: treating lysosomal disorders of the brain. Nat Rev Neurosci 2005; 6(9):713-725.

Jović M, Kean MJ, Szentpetery Z, Polevoy G, Gingras AC, Brill JA, Balla T. Two phosphatidylinositol 4-kinases control lysosomal delivery of the Gaucher disease enzyme, β-glucocerebrosidase. Mol Biol Cell. 2012; 23(8):1533-1545

Kasper D, Dittmer F, von Figura K, and Pohlmann, R. Neither type of mannose 6-phosphate receptor is sufficient for targeting of lysosomal enzymes along intracellular routes. J. Cell Biol. 1996; 134(3):615–623.

Kim JW, Liou BB, Lai MY, Ponce E, Grabowski GA.. Gaucher disease: identification of three new mutations in the Korean and Chinese (Taiwanese) populations. Hum Mutat 1996; 7(3):214–218.

Koprivica V, Stone DL, Park JK et al: Analysis and classification of 304 mutant alleles in patients with type 1 and type 3 Gaucher disease. Am J Hum Genet 2000; 66(6):1777–1786.

Kowarz L, Goker-Alpan O, Banerjee-Basu S, LaMarca ME, Kinlaw L, Schiffman R, Baxevanis AD, Sidransky E. Gaucher mutation N188S is associated with myoclonic epilepsy. Hum Mutat 2005; 26(3):271–273.

Krieger, M. Scavenger receptor class B type I is a multiligand HDL receptor that influences diverse physiologic systems. J. Clin. Invest. 2001; 108(6):793–797.

Kraoua I, Sedel F, Caillaud C, Froissart R, Stirnemann J, Chaurand G, Flodrops H, Tari S, Gourfinkel-An I, Mathieu S et al. A French experience of type 3 Gaucher disease: Phenotypic diversity and neurological outcome of 10 patients. Brain Dev. 2011; 33(2):131-139.

Kuchař L, Ledvinová J, Hřebíček M, Myšková H, Dvořáková L, Berná L, Chrastina P, Asfaw B, Elleder M, Petermöller M et al. Prosaposin deficiency and saposin B deficiency (activator-deficient metachromatic leukodystrophy): Report on two patients detected by analysis of urinary sphingolipids and carrying novel PSAP gene mutations. Am J Med Genet A. 2009; 149A:613–621.

Kuronita T, Eskelinen EL, Fujita H, Saftig P, Himeno M, Tanaka Y. A role for the lysosomal membrane protein LGP85 in the biogenesis and maintenance of endosomal and lysosomal morphology. J. Cell Sci. 2002; 115(21):4117–4131.

Lachmann RH, Grant IR, Halsall D, Cox TM, Twin pairs showing discordance of phenotype in adult Gaucher disease. QJM 2004; 97(4):199–204.

Le Borgne R, Alconada A, Bauer U, Hoflack B. The mammalian AP-3 adaptor-like complex mediates the intracellular transport of lysosomal membrane glycoproteins. J Biol Chem. 1998; 273(45):29451-29461.

Lefrancois S, Zeng J, Hassan AJ, Canuel M. Morales CR, The lysosomal trafficking of sphingolipid activator proteins (SAPs) is mediated by sortilin, EMBO J. 2003; 22(24):6430–6437.

Legler G, Bieberich E. Active site directed inhibition of a cytosolic beta-glucosidase from calf liver by bromoconduritol B epoxide and bromoconduritol F. Arch Biochem Biophys 1988; 260(1):437-442.

Liou B, Kazimierczuk A, Zhang M, Scott CR, Hegde RS, and Grabowski GA Analyses of variant acid b-glucosidases: effects of Gaucher disease mutations. J. Biol. Chem. 2006; 281(17):4242–4253.

Ludwig T, Munier-Lehmann H, Bauer U, Hollinshead M, Ovitt C, Lobel P, and Hoflack B. Differential sorting of lysosomal enzymes in mannose 6-phosphate receptor-deficient fibroblasts. EMBO J. 1994; 13(15):3430–3437.

Maley F, Trimble RB, Tarentino AL and Plummer TH. Characterization of glycoproteins and their associated oligosaccharides through the use of endoglycosidases. Anal. Biochem. 1989; 180(2):195–204.

Maniwang E, Tayebi N, Sidransky E. Is Parkinson disease associated with lysosomal integral membrane protein type-2? challenges in interpreting association data. Mol Genet Metab. 2013; 108(4):269-271.

Mazella J, Zsürger N, Navarro V, Chabry J, Kaghad M, Caput D, Ferrara P, Vita N, Gully D, Maffrand JP et al. The 100-kDa neurotensin receptor is gp95/sortilin, a non-G-protein-coupled receptor, J. Biol. Chem. 1998; 273(41):26273–26276.

Mazzulli JR, Xu YH, Sun Y, Knight AL, McLean PJ, Caldwell GA, Sidransky E, Grabowski GA and Krainc D. Gaucher disease glucocerebrosidase and α-synuclein form a bidirectional pathogenic loop in synucleinopathies. Cell 2011; 146(1):37-52.

McGlynn R, Dobrenis K, Walkley SU. Differential subcellular localization of cholesterol, gangliosides, and glycosaminoglycans in murine models of mucopolysaccharide storage disorders. J Comp Neurol. 2004; 480(4):415-426.

Meikle PJ, Hopwood JJ, Clague AE, Carey WF. Prevalence of lysosomal storage disorders. JAMA. 1999; 281(3):249–254.

Mistry PK, Wraight EP, and Cox TM. Therapeutic delivery of proteins to macrophages: implications for treatment of Gaucher's disease. Lancet 1996; 348(9041):1555–1559.

Montfort M, Chabás A, Vilageliu L, Grinberg D. Functional analysis of 13 GBA mutant alleles identified in Gaucher disease patients: Pathogenic changes and "modifier" polymorphisms. Hum Mutat. 2004; 23(6):567-575.

Moraitou M, Hadjigeorgiou G, Monopolis I, Dardiotis E, Bozi M, Vassilatis D, Vilageliu L, Grinberg D, Xiromerisiou G, Stefanis L, Michelakakis H. β-Glucocerebrosidase gene mutations in two cohorts of Greek patients with sporadic Parkinson's disease. Mol Genet Metab. 2011; 104(1-2):149-52.

Moran D, Galperin E, Horowitz M. Identification of factors regulating the expression of the human glucocerebrosidase gene. Gene 1997; 194(2):201-213.

Morris JL. Velaglucerase alfa for the management of type 1 Gaucher disease. Clin Ther. 2012; 34(2):259-71.

Myerowitz R. Tay-Sachs disease-causing mutations and neutral polymorphisms in the Hex A gene. Hum Mutat. 1997; 9(3):195–208.

Neculai D, Schwake M, Ravichandran M, Zunke F, Collins RF, Peters J, Neculai M, Plumb J, Loppnau P, Pizarro JC et al. Structure of LIMP-2 provides functional insights with implications for SR-BI and CD36. Nature. 2013; 504(7478):172-176.

Neumann J, Bras J, Deas E, O'Sullivan SS, Parkkinen L, Lachmann RH, Li A, Holton J, Guerreiro R, Paudel R et al. Glucocerebrosidase mutations in clinical and pathologically proven Parkinson's disease. Brain 2009; 132(7):1783-1794.

Ni X, Morales CR. The lysosomal trafficking of acid sphingomyelinase is mediated by sortilin and mannose 6-phosphate receptor, Traffic 2006; 7(7):889–902.

Nishino I, Fu J, Tanji K et al. Primary LAMP-2 deficiency causes X-linked vacuolar cardiomyopathy and myopathy (Danon disease). Nature 2000; 406(6798):906–910.

Neudorfer O, Giladi N, Elstein D, Abrahamov A, Turezkite T, Aghai E, Reches A, Bembi B and Zimran A. Occurrence of Parkinson's syndrome in type I Gaucher disease. QJM 1996; 89(9):691-694.

Pampols T, Pineda M, Giros ML, Ferrer I, Cusi V, Chabas A, Sanmarti FX, Vanier MT, Christomanou H. Neuronopathic juvenile glucosylceramidosis due to sap-C deficiency: clinical course, neuropathology and brain lipid composition in this Gaucher disease variant. Acta Neuropathol 1999; 97(1):91-7.

Park JK, Orvisky E, Tayebi N, Kaneski C, Lamarca ME, Stubblefield BK, Martin BM, Schiffmann R and Sidransky E. Myoclonic epilepsy in Gaucher disease: genotype-phenotype insights from a rare patient subgroup. Pediatr. Res. 2003; 53(3):387–395.

Pasmanik-Chor M, Elroy-Stein O, Aerts H, Agmon V, Gatt S, Horowitz M. Overexpression of human glucocerebrosidase containing different-sized leaders. Biochem J 1996; 317(1):81-88.

Pelled D, Shogomori H, Futerman AH. The increased sensitivity of neurons with elevated glucocerebroside to neurotoxic agents can be reversed by imiglucerase. J Inherit Metab Dis 2000; 23(2):175-84.

Pennelli N, Scaravilli F, Zacchello F. The morphogenesis of Gaucher cells investigated by electron microscopy. Blood 1969; 34(3):331-347.

Perandones C, Micheli FE, Pellene LA, Bayly MA, Berkovic SF, Dibbens LM.
A case of severe hearing loss in action myoclonus renal failure syndrome resulting from mutation in SCARB2. Mov Disord. 2012; 27(9):1200-2001.

Petersen CM, Nielsen MS, Nykjaer A, Jacobsen L, Tommerup N, Rasmussen HH, Roigaard H, Gliemann J, Madsen P, Moestrup SK. Molecular identification of a novel candidate sorting receptor purified from human brain by receptor-associated protein affinity chromatography, J. Biol. Chem. 1997; 272(6):3599–3505.

Puri V, Watanabe R, Dominguez M, Sun X, Wheatley CL, Marks DL and Pagano RE. Cholesterol modulates membrane traffic along the endocytic pathway in sphingolipid-storage diseases. Nat. Cell Biol. 1999; 1(6):386–388.

Reczek D, Schwake M, Schroder J, Hughes H, Blanz J, Jin X, Brondyk W, Van Patten S, Edmunds T, Saftig P. LIMP-2 is a receptor for lysosomal mannose-6-phosphate-independent targeting of betaglucocerebrosidase. Cell 2007; 131(4):770–783.

Reese MG, Eeckman FH, Kulp D, Haussler D: Improved splice site detection in Genie. J Comput Biol 1997; 4(3):311–323.

Reid PC, Sakashita N, Sugii S, Ohno-Iwashita Y, Shimada Y, Hickey WF, Chang TY. A novel cholesterol stain reveals early neuronal cholesterol accumulation in the Niemann-Pick type C1 mouse brain. J Lipid Res. 2004; 45(3):582-591.

Reiner O, Horowitz M. Differential expression of the human glucocerebrosidase-coding gene. Gene 1988; 73(2):469-478.

Reiner O, Wigderson M, Horowitz M. Structural analysis of the human glucocerebrosidase genes. DNA 1988; 7(2):107-116.

Ron I, Horowitz M. ER retention and degradation as the molecular basis underlying Gaucher disease heterogeneity. Hum Mol Genet 2005; 14(16):2387-2398.

Rubboli G, Franceschetti S, Berkovic SF, Canafoglia L, Gambardella A, Dibbens LM, Riguzzi P, Campieri C, Magaudda A, Tassinari CA et al. Clinical and neurophysiologic features of progressive myoclonus epilepsy without renal failure caused by SCARB2 mutations. Epilepsia. 201; 52(12):2356-2363

Salvioli R, Tatti M, Scarpa S, Moavero SM, Ciaffoni F, Felicetti F, Kaneski CR, Brady RO, Vaccaro AM. The N370S (Asn370-->Ser) mutation affects the capacity of glucosylceramidase to interact with anionic phospholipid-containing membranes and saposin C. Biochem J. 2005; 390(1):95-103.

Sardi SP, Clarke J, Kinnecom C, Tamsett TJ, Li L, Stanek LM, Passini MA, Grabowski GA, Schlossmacher MG, Sidman RL et al. CNS expression of glucocerebrosidase corrects {alpha}-synuclein pathology and memory in a mouse model of Gaucher-related synucleinopathy. Proc. Natl. Acad. Sci. USA 2011; 108(29):12101-12106.

Sardiello M, Palmieri M, di Ronza A, Medina DL, Valenza M, Gennarino VA, Di Malta C, Donaudy F, Embrione V, Polishchuk RS et al. A. A gene network regulating lysosomal biogenesis and function. Science. 2009; 325(5939):473-477.

Sarmientos F, Schwarzmann G, Sandhoff K. Direct evidence by carbon-13 NMR spectroscopy for the erythro configuration of the sphingoid moiety in Gaucher cerebroside and other natural sphingolipids. Eur J Biochem 1985; 146(1):59-64.

Sawkar AR, Schmitz M, Zimmer KP, Reczek D, Edmunds T, Balch WE, Kelly JW. Chemical chaperones and permissive temperatures alter localization of Gaucher disease associated glucocerebrosidase variants. ACS Chem Biol. 2006; 1(4):235-251.

Schiffmann R, Fitzgibbon EJ, Harris C, DeVile C, Davies EH, Abel L, van Schaik IN, Benko W, Timmons M, Ries M, Vellodi A. Randomized, controlled trial of miglustat in Gaucher's disease type 3. Ann Neurol. 2008; 64(5):514-522

Schmitz M, Alfalah M, Aerts JM, Naim HY, and Zimmer KP. Impaired trafficking of mutants of lysosomal glucocerebrosidase in Gaucher's disease. Int. J. Biochem. Cell Biol. 2005; 37(11): 2310–2320.

Sidransky E. Gaucher disease: complexity in a "simple" disorder. Mol Genet Metab 2004; 83(1-2):6-15.

Sidransky E, Tayebi N, Stubblefield BK, Eliason W, Klineburgess A, Pizzolato GP, Cox JN, Porta J, Bottani A and DeLozier-Blanchet CD. The clinical, molecular, and pathological characterisation of a family with two cases of lethal perinatal type 2 Gaucher disease. J. Med. Genet. 1996; 33(2):132–136.

Simons, K., and D. Toomre. Lipid rafts and signal transduction. Nat. Rev. Mol. Cell Biol 2000; 1(21): 31–39.

Sleat DE, Wiseman JA, El-Banna M, Kim KH, Mao Q, Price S, Macauley SL, Sidman RL, Shen MM, Zhao Q et al. A mouse model of classical late-infantile neuronal ceroid lipofuscinosis based on targeted disruption of the CLN2 gene results in a loss of tripeptidyl-peptidase I activity and progressive neurodegeneration. J Neurosci. 2004; 24(41):9117-9126.

Sorge JA, West C, Kuhl W, Treger L, Beutler E. The human glucocerebrosidase gene has two functional ATG initiator codons. Am J Hum Genet 1987; 41(6):1016-1024.

Sorge J, West C, Westwood B, Beutler E. Molecular cloning and nucleotide sequence of human glucocerebrosidase cDNA. Proc Natl Acad Sci USA 1985; 82(21):7289-7293.

Staretz-Chacham O, Lang TC, LaMarca ME, Krasnewich D, Sidransky E. Lysosomal storage disorders in the newborn. Pediatrics. 2009; 123(4):1191-1207.

Stenson PD, Ball EV, Mort M, Phillips AD, Shiel JA, Thomas NS, Abeysinghe S, Krawczak M, Cooper DN.. Human Gene Mutation Database (HGMD): 2003 update. Hum Mutat 2003; 21(6):577-581.

Sun Y, Qi X, Grabowski GA. Saposin C is required for normal resistance of acid beta-glucosidase to proteolytic degradation. J Biol Chem 2003; 278(34):31918-31923.

Tabuchi N, Akasaki K, Tsuji H. Two acidic amino acid residues, Asp(470) and Glu(471), contained in the carboxyl cytoplasmic tail of a major lysosomal membrane protein, LGP85/LIMP II, are important for its accumulation in secondary lysosomes. Biochem Biophys Res Commun. 2000; 270(2):557-563.

Tayebi N, Walker J, Stubblefield B, Orvisky E, LaMarca ME, Wong K, Rosenbaum H, Schiffmann R, Bembi B and Sidransky E. Gaucher disease with parkinsonian manifestations: does glucocerebrosidase deficiency contribute to a vulnerability to parkinsonism? Mol. Genet. Metab. 2003; 79(2):104-109.

Tayebi N, Stubblefield BK, Park JK, Orvisky E, Walker JM, LaMarca ME, Sidransky E. Reciprocal and nonreciprocal recombination at the glucocerebrosidase gene region: implications for complexity in Gaucher disease. Am J Hum Genet 2003; 72(3):519-534.

Te Vruchte D, Speak AO, Wallom KL, Al Eisa N, Smith DA, Hendriksz CJ, Simmons L, Lachmann RH, Cousins A, Hartung R, Mengel E et al. Relative acidic compartment volume as a lysosomal storage disorder-associated biomarker. J Clin Invest. 2014 Feb 3. pii: 72835

Trimble RB and Tarentino AL. Identification of distinct endoglycosidase (endo) activities in Flavobacterium meningosepticum: endo F1, endo F2, and endo F3. Endo F1 and endo H hydrolyze only high mannose and hybrid glycans. J. Biol. Chem. 1991; 266(3):1646–1651.

Tsuji S, Choudary PV, Martin BM, Stubblefield BK, Mayor JA, Barranger JA, Ginns EI. A mutation in the human glucocerebrosidase gene in neuronopathic Gaucher's disease. N Engl J Med. 1987; 316(10):570-575.

Tsuji S, Martin BM, Barranger JA, Stubblefield BK, LaMarca ME, Ginns EI. Genetic heterogeneity in type 1 Gaucher disease: multiple genotypes in Ashkenazic and non-Ashkenazic individuals. Proc Natl Acad Sci U S A. 1988 Apr; 85(7):2349-23452.

Tylki-Szymanska A, Czartoryska B, Vanier MT, Poorthuis BJ, Groener JA, Lugowska A, Millat G, Vaccaro AM, Jurkiewicz E. Non-neuronopathic Gaucher disease due to saposin C deficiency. Clin Genet. 2007; 72(6):538–542.

Tylki-Szymanska A, Groener JE, Kaminski ML, Lugowska A, Jurkiewicz E, Czartoryska B. Gaucher disease due to saposin C deficiency, previously described as non-neuronopathic form - No positive effects after 2-years of miglustat therapy. Mol Genet Metab. 2011; 104(4):627–630

Uyama E, Takahashi K, OwadaM, Okamura R, NaitoM, Tsuji S, Kawasaki S, Araki S. Hydrocephalus, corneal opacities, deafness, valvular heart disease, deformed toes and leptomeningeal fibrous thickening in adult siblings: a new syndrome associated with b-glucocerebrosidase deficiency and a mosaic population of storage cells. Acta Neurol Scand 1992; 86(4):407–420.

Velayati A, DePaolo J, Gupta N, Choi JH, Moaven N, Westbroek W, Goker-Alpan O, Goldin E, Stubblefield BK, Kolodny E, Tayebi N, Sidransky E. .A mutation in SCARB2 is a modifier in Gaucher disease. Hum Mutat. 2011; 32(11):1232-1238.

Walkley SU. Pathogenic cascades in lysosomal disease-Why so complex? J Inherit Metab Dis. 2009; 32(2):181-189

Walkley SU, Thrall MA, Haskins ME, Mitchell TW, Wenger DA, Brown DE, Dial S, Seim H. Abnormal neuronal metabolism and storage in mucopolysaccharidosis type VI (Maroteaux-Lamy) disease. Neuropathol Appl Neurobiol. 2005; 31(5):536-544.

Walkley SU, Vanier MT. Secondary lipid accumulation in lysosomal disease. Biochim Biophys Acta. 2009; 1793(4):726-736.

Wong K, Sidransky E, Verma A, Mixon T, Sandberg GD, Wakefield LK, Morrison A, Lwin A, Colegial C, Allman JM et al. Neuropathology provides clues to the pathophysiology of Gaucher disease. Mol. Genet. Metab. 2004; 82(3):192–207.

Xu YH, Sun Y, Ran H, Quinn B, Witte D and Grabowski GA. Accumulation and distribution of α-synuclein and ubiquitin in the CNS of Gaucher disease mouse models. Mol. Genet. Metab. 2011; 102(4):436-447.

Yeo G, Burge CB: Maximum entropy modeling of short sequence motifs with applications to RNA splicing signals. J Comput Biol 2004; 11(2-3):377–394

Yoshizawa T, Kohno Y, Nissato S, Shoji S. Compound heterozygosity with two novel mutations in the HEXB gene produces adult Sandhoff disease presenting as a motor neuron disease phenotype. J Neurol Sci 2002; 195(2):129–138.

Yu Z, Sawkar AR, Kelly JW. Pharmacologic chaperoning as a strategy to treat Gaucher disease. FEBS J 2007; 274(19):4944-4950.

Zachos C, Blanz J, Saftig P, Schwake M. A critical histidine residue within LIMP-2 mediates pH sensitive binding to its ligand β-glucocerebrosidase. Traffic. 2012; 13(8):1113-1123.

Zervas M, Dobrenis K, Walkley SU. Neurons in Niemann-Pick disease type C accumulate gangliosides as well as unesterified cholesterol and undergo dendritic and axonal alterations.J Neuropathol Exp Neurol. 2001; 60(1):49-64.

Zhao H, Bailey LA, Elsas LJ 2nd, Grinzaid KA, Grabowski GA. Gaucher disease: in vivo evidence for allele dose leading to neuronopathic and nonneuronopathic phenotypes. Am J Med Genet 2003; 116A(1):52–56.

Zimran A. How I treat Gaucher disease. Blood. 2011; 118(6):1463-1471.

List of pubblications

1. **Malini E**, Grossi S, Deganuto M, Rosano C, Parini R, Dominisini S, Cariati R, Zampieri S, Bembi B, Filocamo M, Dardis A. Functional analysis of 11 novel GBA alleles. Eur J Hum Genet. 2013 Sep 11. doi: 10.1038/ejhg.2013.182

2. **Malini E**, Maurizio E, Bembich S, Sgarra R, Edomi P, Manfioletti G. HMGA Interactome: New Insights from Phage Display Technology. Biochemistry. 2011 May 3; 50(17):3462-8.

Acknowledgements - Ringraziamenti

Questi tre anni di dottorato sono stati occasione per acquisire nuove conoscenze scientifiche ma soprattutto stimolo di crescita.

Desidero ringraziare tutto il Centro di Coordinamento Regionale per le Malattie Rare di Udine presso cui ho svolto questo lavoro.

In particolare ringrazio il mio supervisor, la dott.ssa Andrea Elena Dardis, per avermi guidato nel progetto e il dott. Bruno Bembi, direttore del centro per avermi permesso di svolgere il dottorato nel suo laboratorio.

Un grazie alle colleghe vecchie e nuove del laboratorio Malattie Rare: dott.ssa Stefania Zampieri, dott.ssa Silvia Cattarossi, dott.ssa Roberta Cariati, dott.ssa Milena Romanello, dott.ssa Annalisa Pianta e dott.ssa Irene Zanin che mi hanno ascoltato, consigliato e aiutato nelle giornate belle e brutte di lavoro.
Un ringraziamento speciale va alla dott.ssa Marta Deganuto per la sua competenza e per avermi sostenuto in questo mio percoso nonché per essere semplicemente una delle persone più belle che ho conosciuto negli ultimi anni.

Ringrazio tutte le altre persone che hanno contribuito a realizzare questo lavoro.
La dott.ssa Mirella Filocamo con cui ho collaborato; la dott.ssa Barbara Toffoletto e dott.ssa Daniela Cesselli per il loro contributo nelle analisi di citofluorimetria.

Ringrazio i miei affetti più cari: i miei genitori e Lorenzo, grazie per non avermi mai fatto mancare il vostro sostegno e amore in questi anni.